Zootaxa 4948 (4): 451–500
https://www.mapress.com/j/zt/

Article

ISSN 1175-5326 (print edition)
ZOOTAXA
ISSN 1175-5334 (online edition)

https://doi.org/10.11646/zootaxa.4948.4.1
http://zoobank.org/urn:lsid:zoobank.org:pub:44061E80-81B7-46AF-AD51-9B461C2E2B67

Taxonomy and phylogeny of Koinocystididae (Platyhelminthes, Kalyptorhynchia), with the description of three new genera and twelve new species

YANDER L. DIEZ[1, 2, *], MARLIES MONNENS[2,3], ROSA ISABEL AGUIRRE[10], RANA YURDUSEVEN[2,4], PHILIPPE JOUK[2,5,11], NIELS W. L. VAN STEENKISTE[12,13], BRIAN S. LEANDER[12,14], ERNEST SCHOCKAERT[2,6], PATRICK REYGEL[2,7], KAREN SMEETS[2,8] & TOM ARTOIS[2,9]

[1]*Universidad de Oriente, Biology & Geography Department, Ave. Patricio Lumumba s/n, CP 90500, Santiago de Cuba, Cuba.*
yanderluis87@gmail.com, yander@uo.edu.cu; https://orcid.org/0000-0001-8741-4799
[2]*Hasselt University, Centre for Environmental Sciences, Research Group Zoology: Biodiversity and Toxicology, Universitaire Campus Gebouw D, B-3590 Diepenbeek, Belgium*
[3] *marlies.monnens@uhasselt.be; https://orcid.org/0000-0002-91331512*
[4] *rana.yurduseven@hotmail.com; https://orcid.org/0000-0002-2047-5375*
[5] *philippe.jouk@kmda.org; https://orcid.org/0000-0002-6436-2401*
[6] *ernest.schockaert@uhasselt.be; https://orcid.org/0000-0003-0666-5604*
[7] *patrick.reygel@uhasselt.be; https://orcid.org/0000-0001-8721-6290*
[8] *karen.smeets@uhasselt.be; https://orcid.org/0000-0001-9673-8824*
[9] *tom.artois@uhasselt.be; https://orcid.org/0000-0002-2491-7273*
[10]*Centro Oriental de Ecosistemas y Biodoversidad (BIOECO). Museo Tomás Romay, Calle Enramadas 601, CP 90100, Santiago de Cuba, Cuba. iaguirrealcolea@gmail.com; https://orcid.org/0000-0002-7311-2308*
[11]*Royal Zoological Society of Antwerp, Centre for Research & Conservation, Koningin Astridplein 20-26, B-2018 Antwerp, Belgium.*
[12]*University of British Columbia, Departments of Botany and Zoology, 6270 University Blvd., Vancouver, BC, V6T 1Z4 Canada.*
[13] *niels_van_steenkiste@hotmail.com; https://orcid.org/0000-0002-2676-7862*
[14] *bleander@mail.ubc.ca; https://orcid.org/0000-0003-0798-0470*
[*]*Corresponding author. yanderluis87@gmail.com; yander@uo.edu.cu*

Table of contents

Accepted by W. Sterrer: 4 Aug. 2020; published: 23 Mar. 2021

Abstract

The taxon Koinocystididae is the third most species-rich family within Eukalyptorhynchia. However, its diversity and phylogeny have been largely neglected in former studies. We introduce three new genera and twelve new species of Koinocystididae including *Simplexcystis asymmetrica* **gen. n. sp. n.**, *Galapagetula cubensis* **sp. n.**, eight species of *Reinhardorhynchus* **gen. n.** and two species of *Itaipusa*. This raises the total number of species within Koinocystididae from 51 to 63. We also report on new distribution records for six known species: *I. divae* (Cuba, Panama and New Caledonia), *I. karlingi* (Sardinia and Lanzarote), *Reinhardorhynchus riegeri* **comb. n.** (Cuba), *R. ruffinjonesi* **comb. n.** (Cuba and Panama), *Utelga heinckei* (Cuba and Lanzarote), and *U. pseudoheinckei* (Sardinia). *Simplexcystis asymmetrica* **gen. n. sp. n.** is characterised by a male duct running eccentrically through the copulatory bulb, lack of any hard structures in the male system, lack of a bursa, and the fact that the epithelia of the female, the male, and part of the common atrium are covered by a brush border. *Galapagetula cubensis* **sp. n.** has a caudal gonopore, a divisa-type copulatory bulb with an unarmed penis papilla, and a female duct without a sphincter. The new species of *Itaipusa* and *Reinhardorhynchus* **gen. n.** differ from their congeners in the detailed structure of the copulatory bulb and especially the hard structures associated with it. In a molecular phylogenetic analysis based on all available 18S and 28S rDNA sequences of koinocystidids, we found support for the monophyly of the family and the genus *Utelga* Marcus, 1949. The genus *Itaipusa* is not monophyletic in that *I. sinensis* forms a clade with *Rhinolasius dillonicus*, while other species of *Itaipusa* that have a copulatory bulb armed with hooks form a clade together with *Sekerana stolzi*. As the type species of *Itaipusa* (*I. divae*) is in neither of these clades, we erected a new genus for *I. sinensis* (*Koinogladius* **gen. n.**) and one for species of *Itaipusa* having a hook-bearing copulatory bulb (*Reinhardorhynchus* **gen. n.**), respectively. Whether the remaining species of *Itaipusa* form a monophylum remains uncertain.

Key words: Kalyptorhynchia, microturbellarian, Rhabdocoela, systematics, phylogeny

Introduction

The rhabdocoel family Koinocystididae Meixner, 1924 was introduced by Meixner (1924), who initially ranked it as a subfamily (Koinocystidini) within Polycystididae Graff, 1905. Afterward, he considered it a separate family (Meixner, 1925), at that moment including three species: *Koinocystis sophiae* Graff (1905) [now *Itaipusa sophiae* (Graff, 1905) Karling, 1978], *K. neocomensis* (Fuhrmann, 1904) Meixner, 1924 and *Anoplorhynchus piger* Meixner, 1925 [= *Sekerana stolzi* (Sekera, 1912) Strand, 1914; see Karling 1980]. Since then many new species and genera have been described, and the taxonomy was discussed and refined by several authors: Marcus (1949, 1951, 1954), Karling (1952a, 1952b, 1954, 1964, 1978, 1980), Brunet (1972), Reygel *et al.* (2011), Willems *et al.* (2017), and Lin *et al.* (2017). Currently, Koinocystididae includes 24 accepted genera and 51 accepted species (Tyler *et al.* 2006–2020).

Representatives of Koinocystididae are recognised by bearing a proboscis with cell nuclei within the bulb, lacking a cellular mantle, muscle plates, cuticular hooks or secretory girdle. The copulatory organ is of conjuncta duplex type and armed with sclerotised structures, exceptionally unarmed. The paired oviducts and the common vitelloduct open in a seminal receptacle (female duct) with a strong distal sphincter. The common atrium is ventrocaudally located, with anterior stalked uterus and posterior copulatory bursa (lacking in some species) (Karling 1978, 1980). However, few species of the family bear a copulatory organ of divisa duplex type and the number and morphology of the atrial organs is exceptionally diverse.

The fact that so many new taxa are described on a regular basis is indicative of the poorly known diversity of

this family, as is the case for most microturbellarian taxa, and even meiofauna in general. Vast areas of the world are indeed still completely unexplored as far as this particular fauna is concerned. Moreover, the morphological complexity of koinocystidids poses challenges to species identification and description. Both the female and male genital systems provide most of the distinguishing features, but indeed can show such high levels of complexity that several taxa had to be classified in monospecific genera (for details see Karling 1980).

Considering the above and a lack of DNA sequence data for most species, it is not surprising that the phylogenetic relationships within Koinocystididae have hardly been explored. In the most recent exhaustive phylogenetic analysis of Kalyptorhynchia (Tessens *et al.* 2014), only four koinocystidid species, two of which were undescribed species of *Itaipusa* Marcus, 1954, were included, representing less than 5% of the known diversity of Koinocystididae. More recently, Lin *et al.* (2017) described a new species of *Itaipusa* from China and discussed its relationships with the latter two undescribed species. Koinocystididae and *Itaipusa* were provisionally recovered as clades in these studies, but corroboration based on a more extensive dataset is needed. Such analyses will also elucidate the intrafamilial relationships of Koinocystididae, enabling a re-evaluation of the morphological treatment of this family by Karling (1980).

In this work, the phylogenetic relationships of Koinocystididae are explored in detail, using partial sequences of 18S and 28S ribosomal DNA (rDNA) subunits. Our results have important taxonomical consequences especially for the genus *Itaipusa*. Furthermore, we also describe 12 new species and three new genera collected at several localities around the world. New distribution records are provided for *I. divae* Marcus, 1949, *I. karlingi* Mack-Fira, 1968, *Reinhardorhynchus riegeri* (Karling, 1978) **comb. n.**, *R. ruffinjonesi* (Karling, 1978) **comb. n.**, *Utelga heinckei* (Attems, 1897) Karling, 1954, and *U. pseudoheinckei* Karling, 1980.

Material and methods

Collecting and morphological study. Representatives of Koinocystididae have been collected by members of the research group "Zoology: Biodiversity and Toxicology" of Hasselt University at several locations around the world: Brazil (October 2012), Panama (December 2011 & February 2016), Cuba (January 2016 to May 2018), Lanzarote (February 2010), Sardinia (September 2018), French Polynesia (March 2016), and New Caledonia (October 2003). Live specimens were extracted from the sediment and algae using the $MgCl_2$ method (see Schockaert 1996). They were studied alive and whole-mounted with lactophenol. Drawings of the sclerotised structures were made with a camera lucida on a Nikon Eclipse 80i microscope or a Leica DM 2500 LED microscope, using Nomarski interference contrast. Measurements were taken along the central axis of the measured object. The position of structures is expressed in percentages of the total body length (distance from the anterior tip of the body). Body length, pharynx diameter and proboscis length were measured on whole mounts. However, when the pharynx and proboscis had been damaged during fixation, their measurements were denoted as a percentage of the body length in live specimens. Specimens selected for histological studies were fixed in hot Bouin's fixative (50 °C), embedded in paraffin, serially sectioned (3 µm) and stained with Heidenhain's haematoxylin, using erythrosin as a counterstain. Specimens for molecular studies were preserved in ethanol (99 %) and stored at -20ºC.

Specimens collected in Panama were carried to and processed at the Laboratory of Analytical Biology at the Smithsonian Institution National Museum of Natural History, in Washington, D.C. Export permits were issued to Dr. Francesca Leasi by Samuel Valdés Díaz, Director de Áreas Protegidas y Vida Silvestre (Permiso Científico No SEX/A-32-16; April 27th, 2016) as was the Permiso Científico No SE/A-2-16; January 4th, 2016. Type and reference specimens of the species collected in Panama were deposited in the collections of the US National Museum of Natural History (USNM). Type specimens of the species collected in all other localities were deposited in the collection of the Finnish Museum of Natural History (FMNH) and the reference material in the collection of Hasselt University (HU).

For comparative purposes, the holotypes of *Itaipusa riegeri* (SMNH Type-2957), *I. ruffinjonesi* (SMNH Type-2958), *I. bispina* Karling, 1980 (SMNH Type-3127), and *I. variodentata* (Karling, Mack-Fira & Dörjes, 1972) Karling, 1978 (SMNH Type-2481) were studied. Also, we examined the reference material present in Hasselt University of *I. divae* (HU Nrs. IV.4.11–17) and the paratypes of *I. sbui* Willems & Artois, 2017 (in Willems *et al.* 2017) (paratypes HU Nrs. 577 & 578) and the reference material in the SMNH of *I. bispina* (Nrs. 94020 & 94021).

The discussion on the individual species is given after the descriptions of all species of a genus. The authors variously contributed to the descriptions of the species and this is indicated by the different authorship of each species.

DNA extraction, PCR amplification and sequencing. DNA was extracted from complete specimens using the QIAampH DNA Micro Kit with QIAamp MinEluteH columns (QIAGEN), following the manufacturer's protocol. Extracts were stored in duplicate (40 and 20 µl). Partial 18S and 28S rDNA gene fragments were amplified using the primers and PCR protocols listed in Table 1.

TABLE 1. Primer sequences and PCR regimes used for PCR amplification.

Primer	Direction	Primer sequence (5'-3')	Reference
Subunit 18S			
TimA	Forward	AMCTGGTTGATCCTGCCAG	Tessens *et al.* 2014
Poly18SR2	Reverse	GCMRGKTCACCTACRGAAACCTTGTT	Tessens *et al.* 2014
95ºC * 5 min 10 s, 30X (94ºC * 30 s, 55ºC * 30 s, 72ºC * 90 s), 72ºC * 5 min			
Subunit 28S			
LSU5	Forward	TAGGTCGACCCGCTGAAYTTA	Van Steenkiste *et al.* 2013
LSU6-3B	Reverse	GCTGTTCACATGGAACCCTTCTC	Van Steenkiste *et al.* 2013
95ºC * 5 min 10 s, 30X (94ºC * 60 s, 50ºC * 60 s, 72ºC * 90 s), 72ºC * 5 min			

PCR reactions were carried out using 0.2 ml PuReTaq Ready-To-Go PCR beads (GE Healthcare). Each reaction included 2.5 µl of each primer (5 µM), 1 µl of DNA and 17 µl of purified water for a final volume of 25 µl. PCR reactions were carried out on a Bio-Rad PCR T-100 Touch thermal cycler. PCR products were verified on a 1.4% agarose gel, stained with GelRed™. DNA quantities were assessed on a Qubit Fluorometer using the Qubit™ dsDNA HS Assay Kit (ThermoFisher Scientific). PCR products were commercially purified and sequenced by Macrogen Europe B.V. (Amsterdam) under BigDye™ terminator cycling conditions on an ABI3730XL DNA Sequencer. Specimens collected in Vancouver, Canada (*U. heinckei*, *Rhinolasius dillonicus* Karling, 1980 and *Itaipusa biglandula* Reygel, Willems & Artois, 2011) were processed following the methodology of Van Steenkiste *et al.* (2018).

Phylogenetic molecular analysis. An overview of all used sequences and corresponding accession numbers is presented in Table 2. Raw reads were quality-trimmed (error probability = 0.05) and assembled in Geneious v11.1.5 (Kearse *et al.* 2012). Consensus sequences were subjected to a BLAST search (Altschul *et al.* 1990) on the NCBI website (ncbi.nlm.nih.gov) to check for signs of contamination. All available koinocystidid sequences were mined from GenBank (Benson *et al.* 2012) and a separate dataset was compiled for both 18S (18 sequences) and 28S rDNA (17 sequences). *Cystiplex axi* Karling, 1964 was included as an outgroup taxon.

Both datasets were aligned using the online version of MAFFT v7 (Katoh & Standley 2013; Katoh *et al.* 2017), specifying the Q-INS-i algorithm to account for secondary structures. Ambiguously-aligned regions were identified and eliminated on the Gblocks v0.91b server (Castresana 2000), employing options for a less stringent selection. Resulting alignments were concatenated in Geneious. An initial partitioning scheme, defining gene boundaries was constructed manually. The concatenated alignment and partition file were used as input for the ModelFinder tool (Kalyaanamoorthy *et al.* 2017) on the IQ-TREE webserver (Trifinopoulos *et al.* 2016). Model fit was evaluated using the Akaike Selection Criterion and partition merging was enabled (Lanfear *et al.* 2012). The latter feature determines the best-fit partitioning scheme for a particular dataset, while also calculating the best-fitting evolutionary models for each selected subset.

Maximum likelihood (ML) analyses were conducted using the 'Tree Inference' tool on the IQ-TREE server (Nguyen *et al.* 2015), using edge-linked partitions. Branch support was assessed by ultrafast bootstrapping (UFBoot) (Hoang *et al.* 2017) and SH-aLRT branch tests (Guindon *et al.* 2010), both with 1000 replicates. Bayesian inference (BI) was carried out using the Metropolis-coupled Markov Chain Monte Carlo (MC^3) algorithm, implemented in MrBayes v3.2.6 (Ronquist *et al.* 2012) on the CIPRES Science Gateway (Miller *et al.* 2010). Two partitions under the GTR+G+I model were specified (as inferred by ModelFinder). Two independent runs were conducted simultaneously for 10,000,000 generations, each including one cold and three heated chains. Trees were sampled every 1000th generation, the first 25% being discarded as burn-in. Chain convergence was confirmed by the average standard deviation of split frequencies dropping below 0.01, the potential scale reduction factor approaching 1.0 and the log probability reaching a stationary distribution. Obtained topologies were summarised in a majority-rule consensus tree. Inferred posterior probabilities (pp) were employed as support values. ML and BI trees were visualised and rooted in FigTree v1.4.3 (Rambaut 2006–2019). Weakly-supported clades (UFboot < 0.95 and/or SH-aLRT < 0.80 and/or pp < 0.95) were collapsed.

TABLE 2. GenBank accession numbers used in the study (*new sequences).

Species	18S rDNA	28S rDNA
*Itaipusa divae**	MW081596	MW054455
*Itaipusa biglandula**	MW081601	MW054460
*Itaipusa karlingi**	MW081598	MW054457
Itaipusa novacaledonica **sp. n.**	KJ887481	KJ887528
Itaipusa sp. n. 1	KJ887451	KJ887557
Koinogladius sinensis **comb. n.** YTP1	MF443159.1	MF443174.1
Koinogladius sinensis **comb. n.** YTP2	MF443160.1	MF443175.1
Koinogladius sinensis **comb. n.** YTP3	MF443161.1	MF443176.1
Reinhardorhynchus anamariae **sp. n.***	MW081597	MW054456
Reinhardorhynchus hexacornutus **sp. n.***	MW054464	MW054451
Reinhardorhynchus riegeri **comb. n.***	MW081595	MW054454
Reinhardorhynchus tahitiensis **sp. n. A***	MW054463	MW054452
Reinhardorhynchus tahitiensis **sp. n. B***	MW054462	MW054453
Koinocystididae sp. 1	KR339027.1	-
*Utelga heinckei**	MW081600	MW054459
*Utelga pseudohenckei**	MW081599	MW054458
*Rhinolasius dillonicus**	MW081602	MW054461
Mesorhynchus terminostylis	AY775741.1	KJ887500.1
Sekerana stolzi	-	KJ887537
Cystiplex axi	KJ887437.1	KJ887549.1

Abbreviations used in the figures. ac, accessory cirrus; **ag,** atrial glands; **b,** bursa; **bb,** brush border; **b1,** resorptive bursa; **b2,** muscular bursa; **br,** brain; **bs,** bursal stalk; **ca,** common genital atrium; **cb,** copulatory bulb; **cds**: spines of distal part of spiny belt; **cg,** common gonopore; **cgl,** caudal glands; **ci,** cirrus; **cir,** spiny belt of cirrus; **cis,** cirrus spines; **cm,** circular muscles; **cms,** spines of middle part of spiny belt; **cps,** spines of proximal part of spiny belt; **cret,** cone retractors; **dil**, dilatators; **dip,** digestive parenchyma; **div,** diverticulum; **ds,** distal-most spines of spiny belt; **e**, eye; **ec,** ejaculatory cirrus; **ed,** ejaculatory duct; **egl,** epithelial eosinophilic glands; **em,** embryo; **epg,** epithelium glands; **fa,** female atrium; **fd,** female duct; **fd1,** proximal compartment of the female duct; **fd2,** distal compartment of female duct; **fgl,** female glands; **fh,** funnel-like structure of hook; **fp,** folded projection; **gl,** glands; **h,** hook; **ilm,** internal longitudinal muscles; **iret,** integumental retractors; **js,** juncture sphincter; **lm,** longitudinal muscles; **m,** mouth; **ma,** male atrium; **ne,** nucleated epithelium; **np,** nucleated parenchyma; **od,** oviduct; **oe,** oesophagus; **oeg,** oesophagic glands; **om,** oblique muscles; **os,** ovary black spot; **ov,** ovary; **pa,** papilla; **pc,** papillary cirrus; **pep,** proboscis sheath epithelium; **pfix,** proboscis fixators; **pg (1–4),** prostate glands (type 1–4); **ph,** pharynx; **phg,** pharyngeal glands; **pl,** cirrus plate; **pp,** penis papilla; **ppc,** prepharyngeal cavity; **pr,** proboscis; **pret,** proboscis retractors; **prg1–3,** proboscis glands type 1–3; **prp,** proboscis pore; **pv,** prostate vesicle; **rb,** receptacle bursa; **rh,** rhabdites; **rm,** radial muscles; **sd,** seminal duct; **sfp,** small folded pieces; **slm,** sheet of longitudinal muscles; **sp (1–2),** spines (1–2); **sph,** sphincter; **spr1–4,** spine rows 1–4; **sv,** seminal vesicle; **t,** testis; **tl,** layer of muscles and connective tissue; **ubg,** uterine basophilic glands; **ueg,** uterine eosinophilic glands; **ug,** uterine glands; **ut,** uterus; **vi**, vitellarium.

Results

Taxonomic account

Platyhelminthes Claus, 1887

Rhabditophora Ehlers, 1985

Rhabdocoela Ehrenberg, 1831
Kalyptorhynchia Graff, 1905

Eukalyptorhynchia Meixner, 1928

Koinocystididae Meixner, 1924

***Itaipusa* Marcus, 1949**

Emended diagnosis of *Itaipusa* (after Marcus 1949 and Karling 1980). Representative of Koinocystididae with a proboscis with a juncture sphincter. Copulatory bulb of conjucta duplex-type. Male duct armed with spiny rows (the cirrus), except in *I. biglandula* Reygel *et al.* (2011), where it is unarmed. Without accessory sclerotised structures such as stylets or hooks.

Type species. *Itaipusa divae* Marcus, 1949, by original designation.

Other species. *Itaipusa aberrans* **sp. n.**, *I. acerosa* (Brunet, 1972) Karling, 1978, *I. biglandula*, *I. karlingi* Mack-Fira, 1968, *I. novacaledonica* **sp. n**., *I. sbui* Willems & Artois in Willems *et al.*, 2017, *I. similis* (Brunet, 1972) Karling, 1978, *I. sophiae* (Graff, 1905) Karling, 1978, and *I. spinibursa* Karling, 1978.

***Itaipusa divae* Marcus, 1949**
(Fig. 1A–C)

Known distribution. Bahia de Santos (Type Locality) and Pitangueiras, São Sebastião, Brazil (see Marcus 1949 for details). Three localities in Galapagos Islands and several in Curaçao (see Reygel *et al.* 2011 for details).

New records and material. Observations on live specimens. Three whole mounts from Siboney (19°57’34”N; 75°42’07”W), Santiago de Cuba, Cuba (February 7 & May 15, 2016; April 4, 2017) (HU XIII.2.42–XIII.2.44), intertidal up to 0.6 m deep, fine-grained sand, salinity 32–35 ‰. One whole mount from La Mula (19°56’44”N; 76°45’19”W), Guamá, Santiago de Cuba, Cuba (June 29, 2016) (HU XIII.2.45), intertidal rocky pools, on the algae *Digenia simplex* and *Cladophoropsis macromeres*, salinity 33 ‰. One whole mount from Macabí (20°54’13”N; 75°43’40”W), Banes, Holguín, Cuba (April 23, 2017) (HU XIII.2.46), fine-grained sand, 0.3 m deep, salinity 34 ‰. Three whole mounts from a beach east of the Marine Research Station of Achotines (07°24’47”N; 80°10’20”W), Vera Cruz, Panama (February 28, 2016) (USNM 1642500–1642502), just over the rocky hill, on green algae (*Blidingia*/*Enteromorpha*-like). One whole mount (HU XIII.2.47) and one serially-sectioned specimen (HU XIII.2.48) collected in Anse Vata Bay (22°18’19”S; 166°26’50”E), Nouméa, New Caledonia (October 22, 2003), on algae (*Ulva*-like) and sediment taken from rocks in the mouth of a small river.

Remarks. Habitus and overall anatomical organisation of our specimens correspond to the description by Marcus (1949). The specimens are unpigmented, with two eyes. The specimens from Cuba are 0.8–1 mm long ($\bar{x}$= 0.9 mm; n = 5), the specimens from Panama are 0.9–1.3 mm long ($\bar{x}$= 1.1 mm; n = 2), and the specimen from New Caledonia is 1 mm long. The syncytial epidermis is 3 µm thick (in the serially-sectioned specimen from New Caledonia) and completely ciliated. Cilia 2–3 µm long. The epidermis has a thin basal lamina and is lined internally by a thick layer of circular muscles. Rhabdites present over the entire body surface, more numerous in the posterior body half, 2–3 µm long.

The proboscis has the characteristic koinocystidid construction, with a strong juncture sphincter (see Brunet 1972; Karling 1980). It is 10% of the body length in live specimens from Panama and 15% in the specimens from Cuba and New Caledonia.

The pharynx (Fig. 1A) is located in the anterior body half. Its diameter is 15% of the body length in live specimens from Panama and New Caledonia and 20% in specimens from Cuba. The prepharyngeal cavity (Fig. 1A: ppc) is lined by a low, nucleated epithelium (thicker in the distal 1/3 of the lumen) and surrounded by an external layer of longitudinal muscles. Four types of glands open very close to each other in the distal part of the pharynx lumen: two types containing a coarse-grained eosinophilic secretion, one stained yellowish (Fig. 1A: phg4) and the other stained brownish (Fig. 1A: phg1), one containing a fine-grained eosinophilic secretion (stained pinkish) (Fig. 1A: phg2), and one a coarse-grained basophilic secretion (stained dark blue-black) (Fig. 1A: phg3). Coarse-grained basophilic

glands (Minot's glands; Fig. 1A: oeg) open into the oesophagus (Fig. 1A: oe). The musculature of the pharynx consists of a layer of longitudinal muscles outside of the septum (Fig. 1A: lm), which is continuous with that surrounding the prepharyngeal cavity, and a circular one just inside of the septum (Fig. 1A: cm1). The distal opening of the pharynx is lined by a thick layer of longitudinal muscles, which in sagittal sections gives the impression of forming a lip-like structure (Fig. 1A: slm). The pharynx lumen is surrounded by a low epithelium and an outer layer of circular muscles (Fig. 1A: cm2) and an inner layer of longitudinal muscles (Fig. 1A: ilm). Radial muscles (Fig. 1A: rm) run between the internal and the external walls. The mouth (Fig. 1A: m) is surrounded by a sphincter (Fig. 1A: sph).

The oviform copulatory bulb (Fig. 1B–C) is 76–86 μm long ($\bar{x}$= 81 μm; n = 5) in the specimens from Cuba, 86–89 μm long ($\bar{x}$= 88 μm; n = 2) in the specimens from Panama, and 130 μm long in the specimen from New Caledonia. The spiny cirrus as a whole (Fig. 1B–C: ci) is 35–41μm long ($\bar{x}$= 38 μm; n = 5) and 29–37 μm wide ($\bar{x}$= 33 μm; n = 2) in the specimens from Cuba, 20–36 μm long ($\bar{x}$= 29 μm; n = 3), and 28–44 μm wide ($\bar{x}$= 36 μm; n = 2) in the specimens from Panama, and 57 μm long and 36 μm wide in the specimen from New Caledonia. The cirrus is formed by transverse, sclerotised folds bearing tightly-packed spines. Spines are 2–3 μm long ($\bar{x}$= 2 μm; n = 25) in the specimens from Cuba and New Caledonia, and 3–4 μm long ($\bar{x}$= 4 μm; n = 25) in the specimens from Panama.

Itaipusa karlingi Mack-Fira, 1968

(Fig. 1D–E)

Known distribution. Several localities in Romania, Black Sea (Mack-Fira 1968, 1974). Toulon and Le Brusc, France (Brunet 1972). Lussin Grande, Croatia (Karling 1980).

New records and material. Observations on live specimens. Two whole mounts (HU XIII.2.49–XIII.2.50) from Punta Negra (40°57'12"N, 08°13'43"E), Stintino, Sardinia, Italy (September 9, 2018), on silty algae, 0.5 m deep, salinity 40 ‰. Three whole mounts (HU XIII.3.01–XIII.3.04) and two serially-sectioned specimens (HU XIII.3.05–XIII.3.06) from a sheltered beach at the south of Orzola (29°13'23"N; 13°27'05"W), Lanzarote, Canary Islands (October 6, 2011), medium-coarse sand with holes from burrowing animals, taken at low tide, just below the water line, one specimen collected at the same previous mentioned conditions but the sand was covered by a green organic material, salinity 35 ‰.

Remarks. Habitus and general organisation of the newly-collected specimens as described by Mack-Fira (1968) and Karling (1980). Sardinian specimens are 0.8–0.9 mm long and the specimens from Lanzarote are 1–1.4 mm long ($\bar{x}$= 1.1 mm; n = 3). The syncytial epidermis is 3–4 μm thick, fully ciliated. Rhabdites distributed over the entire surface, 1–2 μm long, most of them stain pinkish in sections, few are stained black. Cilia 4 μm long.

The proboscis is 15% of the body length in live animals. It has the typical koinocystidid morphology (see Brunet 1972; Karling 1980), with a strong juncture sphincter. Only two pairs of integument retractors were observed: a ventral and a dorsal one.

The pharynx morphology does not deviate from that of *Itaipusa divae* (see above). The pharynx is located at 40% and its diameter represents 15% of the body length in live animals. A sphincter surrounds the mouth. Four types of glands open close to each other in the distal part of the pharynx lumen: three types of eosinophilic glands with a coarse-grained secretion (staining dark pink, pinkish, and brownish, respectively) and one type of basophilic glands with a coarse-grained secretion (staining dark purple).

The oviform copulatory bulb (Fig. 1D–E: cb) is 174–184 μm long ($\bar{x}$= 179 μm; n = 2) in the specimens from Sardinia and 188–213 μm long ($\bar{x}$= 200 μm; n = 3) in the specimens from Lanzarote. The copulatory bulb encloses the prostate vesicle, the armed cirrus, and more distally a sclerotised penis papilla. Two types of filiform gland ducts containing a coarse-grained secretion (eosinophilic and basophilic) occur in the prostate vesicle. The cirrus bears two spiny belts, armed with scale-like spines provided with 1-μm-long apical denticles. The proximal spiny belt (Fig. 1D–E: cir1) in the Sardinian specimens is 106–127 μm long ($\bar{x}$= 117 μm; n = 2), with the lateral spines 2–5 μm long ($\bar{x}$= 3 μm; n = 12), those more in the middle of the row 7–9 μm long ($\bar{x}$= 8 μm; n = 20). In the specimens from Lanzarote the proximal spiny belt is 138–153 μm long ($\bar{x}$= 146 μm; n = 2), with the lateral spines 3–5 μm long ($\bar{x}$= 4 μm; n = 12) and the central ones 8–10 μm long ($\bar{x}$= 9 μm; n = 10). The distal spiny belt (Fig. 1D: cir2) is 41–58 μm long ($\bar{x}$= 50 μm; n = 2) in the specimens from Sardinia and does not show marked differences in the

length of the spines, each measuring 3–5 µm ($\bar{x}$ = 4 µm; n = 20). In the specimens from Lanzarote the distal belt is 59–75 µm long ($\bar{x}$ = 66 µm; n = 2), with spines 4–5 µm long ($\bar{x}$ = 5 µm; n = 10). The penis papilla (Fig. 1D–E: pp) is 34–43 µm long ($\bar{x}$ = 39 µm; n = 2) and 31–34 µm wide ($\bar{x}$ = 33 µm; n = 2) in the specimens from Sardinia and 41–48 µm long ($\bar{x}$ = 45 µm; n = 3) and 25–48 µm wide ($\bar{x}$ = 39 µm; n = 3) in the specimens from Lanzarote.

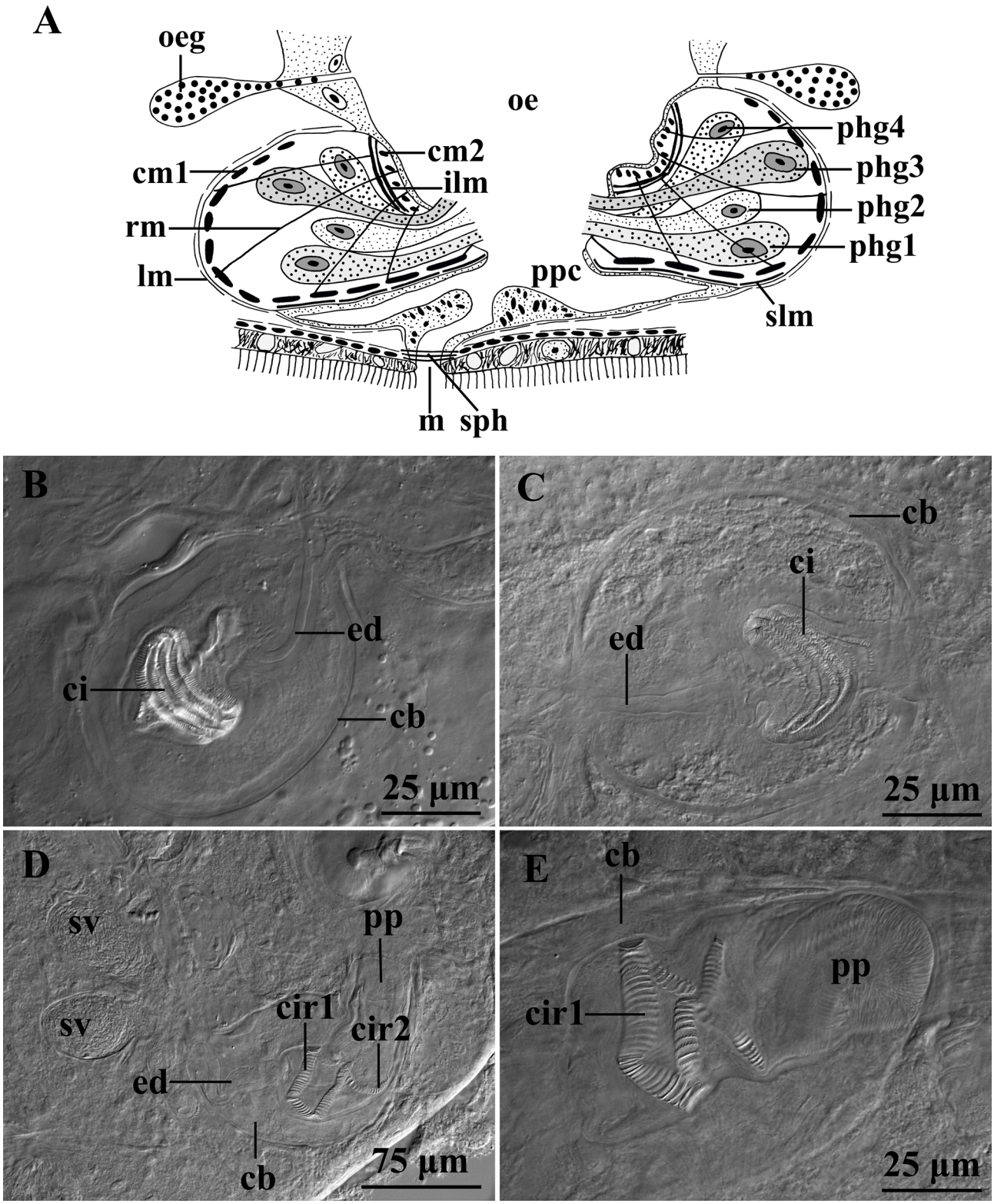

FIGURE 1. A–C, *Itaipusa divae* Marcus, 1949. A, sagittal reconstruction of the pharynx from the left hand side. B–C, copulatory bulb (specimens from Cuba and Panama, respectively). D–E, *Itaipusa karlingi* Mack-Fira, 1968. D, copulatory bulb. E, cirrus and penis papilla. A–B with proximal end toward top of figure, C–E with proximal end toward left of figure.

The uterus enters the common atrium rostro-ventrally. There are no sphincters surrounding the distal part of the uterus. It is lined by a nucleated epithelium and surrounded by longitudinal muscles. Three types of glands open into the uterus: one producing a very coarse-grained eosinophilic secretion, and two producing an eosinophilic secretion (fine-grained and coarse-grained, respectively). The bursal stalk shows the typical sclerotised membranes described for the species (see Mack-Fira 1974; Karling 1980). The female duct opens into the bursa through the typical strong sphincter.

***Itaipusa aberrans* Diez, Aguirre, Reygel & Artois sp. n.**
(Fig. 2)
urn:lsid:zoobank.org:act:171C2F91-B386-4BD4-B07A-CCDC27FAD1F1

Material and distribution. One specimen studied alive and whole mounted, designated holotype (FMNH https://id.luomus.fi/KV.646), collected in Siboney (19°57'34"N; 75°42'07"W) (Type Locality), Santiago de Cuba, Cuba (April 5, 2017), fine-grained sand rich in organic matter, 0.3 m deep, salinity 34 ‰.

Etymology. Species named after the unique and aberrant structure of the cirrus.

Diagnosis. Species of *Itaipusa* with an armed cirrus subdivided into two short, heavily folded plates, connected to each other by a thin duct lined by some small teeth. One plate is 32 µm long and bears a few spines 3–4 µm long. The second plate is spiral-shaped and armed with a few 1–9 µm long spines.

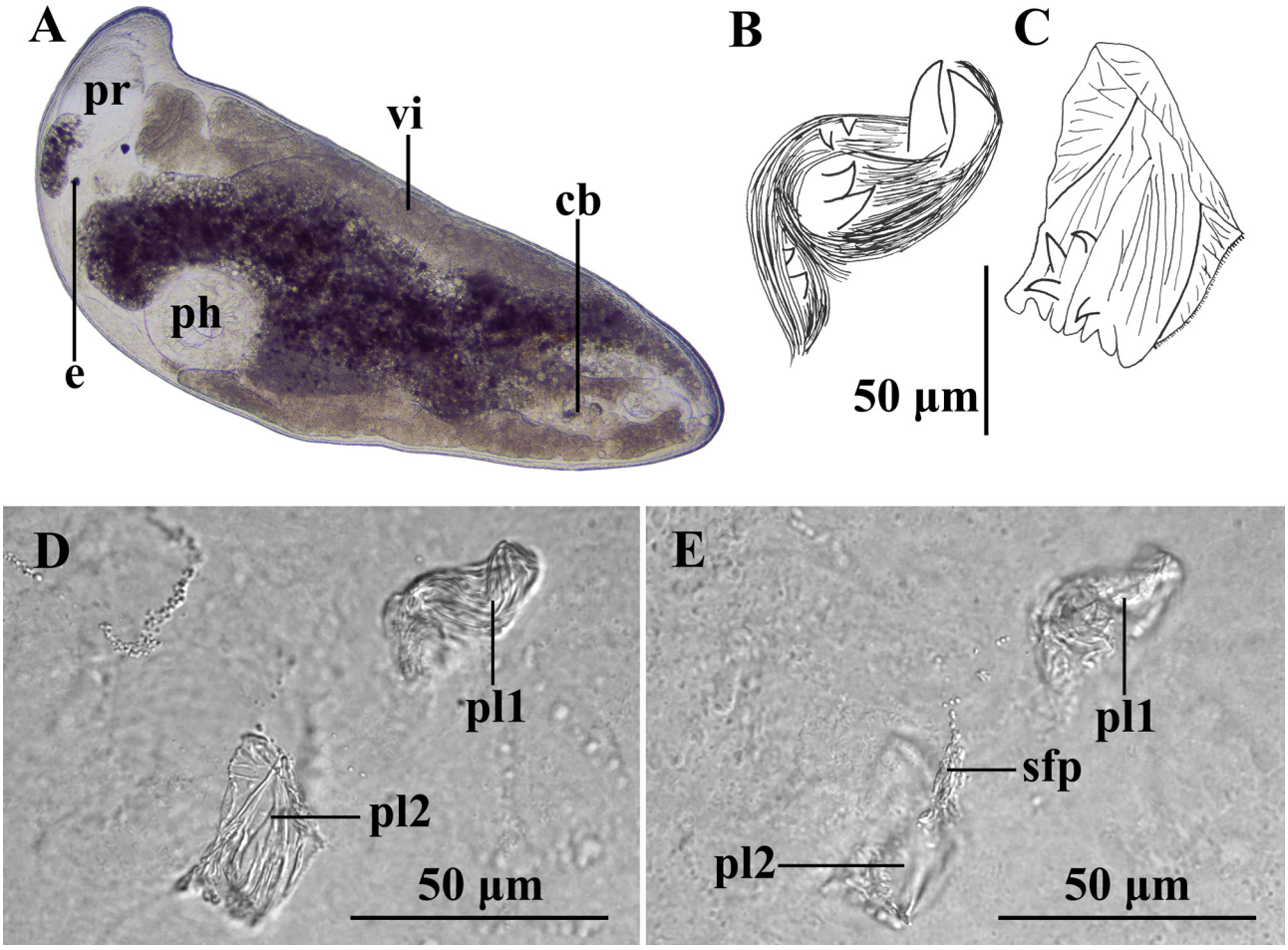

FIGURE 2. *Itaipusa aberrans* **sp. n.**. A, general organisation (live animal). B–E, sclerotised structures of the cirrus (from the holotype). B–E with proximal end toward top of figure.

Description. The specimen is 1.7 mm long, unpigmented, with two eyes (Fig. 2A: e). Proboscis (Fig. 2A: pr) of the typical koinocystidid construction (see Brunet 1972; Karling 1980); it is 10% of the body length in the live animal. The pharynx (Fig. 2A: ph) has a diameter of 15% of the body length in the live specimen, situated at 50%.

A pair of testes is located antero-laterally from the pharynx. Paired elongated seminal vesicles fuse to form a short seminal duct just before entering into the copulatory bulb. The ovoid copulatory bulb (Fig. 2A: cb) encloses the prostate vesicle (typically encompassing numerous filiform ducts) and the armed cirrus (Fig. 2B–E). The cirrus is subdivided into two short, armed plates connected to each other by a narrow structure with some small folded sclerotised pieces (Fig. 2E: sfp). The first plate (Fig. 2B, 2D–E: pl1) is a heavily folded spiral and bears few 4–9-µm-long spines ($\bar{x}$ = 7 µm; n = 5). The second plate (Fig. 2C, D–E: pl2) is 32 µm long, and also shows numerous folds and bears a few spines of 4–5 µm long ($\bar{x}$ = 4 µm; n = 4). The spines of the structure connecting both plates are 1–2 µm long ($\bar{x}$ = 1 µm; n = 8).

The two elongated ovaries lie at midbody. The oocytes are organised in a row, increasing in diameter from the most proximal to the most distal one. The ovaries are flanked by the vitellaria (Fig. 2A: vi), which extend from behind the eyes to the caudal body end. The female duct receives the oviducts and opens into the female atrium through a strong sphincter. The caudally-located bursa is weakly muscular and contains sperm. The bursal stalk is very muscular and connects the bursa with the female atrium.

Itaipusa novacaledonica Diez, Schockaert, Reygel & Artois sp. n.

(Fig. 3)

urn:lsid:zoobank.org:act:9433D2B5-29ED-40E6-8DB3-7786947F4C94

Itaipusa n. sp. 2 in Tessens *et al.* (2014)

Material and distribution. Observations on live specimens. Two whole mounts, one of which is designated holotype (FMNH https://id.luomus.fi/KV.647), the other in HU (XIII.3.07), and one serially-sectioned specimen (HU XIII.3.08), collected in Anse Vata Bay (22°18'19"S; 166°26'50"E) (Type Locality), Nouméa, New Caledonia (October 22, 2003), on algae (*Ulva*-like) and sediment taken from rocks in the mouth of a small river.

Etymology. Species named after New Caledonia, where the material was collected.

Diagnosis. Species of *Itaipusa* with a cirrus with two longitudinal rows of triangular spines. One row is inverted U-shaped and ±136 µm long, the other is M-shaped and ±193 µm long. Spines ±3 µm long in both rows, slightly larger at one of the ends (±5 µm long). Distally, the male duct opens in a penis papilla, that is partially sclerotised.

Description. The specimens are ±1 mm long, translucent, with a pair of rounded eyes. Habitus and general morphology do not deviate from other species of *Itaipusa* described above. The proboscis is about 20% of the body length in the live specimens. Basophilic and eosinophilic glands open into the proboscis through its caudal wall. Two pairs of integument retractors were observed: a ventral and a dorsal one. Other muscles were not observed.

The morphology of the pharynx does not differ from that of *I. divae*. It is located at 40% and its diameter is 15% of the body length. Three types of glands open in the distal part of the pharynx lumen: two eosinophilic ones (filled with a coarse-grained or a fine-grained secretion), and basophilic glands with a coarse-grained secretion.

A pair of testes is located antero-lateral to the pharynx. Caudally from the pharynx the vasa deferentia form a pair of seminal vesicles. The seminal vesicles (Fig. 3A & 3C: sv) fuse to form the seminal duct just before entering the copulatory bulb. The seminal vesicles and seminal duct are lined by a nucleated epithelium and surrounded by an external longitudinal muscle layer. The atrial organs are located in the caudal body fourth. The copulatory bulb is 168–196 µm long ($\bar{x}$ = 182 µm; n = 2) and surrounded by an external, longitudinal muscle layer and a thick, internal circular muscle layer. The seminal duct is situated in the proximal half of the copulatory bulb. Where the seminal duct opens into the cirrus, filiform prostate glands containing a coarse-grained eosinophilic secretion also enter the cirrus (Fig. 3A & 3C: pv). The armature of the cirrus (Fig. 3A–C: ci, 3D) consists of two longitudinal spiny rows: one row is M-shaped and 145–240 µm long ($\bar{x}$ = 193 µm; n = 2) (Fig. 3B & 3D: spr1) and the other one is invert U-shaped and 134–138 µm long ($\bar{x}$ = 136 µm; n = 2) (Fig. 3B & 3D: spr2). In both rows, the triangular spines are 2–4 µm long ($\bar{x}$ = 3 µm; n = 2), reaching up to 5 µm at one of the ends. The rows of spines are conspicuous in the distal part of the cirrus, but less noticeable in the more proximal part. The copulatory bulb opens distally in a penis papilla (Fig. 3B: pp), which is partially sclerotised. A number of glands (Fig. 3B: gl) containing fine-grained eosinophilic secretion open distally into the penis papilla.

The elongated ovaries (Fig. 3A: ov) lie beside the copulatory bulb. The oviducts open into the sperm-containing female duct. The female duct (Fig. 3A: fd) opens into the female atrium through a strong sphincter (Fig. 3A: sph1). The walls of the female atrium (Fig. 3A: fa) are weakly muscular. The bursal stalk (Fig. 3A: bs) is tubular in one

specimen and swollen in a second one. It is surrounded by two strong and folded muscle layer consisting of external circular and internal longitudinal muscles. It connects with the caudally-located bursa (Fig. 3A: b), which is lined by feeble circular muscles. The uterus (Fig. 3A: ut) is oriented forward and is surrounded by a sphincter more or less in its midpart (Fig. 3A: sph2).

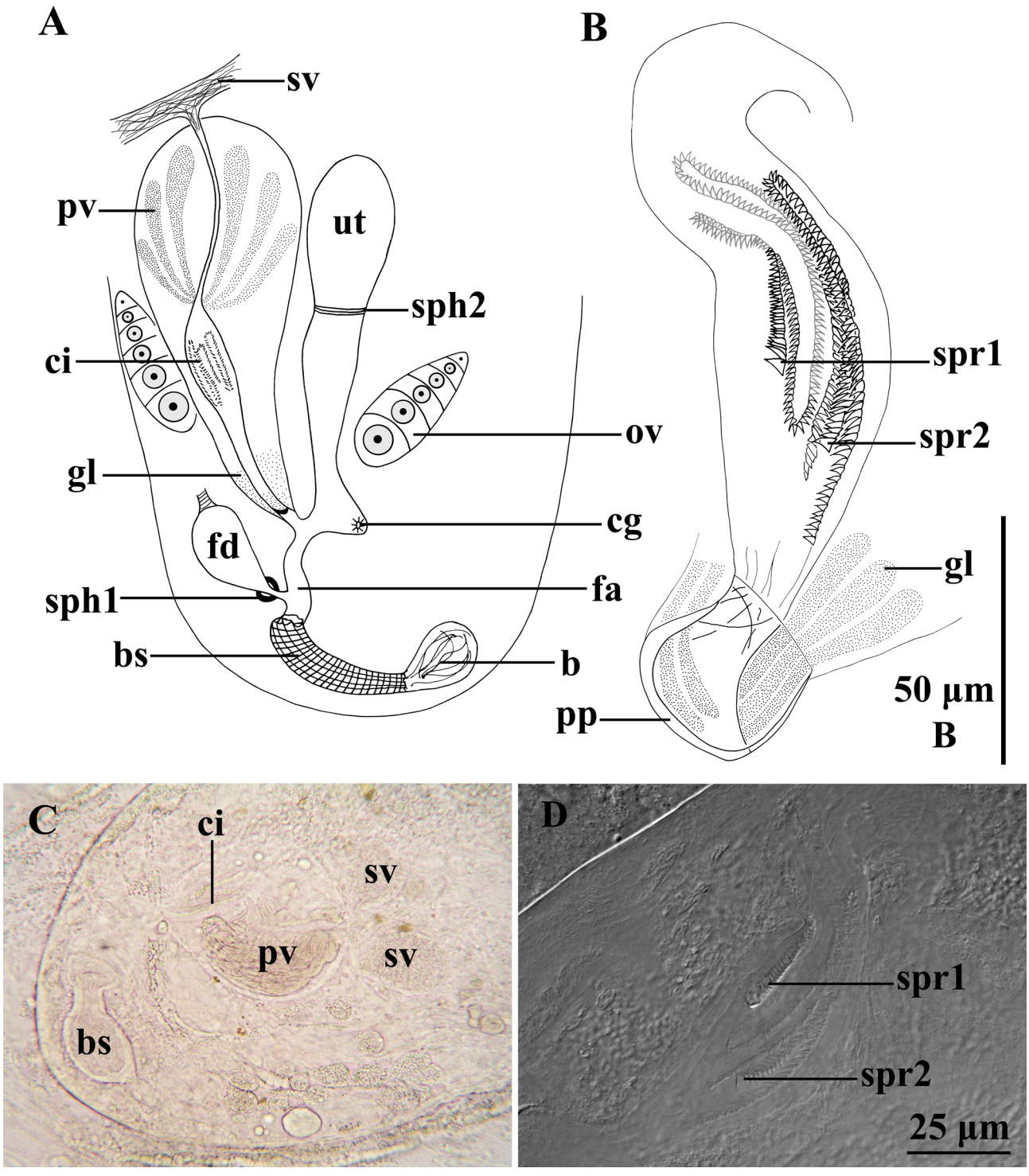

FIGURE 3. *Itaipusa novacaledonica* **sp. n.**. A & C, male and female systems (from a live animal). B & D, cirrus and penis papilla (from the holotype). A–B & D with proximal end toward top of figure, C with distal end toward left of figure.

***Reinhardorhynchus* Diez, Monnens & Artois gen. n.**
urn:lsid:zoobank.org:act:02DC1CAC-6389-459E-B933-42E9647E307E

Diagnosis. Representative of Koinocystididae with a proboscis with a juncture sphincter. Copulatory bulb of the conjuncta duplex-type, except in *R. hexacornutus* **sp. n.** which has a copulatory bulb of the divisa duplex-type. Copulatory organ with an armed or unarmed cirrus. Some species also with a papillary cirrus in the copulatory bulb and one to six accessory hooks distally.

Etymology. In honour of the late Prof. Dr. Reinhard Rieger, for his enormous contribution to turbellarian research.

Type species. *Reinhardorhynchus riegeri* (Karling, 1978) **comb. n.**, here designated.

Other species. *Reinhardorhynchus anamariae* **sp. n.**, *R. beatrizae* **sp. n.**, *R. bispina* (Karling, 1980) **comb. n.**, *R. curvicirra* (Karling, 1980) **comb. n.**, *R. evelinae* (Marcus, 1954) **comb. n.**, *R. hexacornutus* **sp. n.**, *R. pacificus* **sp. n.**, *R. renei* (Reygel, Willems & Artois, 2011) **comb. n.**, *R. riae* **sp. n.**, *R. ruffinjonesi* (Karling, 1978) **comb. n.**, *R. scotica* (Karling, 1954) **comb. n.**, *R. soror* **sp. n.**, *R. tahitiensis* **sp. n.**, *R. unicornis* **sp. n**., and *R. variodentata* (Karling, Mack-Fira & Dörjes, 1972) **comb. n.**

***Reinhardorhynchus riegeri* (Karling, 1978) comb. n.**
(Fig. 4)

Known distribution. Tuckers Town Cove (Type Locality) and Mullet Bay, Rock Hill, Bermuda (Karling 1978).

New records and material. Observations on live specimens. Seven whole mounts (HU XIII.3.08–XIII.3.14) and five serially-sectioned specimens (HU XIII.3.15–XIII.3.19) from Guardalavaca (21°07'32"N; 75°49'39"W), Banes, Holguín, Cuba (February 28, 2017), sandy bottoms and fine-grained sand, in beds of *Syringodium filiforme*, intertidal up to 0.2 m deep, salinity 35 ‰.

Description. Habitus and general organisation of the newly-collected specimens as described by Karling (1978). Specimens unpigmented, 1.4–2 mm long ($\bar{x}$ = 1.8 mm; n = 6), with a pair eyes. The syncytial epidermis is 4 µm thick, fully ciliated. Cilia about 4 µm long. It includes two types of vacuoles: translucent empty ones and others filled with dark granules. Rhabdites present all over the epidermis, 1–2 µm long, some located at the epidermis' surface, others deeply embedded within the epidermis.

The proboscis represents about 10% of the body length in live specimens. It has the typical koinocystidid morphology (see Brunet 1972; Karling 1980), with a strong juncture sphincter and does not differ from that of other species of *Reinhardorhynchus* **gen. n.** (see the description of the proboscis of *R. riae* **sp. n.** below). Only two pairs of integument retractors were observed: a ventral and a dorsal one. The exact number of fixators, dilatators and proboscis retractors could not be determined. The proboscis pore is closed by a sphincter.

The pharynx is located at 30%; its general morphology is as described for *R. riae* **sp. n.** (see below). However, a sphincter around the mouth was not observed. Three types of glands open in the distal part of the pharynx lumen: two eosinophilic ones (coarse-grained and medium-coarse grained, respectively) and a coarse-grained basophilic one.

The two testes are located at both the sides of the pharynx. Each of them is connected to a seminal vesicle by a vas deferens. The seminal vesicles fuse proximally from the copulatory bulb, forming a short seminal duct. The copulatory bulb encompasses the prostate vesicle, two spiny cirri, and two distal hooks. The ejaculatory cirrus (terminology of Karling 1978) (Fig. 4A: ci, 4B) is 50–77 µm long ($\bar{x}$ = 64 µm; n = 4). It is armed with numerous small spines of ± 7 µm long at one side and a group of larger spines 6–17 µm long ($\bar{x}$ = 10 µm; n = 5) at the other. The papillary cirrus (terminology of Karling 1978) (Fig. 4A: pc, 4C) is 110–129 µm long ($\bar{x}$ = 117 µm; n = 7). Its proximal half is provided with ±2-µm-long triangular spines (Fig. 4C: sp1), which in the distal half are 5–8 µm long ($\bar{x}$ = 7 µm; n = 13) (Fig. 4C: sp2). The two larger, strongly sclerotised hooks, which are attached to the wall of the male duct, differ from each other in size. The larger hook (Fig. 4A: h1, 4D) is located next to the papillary cirrus and is 99–120 µm long ($\bar{x}$ = 107 µm; n = 7). Its proximal base is extremely asymmetrical. The smaller one (Fig. 4A: h2; 4E) has a less pronounced asymmetrical base. It is positioned near the proximal end of the ejaculatory cirrus and measures 40–63 µm ($\bar{x}$ = 56 µm; n = 5).

Two elongated ovaries are situated rostral to the copulatory bulb. The oocytes are arranged in a row, increasing in diameter from the most proximal to the most distal one. The female duct receives the pair of oviducts proximally and opens into a distally located bursa through a strong sphincter. Embryos (4–5) without a surrounding shell were observed in some specimens, suggesting the species is (ovo-) viviparous.

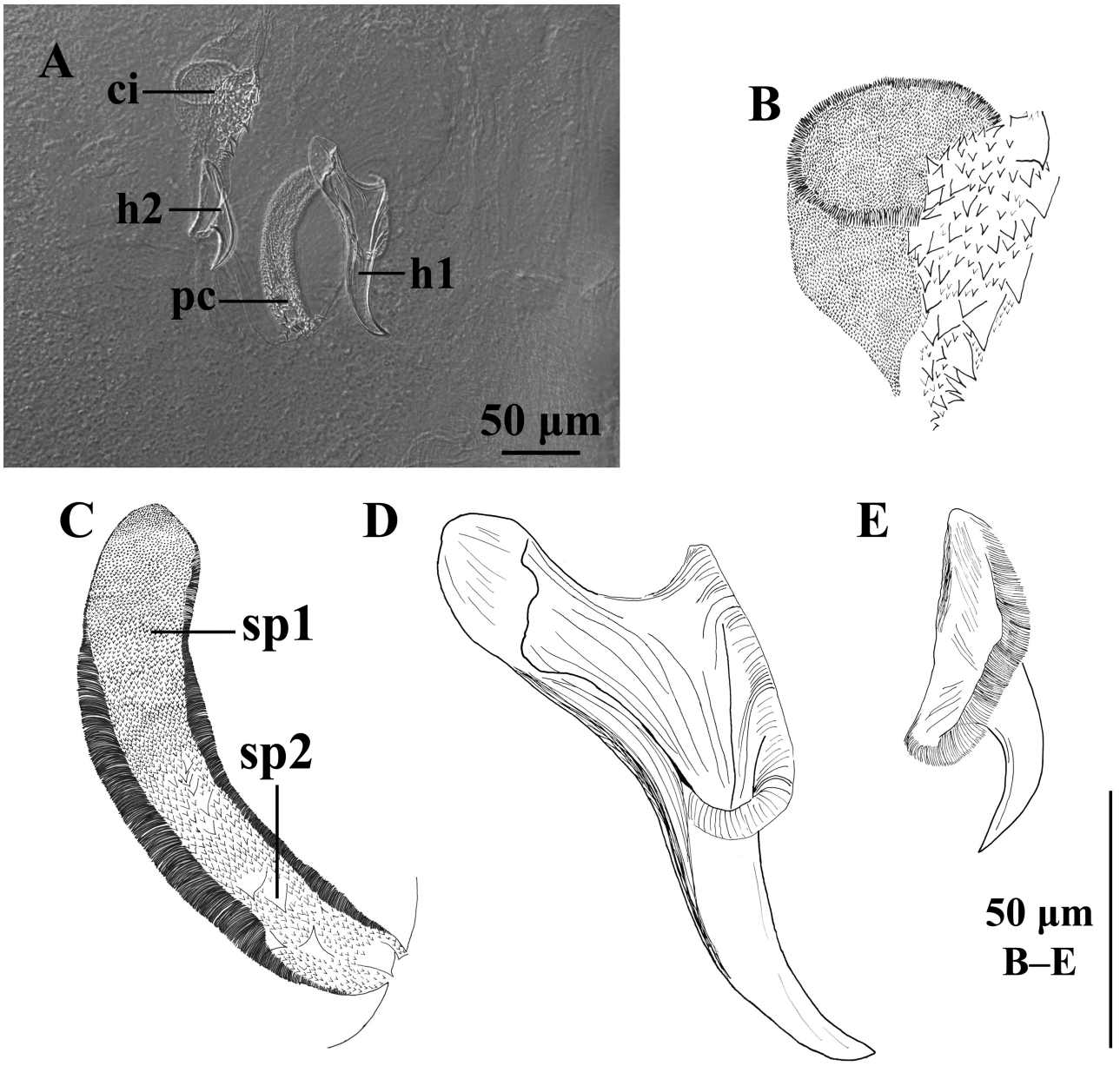

FIGURE 4. *Reinhardorhynchus riegeri* (Karling, 1978) **comb. n**. A, sclerotised structures of the copulatory bulb. B, ejaculatory cirrus. C, papillary cirrus. D, larger hook. E, smaller hook. All with proximal end toward top of figure.

***Reinhardorhynchus ruffinjonesi* (Karling, 1978) comb. n.**
(Fig. 5–6)

Known distribution. St. George, Tobacco Bay, Bermuda (Type Locality) (Karling 1978).

New records and material. Observations on live specimens, whole mounted afterwards. Two whole mounts from Las Sardinas (19°56'24"N; 76°46'41"W), Guamá, Santiago de Cuba, Cuba (June 22, 2017), on the alga *Dictyota menstrualis* with some sand, 0.5 m deep, salinity 35 ‰ (HU XIII.3.20–XIII.3.21). Two whole mounts from Siboney (19°57'34"N; 75°42'07"W), Santiago de Cuba, Cuba (March 22, 2017), intertidal, sand with organic matter, salinity 35 ‰ (HU XIII.3.22–XIII.3.23). Eight whole mounts from Bueycabón (19°57'38"N; 76°57'28"W), Santiago de Cuba, Cuba (February 6 & 21, 2018), fine-grained sand rich in organic matter, 0.5 m deep, salinity 33 ‰ (HU XIII.3.24–XIII.3.31). Two whole mounts from Punta Culebra (8°54'57"N; 79°31'50"W), Panama (December 13, 2011), intertidal, coarse to fine sand collected in front of the Smithsonian Tropical Research Institution (USNM 1642503–1642504). One whole mount (USNM 1642505) from Bahía Can Can (09°32'23"N; 79°40'31"W), near Portobello, Panama (March 3, 2016), intertidal, very coarse sand. One whole mount from a beach at Araça Bay (23°48'47"S; 45°24'31"W), São Sebastião, São Paulo, Brazil (October 26, 2012), intertidal (HU XIII.3.32).

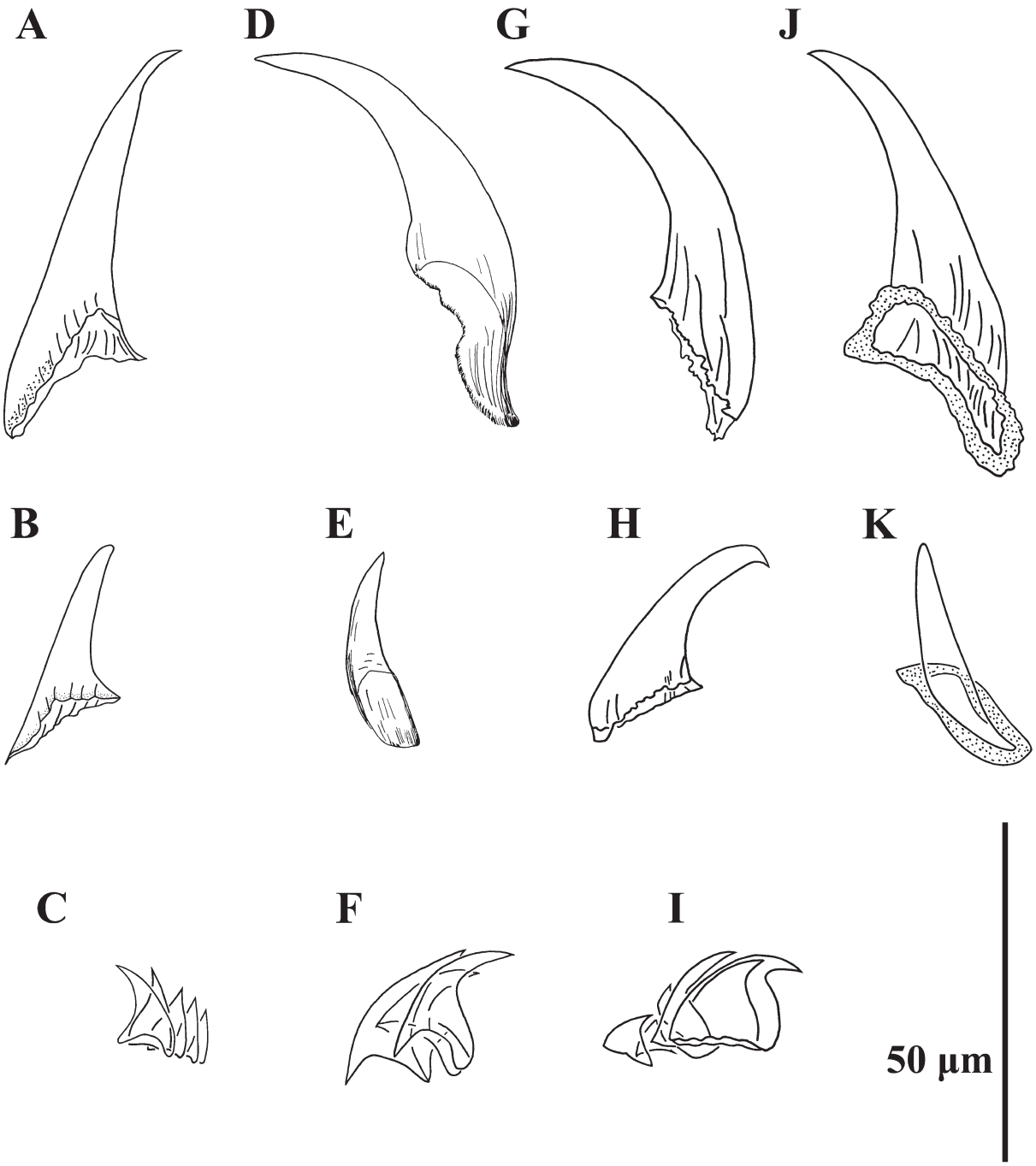

FIGURE 5. *Reinhardorhynchus ruffinjonesi* (Karling, 1978) **comb. n.**. A, D, G & J, larger hook [specimens from Cuba, Punta Culebra (Panama), Brazil, and Bahía Can Can (Panama), respectively]. B, E, H & K, smaller hook [specimens from Cuba, Punta Culebra (Panama), Brazil, and Bahía Can Can (Panama), respectively]. C, F & I, distal spines of the cirrus [specimens from Cuba, Punta Culebra (Panama), and Brazil, respectively]. All with distal end toward top of figure.

Remarks. According to Karling (1978), *R. ruffinjonesi* **comb. n.** is characterised by a cirrus with small sclerotised dots, a curved row of scale-like spines (15 µm maximum length), and two distal hooks (72 µm and 45 µm long, respectively). In addition, Karling (1978) describes a "small, easily overlooked spiny diverticulum" in the cirrus. Our re-examination of the holotype of *R. ruffinjonesi* **comb. n.** (Fig. 6A–B) reveals that the "small sclerotised dots" of the cirrus described by Karling (1978) are in fact triangular spines of 1–2 µm long ($\bar{x}$ = 2 µm; n = 20). These spines are larger in the "spiny diverticulum" (4 µm; n = 9). The curved belt described by Karling (1978), consists of a proximal part of large and scale-like spines, followed by a middle part of small spines, and a distal part of strong, more or less triangular spines. In the holotype, the spines in the proximal part of the row (Fig. 6A: cps) are 6–9 µm

long ($\bar{x}$ = 8 µm; n = 15), smaller toward the distal end. The spines of the middle part are 1–2-µm-long ($\bar{x}$ = 2 µm; n = 10). In the distal part of the belt (Fig. 6A: cds), the spines are 4–20 µm long ($\bar{x}$ = 13 µm; n = 20), the most distal ones of which are curved (Fig. 6B: ds) and 13–21 µm long ($\bar{x}$ = 18 µm; n = 5).

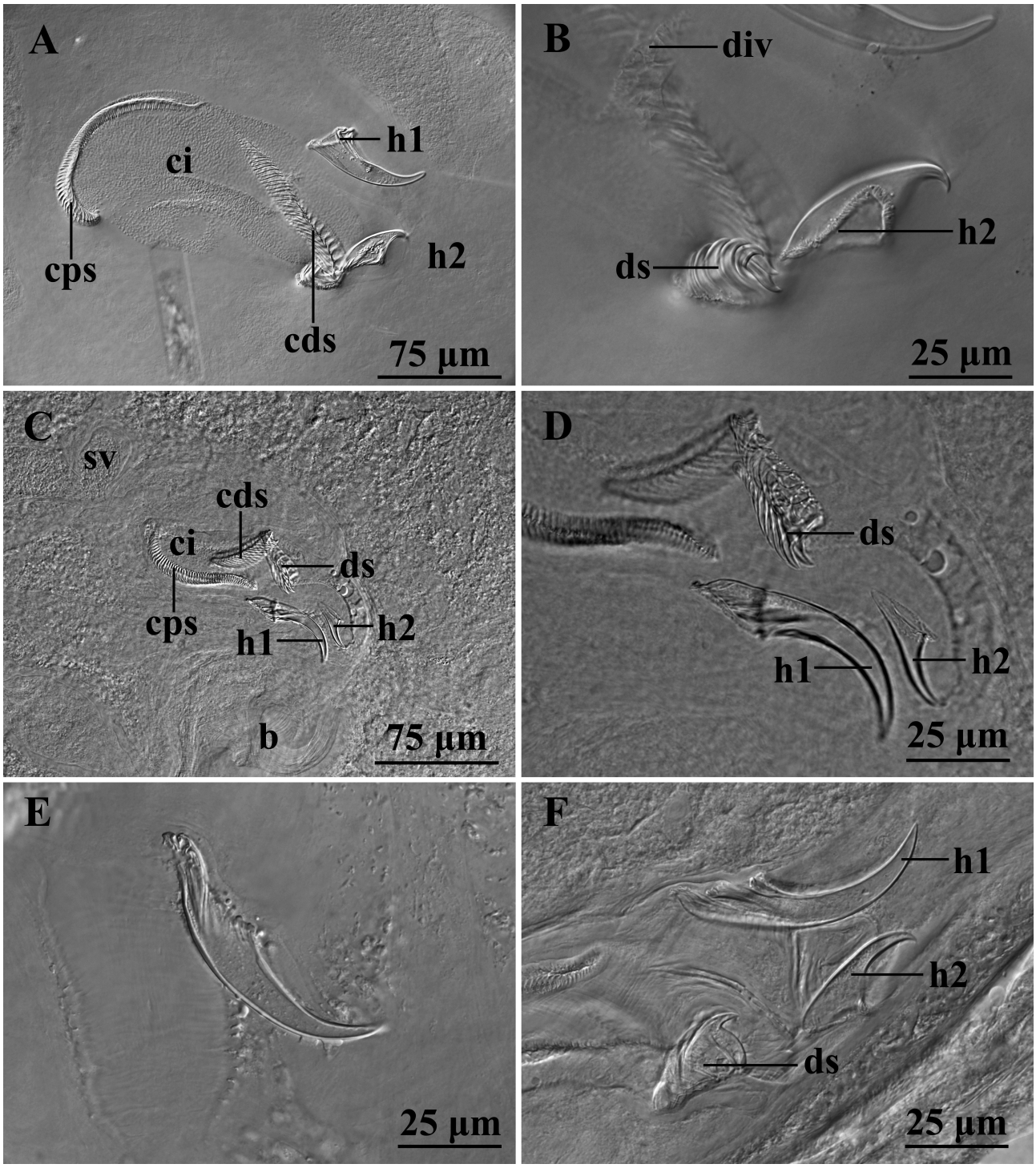

FIGURE 6. *Reinhardorhynchus ruffinjonesi* (Karling, 1978) **comb. n.**. A–F, hard structures of the copulatory bulb. A–B, from the holotype. C–D, specimen from Cuba. E, specimen from Punta Culebra (Panama). F, specimen from Brazil. E oriented with proximal end toward top of figure; the others with proximal end toward left of figure.

In the specimens from Cuba (Fig. 5A–C & 6C–D), the copulatory bulb is 162–220 µm long ($\bar{x}$ = 192 µm; n = 6). The cirrus (Fig. 6C: ci) is armed with triangular spines of 1–2 µm long ($\bar{x}$ = 2 µm; n = 27). The spiny belt is 149–247 µm long ($\bar{x}$ = 176 µm; n = 10). In the proximal part of the belt (Fig. 6C: cps), the spines are 5–9 µm long ($\bar{x}$ = 7 µm; n = 31), with the size of the spines decreasing distally. In the middle part, the spines are 2–3-µm-long

($\bar{x}$ = 3 µm; n = 25). In the distal part (Fig. 6C: cds), the spines are 6–18 µm long ($\bar{x}$ = 12 µm; n = 26), the most distal ones of which (Fig. 5C, 6C–D: ds) are 6–15 µm long ($\bar{x}$ = 12 µm; n = 9). The distal sclerotised hooks differ in size. The larger hook (Fig. 5A, 6C–D: h1) is 46–60 µm long ($\bar{x}$ = 54 µm; n = 10) and 15–27 µm wide at its base ($\bar{x}$ = 21 µm; n = 10). The smaller hook (Fig. 5B, 6C–D: h2) is 21–32 µm long ($\bar{x}$ = 27 µm; n = 10) and 11–21 µm wide at its base ($\bar{x}$ = 17 µm; n = 10).

In the specimens from Punta Culebra (Panama) (Fig. 5D–F, 6E) the copulatory bulb is 339–348 µm long ($\bar{x}$ = 344 µm; n = 2). The cirrus is armed with 2–3-µm-long triangular spines ($\bar{x}$ = 3 µm; n = 20). The belt of spines is 253–366 µm long ($\bar{x}$ = 260 µm; n = 2), with spines of 3–13 µm long ($\bar{x}$ = 8 µm; n = 26) in the proximal part and of 9–23-µm-long ($\bar{x}$ = 17 µm; n = 16) in the distal part. The most distal spines of the posterior part (Fig. 5F) are 20–21 µm long ($\bar{x}$ = 21 µm; n = 3) and shark-tooth shaped, with a broad base, curved, and ending in a sharp tip. The larger distal hook (Fig. 5D & 6E) is 62 µm long (n = 2) and 33–34 µm wide at its base (n = 2). The smaller hook (Fig. 5E) is 26–33 µm long ($\bar{x}$ = 30 µm; n = 2) and 15–16 µm wide at its base (n = 2).

In the specimen from Brazil (Fig. 5G–I, 6F) the copulatory bulb is 165 µm long. No triangular spines were observed in the cirrus. The spiny belt is 165 µm long, with spines of 3–6 µm in length ($\bar{x}$ = 5 µm; n = 14) in the proximal part and a of 3–15 µm in length ($\bar{x}$ = 9 µm; n = 14) in the distal part. The most distal spines (Fig. 5I, 6F: ds) of the distal part are shark-tooth shaped, with a broad base and a sharp curved tip, 15–20 µm long ($\bar{x}$ = 18 µm; n = 3). The larger of the distal hooks (Fig. 5G, 6F: h1) is 60 µm long and 22 µm wide at its base. The smaller hook (Fig. 5H, 6F: h2) is 33 µm long and 16 µm wide at its base.

The specimen from Bahía Can Can (Panama) (Fig. 5J–K) has a copulatory bulb of 310 µm long. The cirrus is armed with 2–3-µm-long triangular spines ($\bar{x}$ = 2 µm; n = 20). The belt of spines is 251 µm long, with spines of 4–10 µm in length ($\bar{x}$ = 7 µm; n = 15) in the proximal part and of 2–18 µm in length ($\bar{x}$ = 10 µm; n = 27) in the distal part. The most distal spines of the distal part are triangular and curved, 16–24 µm long ($\bar{x}$ = 18 µm; n = 4). The larger of the distal hooks (Fig. 5J) is 56 µm long and 30 µm wide at its base. The smaller hook (Fig. 5K) is 29 µm long and 20 µm wide at its base, slightly curved, ending in a rounded tip.

Reinhardorhynchus riae Diez, Reygel & Artois sp. n.

(Fig. 7–8)

urn:lsid:zoobank.org:act:65D70F61-74DB-458B-B5EA-18AB0F972270

Material and distribution. Observations on live specimens. Three whole mounts, one designated holotype (FMNH https://id.luomus.fi/KV.651), the others reference material (HU XIII.3.33–XIII.3.34), and one serially-sectioned specimen (HU XIII.3.35) collected in Mala (Lanzarote, Canary Islands) (29°05'01"N; 13°26'59"W), in front of "Cuevita de Mala" (October 10, 2011), sand patch under loose macroalgae, coarse shell gravel, very clean, 12 m deep (Type Locality). One whole mount from the same locality (HU XIII.3.36) (October 8, 2011), medium-fine, calcareous sand from a large parch among rocks, poorly-oxygenated redox layer just below surface, 20 m deep. Four whole mounts and seven serially-sectioned specimens (HU XIII.3.37–XIII.3.47) collected in a sheltered beach, a bit south of Orzola (Lanzarote, Canary Islands) (29°13'23"N; 13°27'05"W) (October 6, 2011), medium-coarse sand, with holes from burrowing animals, taken at low tide, just below the water line. One whole mount (HU XIII.3.48) collected at the same locality (October 7, 2011), sample taken 0.4–0.5 m deep, coarse sand with lava rocks scattered around. Salinity 35 ‰ in all the localities. One whole mount (HU XIII.3.49) from Punta Negra (40°57'12"N, 08°13'43"E), Stintino, Sardinia, Italia (September 2018), on silty algae, 0.5 m deep, salinity 40 ‰.

Etymology. Species dedicated to Ria Vanderspikken (Hasselt University), in acknowledgement of all her help in organising the sampling campaigns, archiving of literature and taking care of the HU specimen collection.

Diagnosis. Species of *Reinhardorhynchus* **gen. n.** with a copulatory organ armed with two transverse spiny belts, a penis papilla, and two distal hooks. Prostate vesicle enclosed in a muscular bulb. This bulb ends in a pseudocuticular plate and is armed with two spiny rows being ±72 µm and ±55 µm long, respectively. Spines ±3 µm long at the sides and ±9 µm long in the middle of the rows. Penis papilla covered by a pseudocuticula, which carries the distal hooks. Hooks flattened, with a broad and rounded distal end, ±14 µm long and ±32 µm wide at their base. Female duct bipartite: proximal compartment lined by a nucleated epithelium and without muscles, distal compartment surrounded by a thick layer of circular muscles.

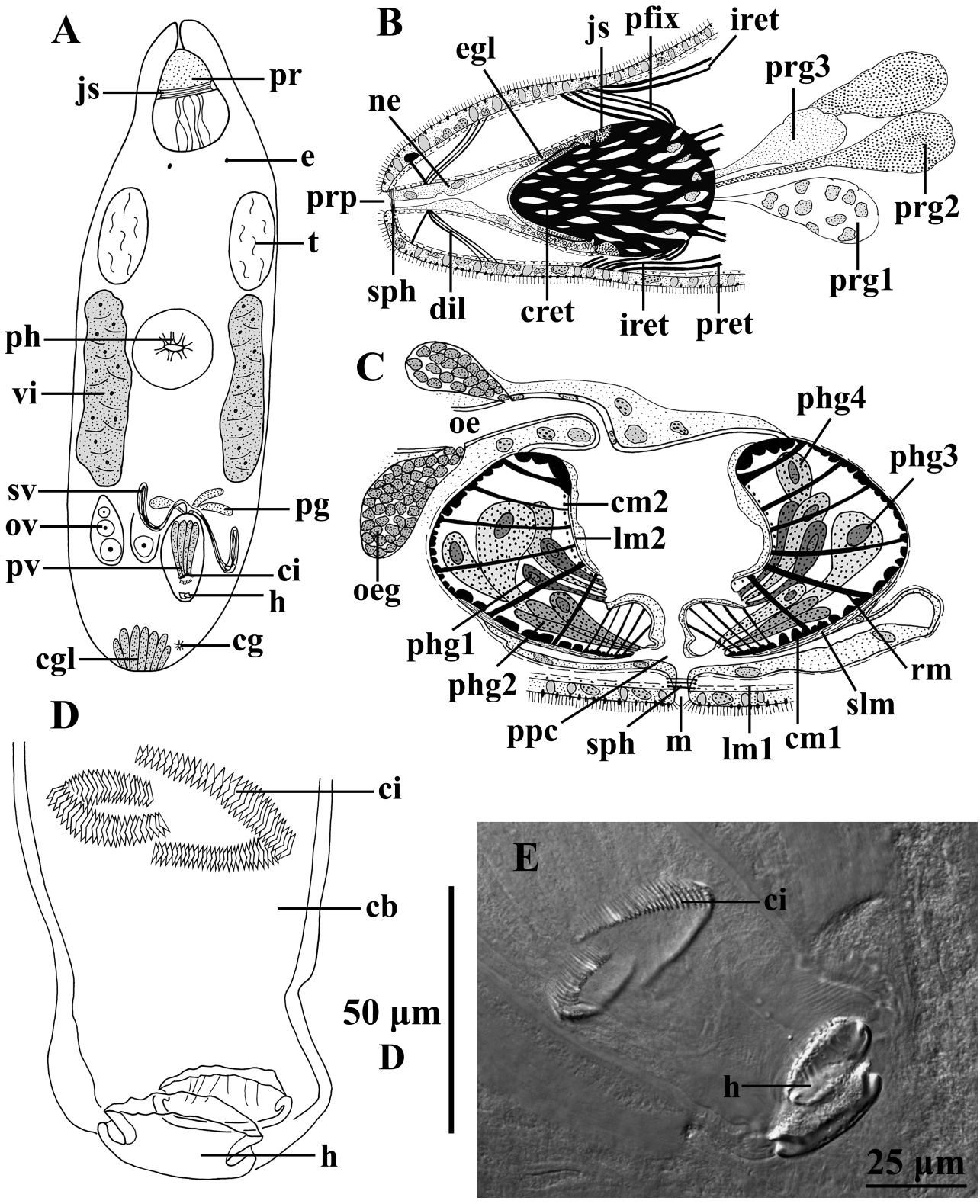

FIGURE 7. *Reinhardorhynchus riae* **sp. n.**. A, general organisation (from a live animal). B, sagittal reconstruction of the proboscis from the left hand side. C, sagittal reconstruction of the pharynx from the right hand side. D–E, cirrus and hooks (from the holotype). D–E with proximal end toward top of figure.

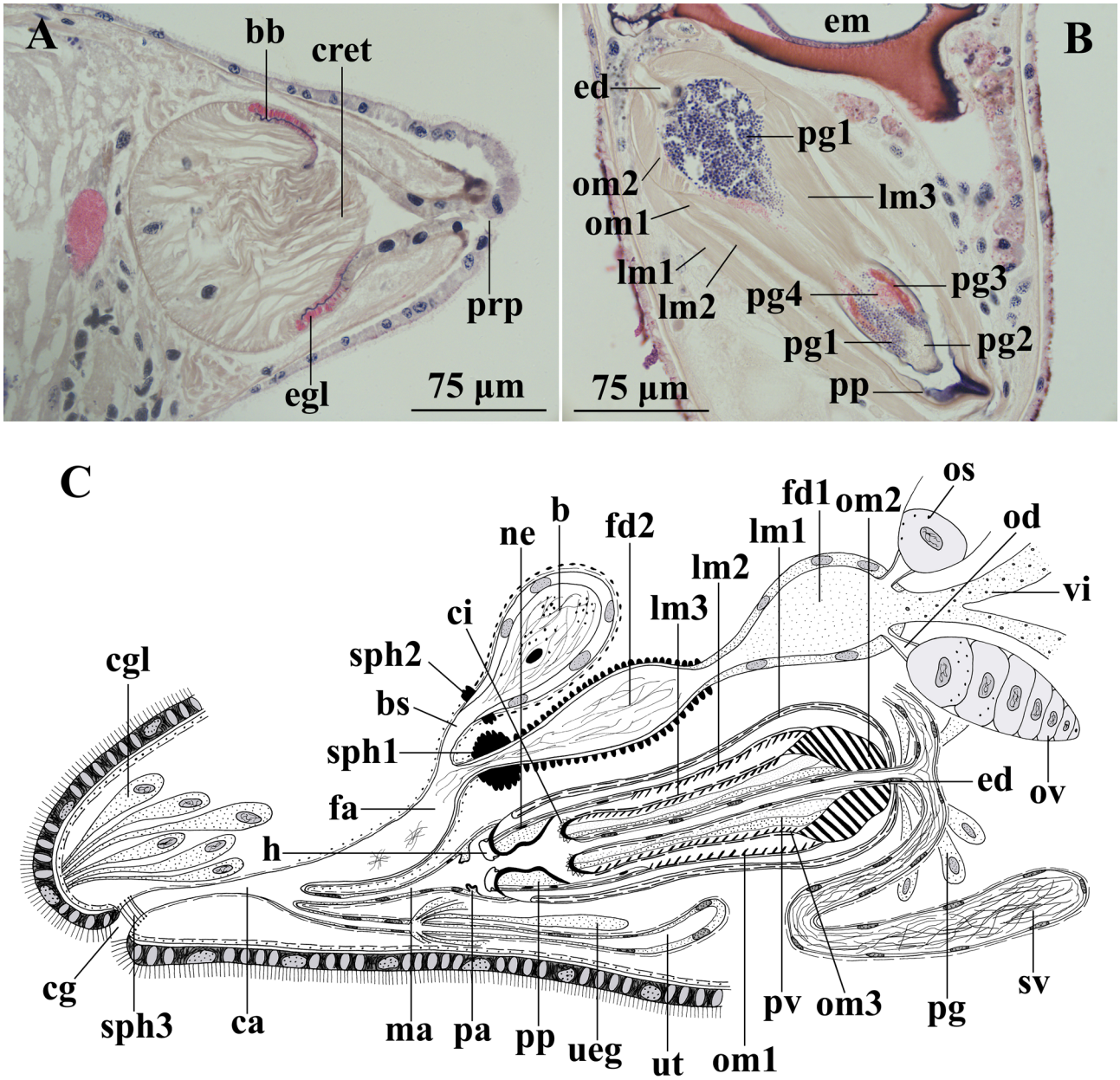

FIGURE 8. *Reinhardorhynchus riae* **sp. n.**. A, proboscis (sagittal section). B, copulatory bulb (sagittal section). C, sagittal reconstruction of the genital system from the right hand side.

Description. The specimens are 1.8–3 mm long ($\bar{x}$ = 2.2 mm; n = 8), translucent, with a pair of eyes (Fig. 7A: e). The coloration of the specimens is due to pinkish glands within the parenchyma. The syncytial epidermis is 7–8 µm thick and completely ciliated; cilia ±4 µm long. The epidermis contains many vacuoles, which are either empty or filled with a dark secretion (coarse- or fine-grained). The 1–2 µm-long rhabdites are located near the apical surface of the epidermis. Caudally in the body some eosinophilic glands occur (Fig. 7A & 8C: cgl).

The proboscis (Fig. 7A: pr, 7B, 8A) is ±15% of the body length and is of the characteristic koinocystidid construction (see Brunet 1972; Karling 1980), displaying a strong juncture sphincter (7A–B: js). The proboscis sheath is surrounded by a nucleated epithelium (Fig. 7B: ne), which is continuous with the epithelium surrounding the proboscis cone. Both epithelia contain oval to circular-shaped glands (reddish stained) (Fig. 7B & 8A: egl). The epithelium surrounding the cone is lined by a brush border (Fig. 8A: bb). Three kinds of glands open through the caudal wall of the proboscis: coarse-grained basophilic ones (dark stained) (Fig. 7B: prg1), coarse-grained eosinophilic ones (pinkish stained) (Fig. 7B: prg2), and fine-grained eosinophilic ones (brownish stained) (Fig. 7B:prg3). The proboscis sheath is surrounded by a layer of circular muscles and a longitudinal one just underneath it. The pro-

boscis pore (Fig. 7B & 8A: prp) is surrounded by a sphincter (Fig. 7B: sph). The cone retractors are well developed (Fig. 7B & 8A: cret). The exact number of proboscis fixators (Fig. 7B: pfix) and dilatators (Fig. 7B: dil) could not be determined. Two pairs of proboscis retractors (Fig. 7B: pret) could be distinguished, however it is not clear if there are more. Two pairs of integument retractors were observed: a ventral and a dorsal one (Fig. 7B: iret).

The pharynx (Fig. 7A: ph, 7C) has a diameter of 15% of the body length in the live specimens, situated at 40%. The prepharyngeal cavity (Fig. 7C: ppc) is lined by a nucleated epithelium and surrounded by an external layer of longitudinal muscles. The mouth (Fig. 7C: m) is surrounded by a sphincter (Fig. 7C: sph). Four types of glands containing a coarse-grained secretion open into the pharynx lumen: dark brown (Fig. 7C: phg1) and pinkish (Fig. 7C: phg2) eosinophilic glands most distally, and brownish eosinophilic (Fig. 7C: phg3) and basophilic glands (Fig. 7C: phg4) more proximally. Coarse-grained basophilic glands (Minot's glands) (Fig. 7C: oeg) open into the oesophagus (Fig. 7C: oe). The musculature of the pharynx consists of a longitudinal muscle layer outside of the septum (Fig. 7C: lm1) and a circular layer just inside of it (Fig. 7C: cm1). These circular muscles are markedly thicker near the proximal and distal tips of the pharynx. The distal opening of the pharynx is lined by a thick layer of longitudinal muscles, which in sagittal section gives the impression of forming a lip-like structure (Fig. 7C: slm). The pharynx lumen is surrounded by an inner circular (Fig. 7C: cm2) and outer longitudinal muscle layer (Fig. 7C: lm2). Radial muscles (Fig. 7C: rm) stretch between the internal and the external walls; the most proximal of these are weaker than the others.

Two testes (Fig. 7A: t) occur latero-rostrally from the pharynx. Caudally from the pharynx, the vasa deferentia form a pair of seminal vesicles (Fig. 7A & 8C: sv). The seminal vesicles are lined by a low, nucleated epithelium and surrounded by an external, longitudinal muscle layer. The seminal vesicles fuse to form a seminal duct just before opening into the copulatory bulb (Fig. 7D: cb), which is located in the caudal body half and represents 15% of the body length in the live specimens. It encompasses the prostate vesicle (Fig. 7A & 8C: pv), the cirrus (Fig. 7A & 7D–E: ci), and two accessory hooks (Fig. 7A, 7D–E & 8C: h). The copulatory bulb ends in a penis papilla (8B–C: pp) and is surrounded by a thick sheath of longitudinal muscles (Fig. 8B–C: lm1). Distally, this muscular sheath is not connected to the penis papilla. A second, internal muscular sheath connects to the proximal part of the prostate vesicle and ends in the penis papilla. This sheath consists of a longitudinal muscle layer (Fig. 8B–C: lm2) and an oblique one just beneath it (Fig. 8B–C: om1). The most distal part of the copulatory bulb is lined by a thin, nucleated epithelium (Fig. 8C: ne), which becomes much thicker and is covered by a sclerotised layer, as a whole forming the penis papilla. The two distal hooks are connected to the distal end of the penis papilla.

The extracapsular prostate glands (Fig. 7A & 8C: pg) open proximally into the copulatory bulb. The prostate vesicle forms a long-drawn muscular bulb. Proximally, it is surrounded by strong oblique muscles (Fig. 8B–C: om2), while over the rest of its length the prostate vesicle is surrounded by an external longitudinal (Fig. 8B–C: lm3) and internal oblique muscle layer (Fig. 8C: om3). The ejaculatory duct (Fig. 8B–C: ed) enters the prostate vesicle through the latter's proximal end and runs axially through it. The duct is lined by a thin nucleated epithelium and surrounded by longitudinal muscles. There are four types of prostate glands: a coarse-grained basophilic one (stained dark purple) (Fig. 8B: pg1), two coarse-grained eosinophilic ones [stained greenish (Fig. 8B: pg2) and reddish (Fig. 8B: pg3), respectively], and an eosinophilic, fine-grained one (stained pinkish) (Fig. 8B: pg4). Distally, these prostate glands open around the distal opening of the ejaculatory duct. The distal tip of the prostate vesicle is covered by a sclerotised layer and armed with teeth, constituting the two spiny rows observed in the live specimens and the whole mounts.

The spiny rows (Fig. 7D–E & 8C: ci) are oriented transversally relative to the copulatory bulb. The larger row is 66–83 μm long ($\bar{x}$ = 72 μm; n = 7), the smaller one 46–65 μm ($\bar{x}$ = 55 μm; n = 7). The triangular spines are smallest at the sides of both rows: 2–4 μm long ($\bar{x}$ = 3 μm; n = 20), compared to 7–12 μm long ($\bar{x}$ = 9 μm; n = 35) in the middle. The distal hooks (Fig. 7A, 7D–E & 8C: h) are similar in length and shape: flattened, distally broad and rounded, 11–20 μm long ($\bar{x}$ = 14 μm; n = 10) and 27–37 μm wide at their base ($\bar{x}$ = 32 μm; n = 10). The male atrium (Fig. 8C: ma) is lined by a low, nucleated epithelium and surrounded by longitudinal muscles. Proximally from the aperture of the ejaculatory duct, the male atrium shows a small, lightly-sclerotised papilla (Fig. 8C: pa). The male atrium opens into the common general atrium (Fig. 8C: ca) through the latter's rostral wall.

The vitellaria (Fig. 7A & 8C: vi) extend along both sides of the body from the level of the testes to the copulatory bulb. The ovaries (Fig. 7A & 8C: ov) are located antero-laterally from the copulatory bulb. The oocytes are organised in a row, increasing in diameter from the most proximal to the most distal one. The most distal oocytes display a number of unidentified black spots (Fig. 8C: os). The oviducts (Fig. 8C: od) are short and not surrounded

by muscles. The female duct is bipartite. The proximal part (Fig. 8C: fd1) is surrounded by a nucleated epithelium, lacks muscles, and narrows towards the second, more distal part (Fig. 8C: fd2). The distal part is lined by a membranous, anucleated epithelium and surrounded by thick, circular muscles. The proximal part receives the broad common vitelloduct and the oviducts and is filled with vitelline material. The distal part contains sperm, hence functioning as seminal receptacle and connects to the female atrium through a strong sphincter (Fig. 8C: sph1). The female atrium (Fig. 8C: fa) also receives the bursal stalk (Fig. 8C: bs), which enters just dorsal to the female duct. The bursa (Fig. 8C: b) is surrounded by an internal longitudinal and external circular muscle layer which continue around the bursal stalk and further around the female atrium. It is lined by a nucleated epithelium, which disappears around the bursal stalk. At the transition between bursa and bursal stalk, a sphincter occurs (Fig. 8C: sph2). The bursa contains disintegrating sperm and different kinds of glandular material in degradation. The female atrium also contains sperm and enters the common genital atrium just dorsal to the opening of the male atrium. The uterus (Fig. 8C: ut) enters the common genital atrium through the latter's rostral wall, ventral to all other systems. The uterus is lined by a nuclear epithelium and is surrounded by a longitudinal muscle layer. Medium-grained eosinophilic uterine glands open into the uterus just proximal to the opening of the female duct (Fig. 8C: ueg). The uterus does not show any sphincters. The common genital atrium is surrounded by longitudinal muscles. An epithelium was not observed and is probably membranous. The common genital atrium opens ventrally and subcaudally through the common gonopore (Fig. 7A & 8C: cg), which is at 95%. This gonopore is surrounded by a sphincter (Fig. 8C: sph3). One live specimen carried two embryos (Fig. 8B: em) not surrounded by a thick egg-shell, suggesting the species is (ovo-)viviparous.

Reinhardorhynchus anamariae Diez, Reygel & Artois sp. n.

(Fig. 9, 12A–C)
urn:lsid:zoobank.org:act:68EBA829-BAD3-4F42-A46E-AC35A1F7F38D

Material and distribution. Observations on live specimens, whole mounted afterwards. Four whole mounts, one of which is designated holotype (FMNH https://id.luomus.fi/KV.648), the others in HU (XIII.3.50; XIII.4.01–XIII.4.02), collected in Bueycabón (19°57'38"N; 76°57'28"W) (Type Locality), Santiago de Cuba, Cuba (February 6, 2018), fine-grained sand with organic matter, 0.5 m deep, salinity 33 ‰.

Etymology. Species dedicated to Prof. Dr. Ana María Suárez Alfonso, researcher at the Marine Research Centre of Havana University, Cuba, specialist in taxonomy and ecology of macroalgae. Awarded with the National Award of Marine Sciences of Cuba (2012).

Diagnosis. Species of *Reinhardorhynchus* **gen. n.** without eyes. Copulatory bulb enclosing a spiny cirrus and two distal hooks. Cirrus armed with rows of spines ±1 μm long and a ±116-μm-long and inverted L-shaped belt of triangular spines. Proximally, the belt bears ±22-μm-long spines, diminishing in length from one end to the other (the proximal largest one is ±42 μm long and the smallest distal one is ±9 μm long). Distally in the belt, the central spines are ±15 μm long; the lateral ones are ±5 μm long. Larger hook ±51 μm long, distally ending in a sharp tip. Smaller hook ±45 μm long, with a blunt distal tip.

Description. Specimens translucent, 0.9–1.4 mm long ($\bar{x}$ = 1.2 mm; n = 4), with pinkish-coloured parenchymal glands, and without eyes. The proboscis (Fig. 9A: pr) is of the typical koinocystidid construction (see Brunet 1972; Karling 1980), possessing a well-developed juncture sphincter; it is 15% of the body length in live specimens. The pharynx (Fig. 9A: ph) has a diameter of 15% of the body length in live specimens and is located at 50%.

The testes (Fig. 9A: t) are rostral to the pharynx. Caudal to the pharynx, the vasa deferentia make up the seminal vesicles. The seminal vesicles fuse to form a short seminal duct just before entering the copulatory bulb. The seminal duct runs through the proximal part of the copulatory bulb and opens into the cirrus. The extracapsular prostate glands open proximally into the copulatory bulb. The oval copulatory bulb is 183–274 μm long ($\bar{x}$ = 222 μm; n = 4). It encompasses the prostate vesicle (Fig. 9B: pv), the spiny cirrus, and two distal hooks. The cirrus (Fig. 9A–B & 12A: ci, 9C, 12B) is armed with rows of spines that are ±1 μm long (Fig. 9C & 12B: sp). Proximally, the rows of spines are oriented longitudinally, while distally they are transversal; these rows join in the middle third of the cirrus. The cirrus includes a belt of large, triangular, hollow spines (Fig. 9C & 12B: cir). This belt has the shape of an inverted L and is 96–129 μm long ($\bar{x}$ = 116 μm; n = 4). The proximal part of the spiny belt is oriented transversally relative to the longitudinal axis of the cirrus, is 31–41 μm long ($\bar{x}$ = 37 μm; n = 4) and includes the largest spines, which are hollow, increasing in diameter from the most proximal to the most distal one. The largest spine

is 37–48 µm long ($\bar{x}$ = 42 µm; n = 4), the rest of the spines are 9–34 µm long ($\bar{x}$ = 22 µm; n = 22). The distal part is oriented longitudinally relative to the axis of the cirrus, measures 65–88 µm ($\bar{x}$ = 79 µm; n = 4), and includes smaller spines than the proximal part. In this part, the spines are larger in the middle (9–18 µm long; $\bar{x}$ = 15 µm; n = 20) than at the sides (2–8 µm long; $\bar{x}$ = 5 µm; n = 25).

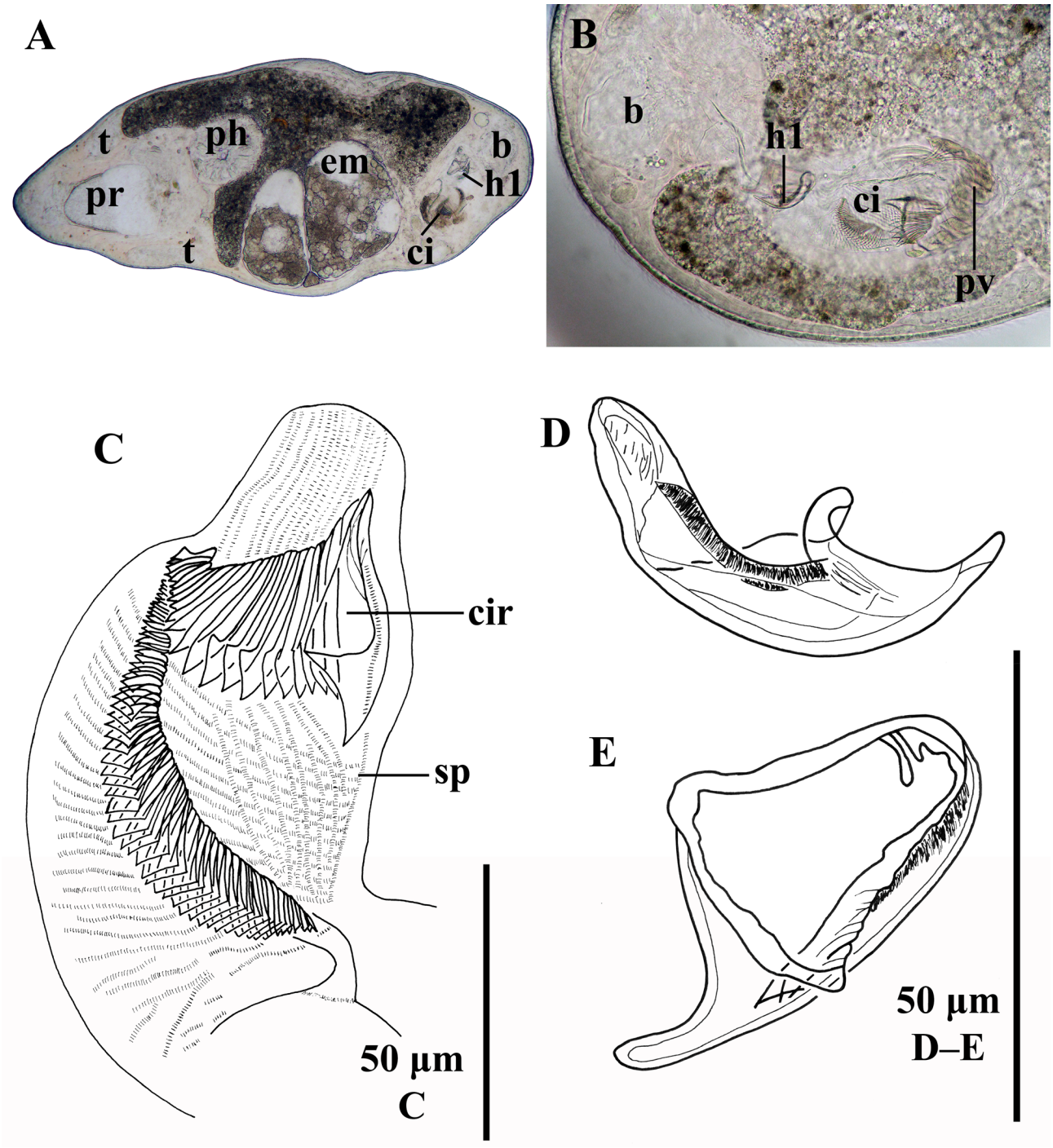

FIGURE 9. *Reinhardorhynchus anamariae* **sp. n.**. A, general organisation. B, caudal body end (both from the live animal). C, cirrus. D, larger hook. E, smaller hook. C–E, from the holotype. C–E with proximal end toward top of figure.

Distally from the cirrus proper, two large hooks are present. The larger hook (Fig. 9A–B, 12A & 12C: h1, 9D) is 48–53 µm long ($\bar{x}$ = 51 µm; n = 4), with an asymmetrical base of 29–36 µm in width ($\bar{x}$ = 31 µm; n = 4). The hook ends in a sharp, distal tip. The smaller hook (Fig. 9E, 12A & 12C: h2) is 44–46 µm long ($\bar{x}$ = 45 µm; n = 4), with a more or less triangular base, 31–35 µm wide ($\bar{x}$ = 33 µm; n = 4), and the distal tip curved and rounded.

The elongated ovaries are lying rostral to the copulatory bulb. The oocytes are organised in a row, increasing in

diameter from the most proximal to the most distal one. The female duct (Fig. 12A: fd) contains sperm and opens into the globular, caudally-located bursa (Fig. 9A–B & 12A: b) through a strong sphincter (Fig. 12A: sph). The common gonopore opens at 90%. One live specimen carried two embryos (Fig. 9A: em) that are not surrounded by a thick egg-shell, suggesting the species is (ovo-)viviparous.

Reinhardorhynchus beatrizae Diez, Aguirre, Reygel & Artois sp. n.

(Fig. 10)

urn:lsid:zoobank.org:act:7191A493-CCA1-421D-88D5-99AD3D7E5705

Material and distribution. Observations on live specimens, whole mounted afterwards. Two whole mounts from Las Sardinas (19°56'24"N; 76°46'41"W) (Type Locality), Guamá, Santiago de Cuba, Cuba (June 22, 2016), one of which is designated holotype (FMNH https://id.luomus.fi/KV.649), the other one in HU (XIII.4.03), silty sand in rock pools protected from wave action, 0.3 m deep, salinity 33 ‰. Six whole mounts and three serially-sectioned specimens (in poor conditions) from Siboney (19°57'34"N; 75°42'07"W), Santiago de Cuba, Cuba (September 4, 2016; March 22 & June 5, 2017), intertidal (upper 10 cm of fine-grained sand) up to 0.5 m deep (fine-grained sand rich in organic matter), salinity 33–35 ‰ (HU XIII.4.04–XIII.4.13). Two whole mounts from Bueycabón (19°57'38"N; 76°57'28"W), Santiago de Cuba, Cuba (February 6 & 21, 2018), fine-grained sand rich in organic matter, 0.5 m deep, salinity 33 ‰ (HU XIII.4.14–XIII.4.15).

Etymology. Species dedicated to Prof. Dr. Beatriz Martínez Daranas, researcher at the Marine Research Centre of Havana University, Cuba), specialist in taxonomy and ecology of seagrass and macroalgae.

Diagnosis. Species of *Reinhardorhynchus* **gen. n.** with the copulatory bulb encompassing the prostate vesicle, an armed cirrus and two distal hooks. Cirrus armed with triangular, ±4-µm-long spines. Cirrus also includes a ±347-µm-long spiny belt. Proximally in the belt the spines are scale shaped and ±23 µm long. Proximal spines followed by a section bearing ±6-µm-long spines that runs distally and ends in the distal comb-shaped part, which is armed with ±32-µm-long spines. Larger hook ±101 µm long and ±59 µm wide at its base. Its base bears a ±45-µm-long and funnel-like hook. Smaller hook ±89 µm long and ±47 µm wide at its base.

Description. Live specimens are 1.5–2 mm long, translucent, with two eyes (Fig. 10A: e). The syncytial and fully-ciliated epidermis is 7–8 µm thick and contains large vacuoles, some of which are filled with a dark granular secretion. Rhabdites occur all over the basal part of the epidermis and measure 2–3 µm.

The proboscis (Fig. 10A: pr) is of the typical koinocystidid construction (see Brunet 1972; Karling 1980), with a strong juncture sphincter, and does not differ in morphology from that of the other species of *Reinhardorhynchus* **gen n**. It is about 15% of the body length in live specimens. Only two pairs of integument retractors were observed: a ventral and a dorsal one. Two pairs of proboscis retractors were observed, but it is not clear whether more are present. The exact number of fixators and dilatators could not be determined. A sphincter around the proboscis pore was not observed.

The pharynx is located at 40–50% (Fig. 10A: ph) and has a diameter of 15% of the body length in live specimens. Its overall morphology does not differ from that previously described for *I. divae* (see above). At least two types of glands open in the distal part of the pharynx lumen: one containing a coarse-grained secretion, the other one a fine-grained secretion.

A pair of testes is located rostral to the pharynx. The seminal vesicles fuse with each other just before entering the copulatory bulb. The copulatory bulb is globular and 253–400 µm long ($\bar{x}$ = 327 µm; n = 7). It is surrounded by an external, longitudinal and a very strong internal, circular muscle layer. The prostate glands open proximally into the copulatory bulb. The copulatory bulb encompasses the prostate vesicle, the cirrus and two distal hooks. The prostate vesicle (Fig. 10A: pv) opens proximally into the cirrus. The filiform prostate ducts contain a coarse-grained secretion. The cirrus is surrounded by an external longitudinal and a very strong internal circular muscle layer. The cirrus (Fig. 10A: ci) is armed with 3–5-µm-long triangular spines (Fig. 10B: cis) ($\bar{x}$ = 4 µm; n = 20). Additionally, the cirrus also shows a 290–382-µm-long spiny belt ($\bar{x}$ = 347 µm; n = 6) (Fig. 10C). Proximally, these scale-like spines are 9–34 µm long ($\bar{x}$ = 23 µm; n = 15) (Fig. 10B–C: cps). This part is followed by a row of triangular and 4–8-µm-long ($\bar{x}$ = 6 µm; n = 31) spines (Fig. 10C: cms). In the distal, comb-shaped part of the belt the spines are 23–48 µm long ($\bar{x}$ = 32 µm; n = 31) (Fig. 10B–C: cds).

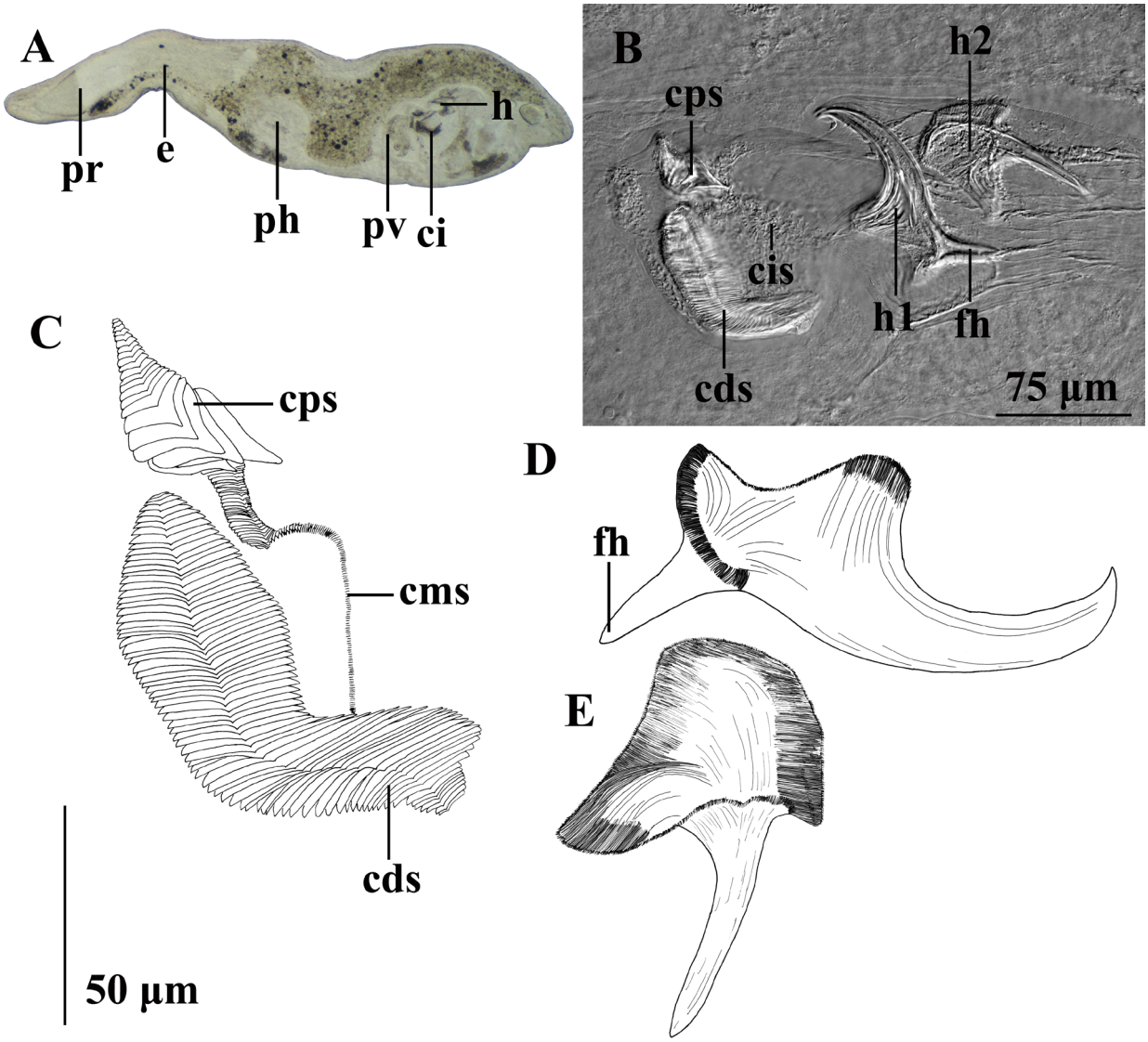

FIGURE 10. *Reinhardorhynchus beatrizae* **sp. n.**. A, general organisation. B, sclerotised structures of the copulatory bulb. C, Cirrus. D, larger hook. E, smaller hook. B–E, from the holotype. C–E with proximal end toward top of figure.

The larger of the two distal hooks (Fig. 10B: h1, 10D; hooks Fig. 10A: h) is 86–121 µm long ($\bar{x}$= 101 µm; n = 7) and 49–72 µm wide at its base ($\bar{x}$= 59 µm; n = 8). The base carries a funnel-like structure of 35–53 µm long ($\bar{x}$= 45 µm; n = 7) (Fig. 10B & 10D: fh). The smaller hook (Fig. 10B: h2, 10E) is 57–94 µm long ($\bar{x}$= 89 µm; n = 6) and 36–55 µm wide at its base ($\bar{x}$= 47 µm; n = 6).

The vitellaria run from the posterior end of the pharynx to the caudal body end. The elongated ovaries are located rostral to the copulatory bulb. The oocytes are organised in one row, increasing in diameter from the most proximal to the most distal one. The oviducts open into the proximal end of the female duct. The female duct opens into the receptacle bursa (terminology of Karling 1981; followed by Reygel *et al.* 2011) through a strong sphincter. The muscular bursal stalk connects the caudally-located bursa with the female atrium. In a live specimen, an egg without shell was observed.

***Reinhardorhynchus hexacornutus* Jouk, Diez, Reygel & Artois sp. n.**

(Fig. 11)

urn:lsid:zoobank.org:act: 45A01032-0A38-4976-9AF0-B2C6F277FC55

Material and distribution. Observations on live specimens, whole mounted afterwards. Five whole mounts, one

of which is designated holotype (FMNH https://id.luomus.fi/KV.650), the others in HU (XIII.4.16–XIII.4.19), collected in Puna'auia (17°36'42"S; 149°36'51"W) (Type Locality), Pape'ete, Tahiti, Society Islands, French Polynesia (March 18, 2016), sediment with ripple marks, 50 cm deep, fine black sand.

Etymology. Species named after the presence of six hooks within the copulatory bulb.

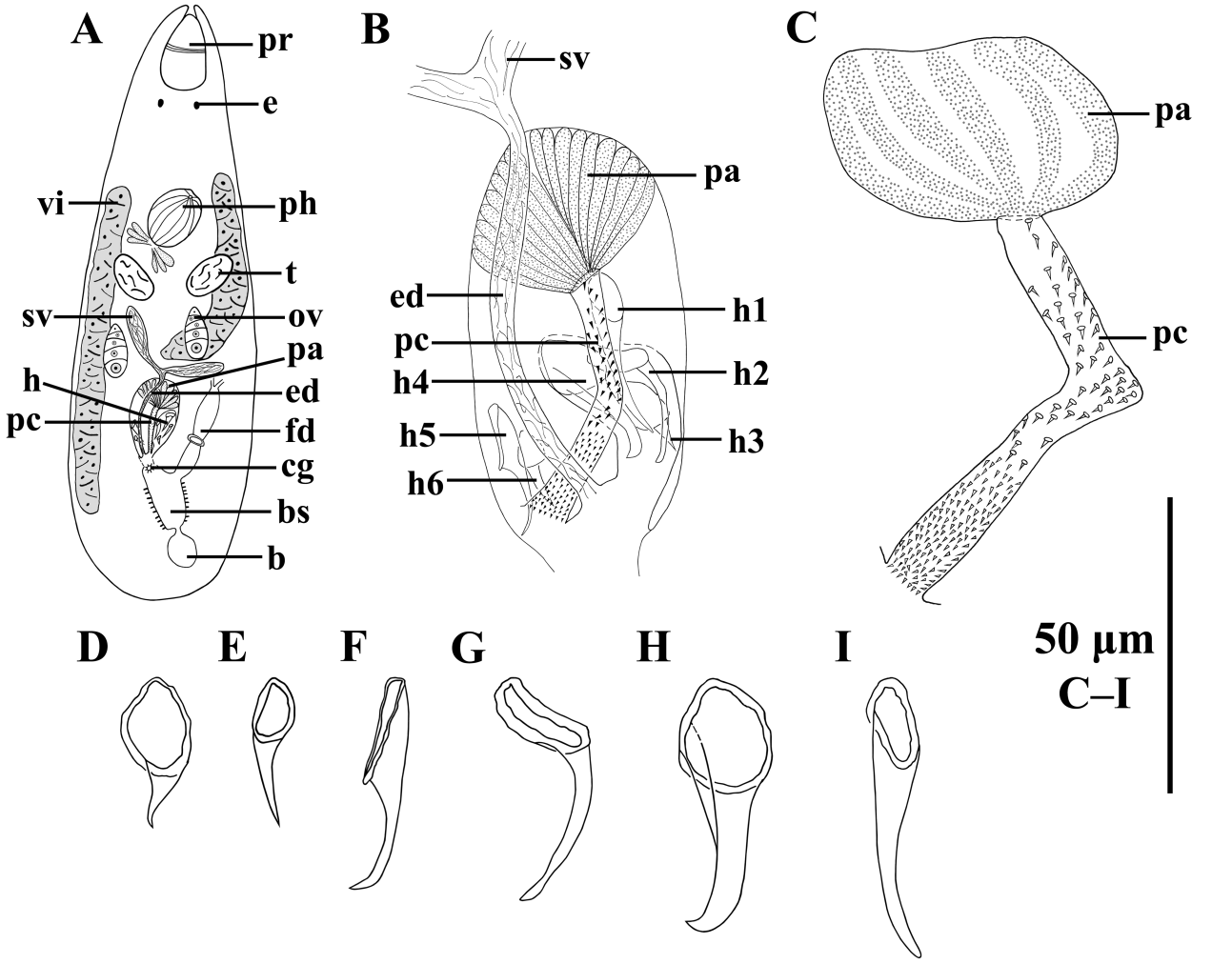

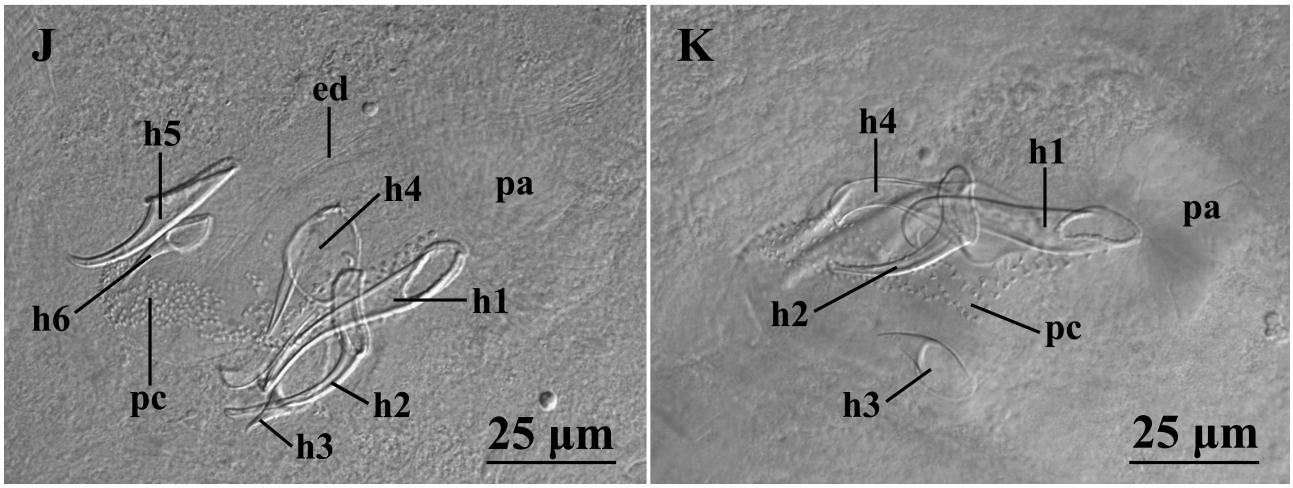

FIGURE 11. *Reinhardorhynchus hexacornutus* **sp. n.**. A, general organisation (from a live animal). B & J–K, copulatory bulb. C, cirrus. D–I: hooks. A–B, from live animals. C–J, from the holotype. K, from a reference specimen (HU XIII.4.16). All oriented with proximal end toward top of figure.

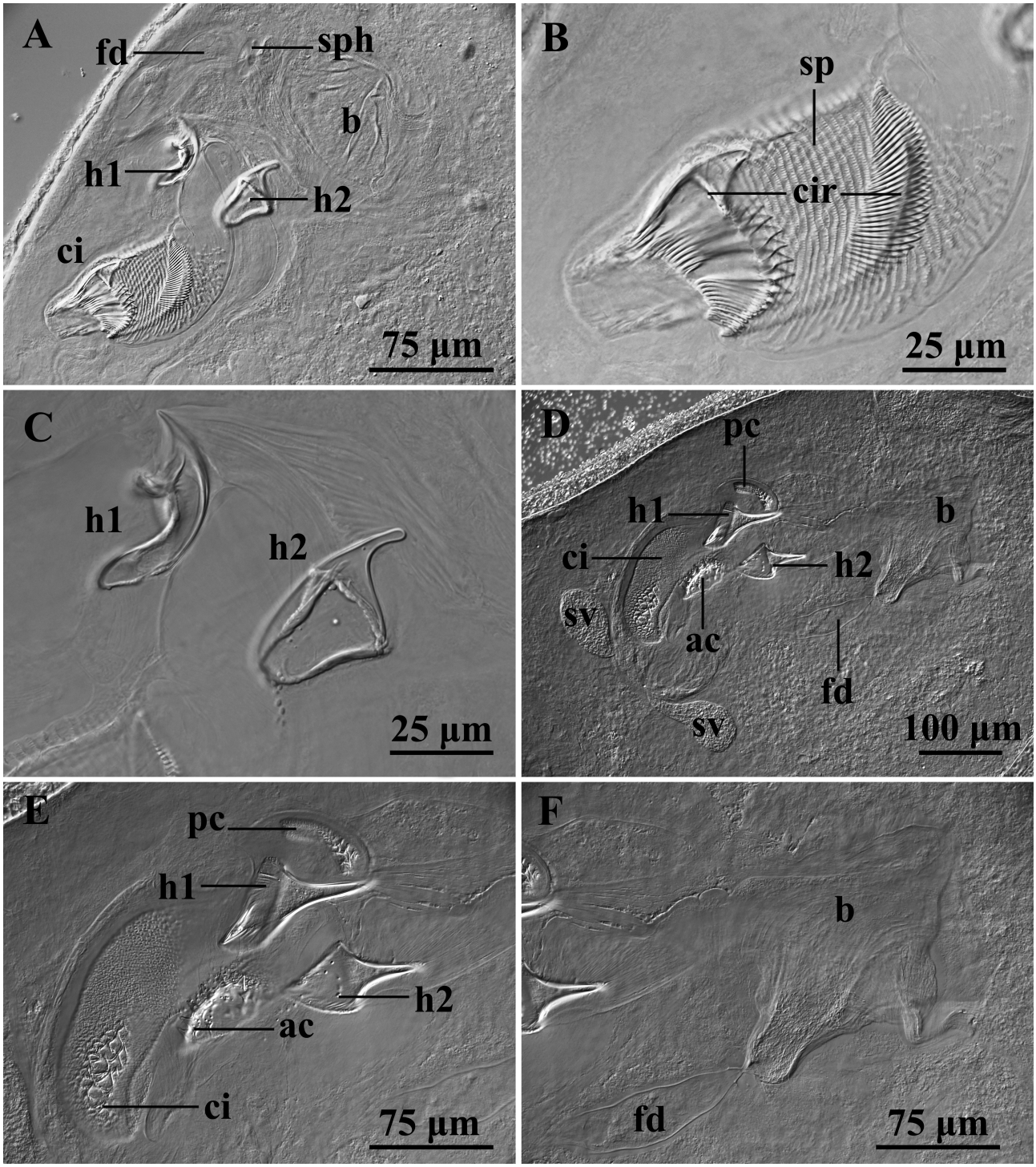

FIGURE 12. A–C, *Reinhardorhynchus anamariae* **sp. n.**. A, sclerotised structures of the cirrus. B, cirrus. C, hooks. D–F, *Reinhardorhynchus pacificus* **sp. n.**. D–E, sclerotised structures of the cirrus. F, female system. All from the holotype. All with proximal end toward left of figure.

Diagnosis. Species of *Reinhardorhynchus* **gen. n.** with the copulatory bulb encompassing the ejaculatory duct, a papillary cirrus, and six hooks. Ejaculatory duct runs through the copulatory bulb and opens distally into the male atrium. Papillary cirrus ±84 µm long, armed with nail-shaped spines, ±2 µm long proximally and ±1.2 µm distally. Hooks funnel-shaped, curved, and ending in a sharp tip, each of different size, ranging from 11µm long and 5 µm wide to 54 µm long and 23 µm wide.

Description. The specimens are 0.9–1.3 mm long ($\bar{x}$ = 1.1 mm; n = 3), translucent, with a pair of eyes (Fig. 11A: e). The proboscis (Fig. 11A: pr) is of the typical koinocystidid construction (see Brunet 1972; Karling 1980),

with a strong juncture sphincter. The pharynx (Fig. 11A: ph) has a diameter of 10% of the body length in live specimens, and is located at 30%.

Two testes (Fig. 11A: t) are positioned behind the pharynx. The vasa deferentia form the seminal vesicles (Fig. 11A–B: sv), which fuse to form a short seminal duct just before entering the copulatory bulb. The oval copulatory bulb is 125 µm long (n = 1) and encompasses the ejaculatory duct, a papillary cirrus, and six accessory hooks. The ejaculatory duct (Fig. 11B & 11J: ed) runs through the proximal part of the copulatory bulb and opens distally into the male atrium. The spiny part of the papillary cirrus (Fig. 11A–C & 11J–H: pc) is 73–91 µm long ($\bar{x}$ = 84 µm; n = 4) and armed with nail-shaped spines. Proximally, these spines are 1.2–2.4 µm long ($\bar{x}$ = 2 µm; n = 20) and distally they decrease in size to ±1.2 µm (n = 15). Proximally, the papillary cirrus is enclosed in a papilla (Fig. 11A–C & 11J–K: pa), with a glandular organ opening into the cirrus. The accessory hooks (Fig. 11A: h, 11B & 11J–K: h1–h6, 11D–I) are funnel-shaped, curved, and ending in a sharp tip. They differ in size, ranging from 11 µm long and 5 µm wide at the base for the smallest one to 54 µm long and 23 µm wide for the largest one. The hooks are organised in two groups; one group is formed by hooks 1–4 (Fig. 11I, 11G, 11D & 11H, respectively) and the other group includes hooks 5–6 (Fig. 11F & 11E, respectively). The hooks 1–4 are located in a well-developed muscular sac.

The vitellaria (Fig. 11A: vi) extend along both sides of the body from the level of the pharynx to the copulatory organs. A pair of ovaries (Fig. 11A: ov) is located at the midbody, rostral to the copulatory bulb. The oocytes are organised in a row. The oviducts open into the proximal end of the female duct. The female duct (Fig. 11A: fd) opens into the female atrium through a strong sphincter. The muscular bursal stalk (Fig. 11A: bs) connects the caudally-located bursa (Fig. 11A: b) to the female atrium. The common gonopore (Fig. 11A: cg) opens at 80%.

Reinhardorhynchus pacificus Diez, Reygel & Artois sp. n.

(Fig. 12D–F, 13)
urn:lsid:zoobank.org:act: C5DDBEEF-C3CA-456D-9330-440CFA8B10E4

Material and distribution. Observations on live specimens, whole mounted afterwards. Two whole mounts collected in Playa Venao (08°53’06”N; 79°36’07”W) (Type Locality), Vera Cruz, Panama (December 2, 2011), one of which is designated holotype (USNM 1642506), the other one in the USNM (1642507), coarse-grained sand with fine silt, salinity 30 ‰.

Etymology. The two specimens were found at the Pacific coast of Panama.

Diagnosis. Species of *Reinhardorhynchus* **gen. n.** with a copulatory bulb encompassing a papillary cirrus, an ejaculatory cirrus, an accessory cirrus, and two hooks. Ejaculatory cirrus ±171 µm long, armed with scale-like spines along its entire length that are ±5 µm wide proximally and ±2 µm wide distally. Few larger triangular spines occur proximally (±10 µm long) and distally (±4 µm long). Accessory cirrus ±92 µm long, proximally armed with ±6-µm-long triangular spines and distally with 3-µm-long triangular spines and ±3-µm-wide and scale-like spines. Distal rims of these spines serrated, bearing ±1-µm-long spinules. Papillary cirrus ±62 µm long, proximally covered by fine spines of ±2 µm long and distally with ±6-µm-long triangular spines. The hooks are ±83 µm long and ±81 µm long, respectively.

Description. The specimens are 1.7 mm long, colourless, with two eyes (Fig. 13A: e). The brain (Fig. 13A: br) is located caudally from the proboscis. The proboscis (Fig. 13A: pr) has the typical koinocystidid morphology (see Brunet 1972; Karling 1980) and shows a strong junction sphincter; it represents 10% of the body length in live specimens. The pharynx (Fig. 13A: ph) has a diameter of ±15% of the body length in live specimens, and is located at 30–40%. Caudally in the body some eosinophilic glands occur (Fig. 13A: cgl).

The two testes (Fig. 13A: t) are located rostrally from the pharynx. The seminal vesicles (Fig. 12D &13A: sv) fuse proximally from the copulatory bulb, forming a short seminal duct. The copulatory bulb is 363–403 µm long ($\bar{x}$ = 383 µm; n = 2). It encompasses the prostate vesicle (Fig. 13A: pv), the ejaculatory cirrus (terminology of Karling 1978), an accessory cirrus, a papillary cirrus (terminology of Karling 1978), and two distal hooks. The ejaculatory cirrus (Fig. 12D–E & 13A: ci, 13B) is 162–180 µm long ($\bar{x}$ = 171 µm; n = 2) and armed with scale-like spines over its entire length. These spines are 5–6 µm wide ($\bar{x}$ = 5 µm; n = 20) proximally and 2–3 µm wide ($\bar{x}$ = 2 µm; n = 20) distally. Additionally, a number of larger triangular spines occur proximally, measuring 6–13 µm ($\bar{x}$ = 10 µm; n = 10), and a group of small triangular spines is present distally, measuring 3–4 µm ($\bar{x}$ = 4 µm; n = 13).

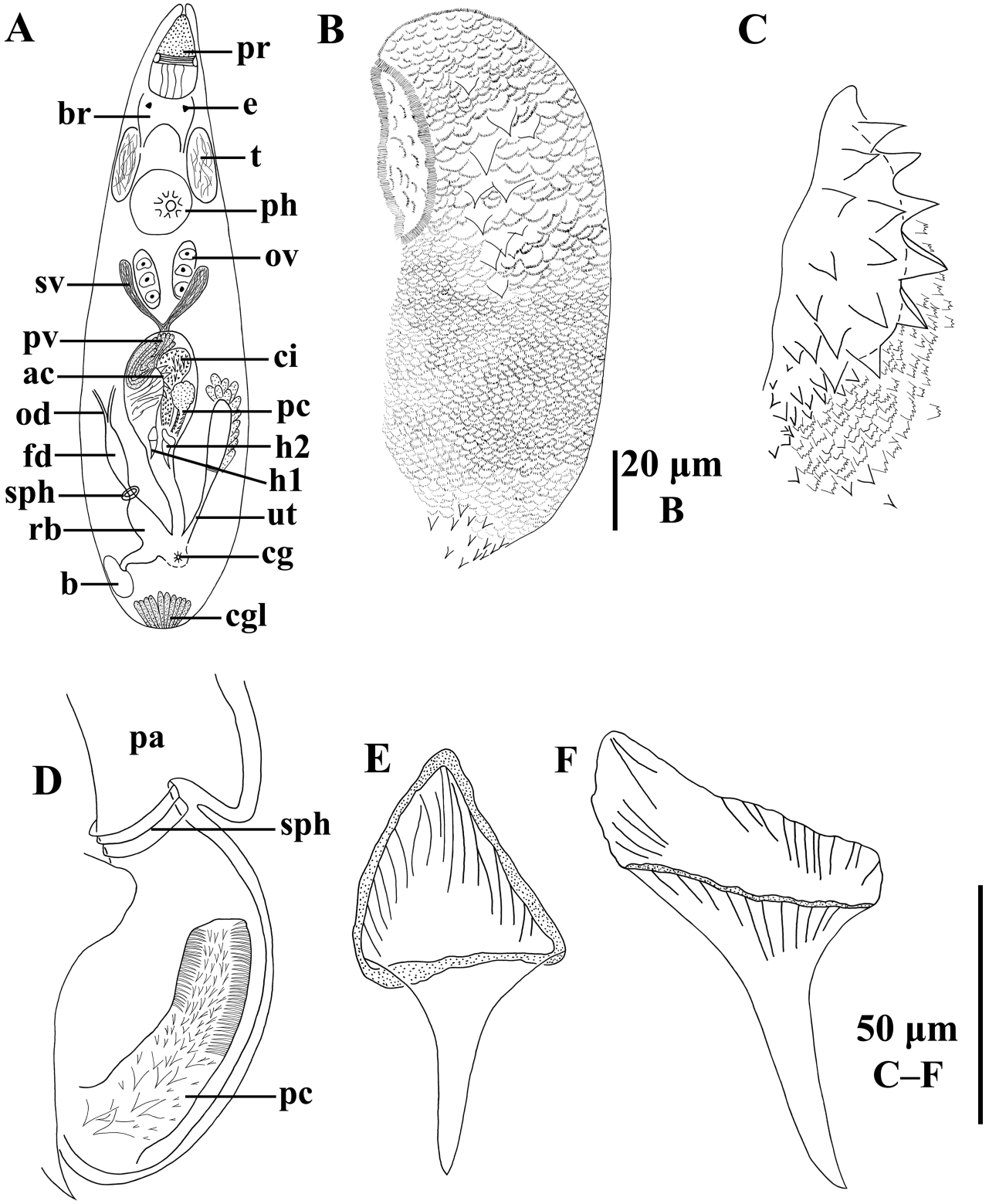

FIGURE 13. *Reinhardorhynchus pacificus* **sp. n.**. A, general organisation (from a live animal). B, ejaculatory cirrus. C, accessory cirrus. D, papillary cirrus. E, larger hook. F, smaller hook. B–F, from the holotype. All with proximal end toward top of figure.

The accessory cirrus (Fig. 12D–E & 13A: ac, 13C) is 89–95 µm long ($\bar{x}$ = 92 µm; n = 2), proximally armed with triangular spines 4–10 µm long ($\bar{x}$ = 6 µm; n = 24) and distally with triangular spines 2–4 µm long ($\bar{x}$ = 3 µm; n = 9) and scale-like spines 2–5 µm wide ($\bar{x}$ = 3 µm; n = 15). The distal rim of the scale-like spines of the accessory cirrus

is serrated, with 1-µm-long spinules. The spiny part of the papillary cirrus (Fig. 12D–E, 13A & 13D: pc) is 55–69 µm long ($\bar{x}$= 62 µm; n = 2) and proximally enclosed in a papilla (Fig. 13D: pa). Papilla and cirrus are separated from each other by a sphincter (Fig. 13D: sph). The papillary cirrus is proximally armed with fine spines, ±2 µm long, and distally with triangular spines, 4–8 µm long ($\bar{x}$= 6 µm; n = 6). The two funnel-shaped distal hooks are nearly equal in size. One hook (Fig. 12D–E & 13A: h1, 13E) is 79–86 µm long ($\bar{x}$= 83 µm; n = 2) and 40–43 µm wide at its base ($\bar{x}$= 42 µm; n = 2). The other hook (Fig. 12D–E & 13A: h2, 13F) is 79–83 µm long ($\bar{x}$= 81 µm; n = 2) and 59–65 µm wide at its base ($\bar{x}$= 62 µm; n = 2).

Vitellaria were not observed. The oval-shaped ovaries (Fig. 13A: ov) are located rostrally from the copulatory bulb. The oocytes are organised in a row. The oviducts (Fig. 13A: od) open into the proximal end of the female duct. The female duct (Fig. 12D, 12F & 13A: fd) opens into the receptacle bursa (terminology of Karling 1981; followed by Reygel *et al.* 2011) (Fig. 13A: rb) through a sphincter (Fig. 13A: sph). The caudally-located bursa (Fig. 12D, 12F & 13A: b) opens into the female genital atrium via the bursal stalk. The uterus (Fig. 13A: ut) has a sphincter more or less at its midpoint. The common gonopore (Fig. 13A: cg) opens at 90%.

Reinhardorhynchus soror Diez, Reygel & Artois sp. n.

(Fig. 14)

urn:lsid:zoobank.org:act:19AA34C8-D7BD-4299-93C0-31856253020B

Material and distribution. Observations on live specimens, whole mounted afterwards. Three whole mounts from Tombolo West (08°48’05”N; 79°33’15”W) (Type Locality), Taboga Island, Panama (December 9, 2011), one of which designated holotype (USNM 1642508), the others in the USNM (1642509–1642510), from medium-coarse sand with ripple marks close to swash zone, small waves, salinity 28 ‰.

Etymology. Species name refers to its similarities with *R. beatrizae* **sp. n**. Lat. *soror*: sister.

Diagnosis. Species of *Reinhardorhynchus* **gen. n.** with a copulatory bulb encompassing a spiny cirrus and two distal hooks. Cirrus armed with triangular, ±5-µm-long spines. It also has a ±437-µm-long belt of spines, which shows three distinct regions: 1) a proximal part with curved and hook-shaped spines fused at their bases, the largest one ±57 µm long, the others measuring 6–40 µm, 2) a middle part with 3-µm-long spines, and 3) a distal, comb-shaped part armed with ±39-µm-long and triangular spines. The larger of the distal hooks curved, ±87 µm long and ±68 µm wide at its base; its base provided with a funnel-like, ±70-µm-long hook. Smaller hook ±59 µm long and ±59 µm wide at its base.

Description. The specimens are 1.5–2.2 mm long ($\bar{x}$= 1.7 mm; n = 3), translucent, with two rounded eyes (Fig. 14A: e). The proboscis (Fig. 14A: pr) is of the typical koinocystidid construction (see Brunet 1972; Karling 1980); it represents 15% of the body length in live specimens. The pharynx (Fig. 14A: ph) has a diameter of 15% of the body length in live specimens and is located at 40–50%.

The testes (Fig. 14A: t) are located rostral to the pharynx. The seminal vesicles (Fig. 14A: sv) fuse just before entering the copulatory bulb. The male copulatory bulb is globular and 320–391 µm long ($\bar{x}$= 356 µm; n = 2). The prostate vesicle (Fig. 14A: pv) opens into the armed cirrus. The cirrus is of the same structure as that of *R. beatrizae* **sp. n**. The cirrus (Fig. 14A: ci) is armed with triangular, 4–5-µm-long spines ($\bar{x}$= 5 µm; n = 35) (Fig. 14F: cis). The cirrus also includes a 437-µm-long belt of spines (n = 1) (Fig. 14A: cir), which consists of three parts. The proximal part is provided with spines that are curved and hook shaped (Fig. 14B, 14F: cps, 14G), the largest one 55–60 µm long ($\bar{x}$= 57 µm; n = 3) and the other ones 6–40 µm long ($\bar{x}$= 18 µm; n = 3). This proximal part forms a continuous 62–72-µm-long row ($\bar{x}$= 66 µm; n = 3). The middle part forms a broad surface consisting of 3-µm-long spines (Fig. 14F: cms) and measuring 109 µm (n = 1). The distal part is 129–135 µm long ($\bar{x}$= 132 µm; n = 2) and consists of a continuous comb-shaped row of spines (Fig. 14C, 14F: cds). The spines in this part are 20–59 µm long ($\bar{x}$= 39 µm; n = 44) and increase in size from the most proximal one to the most distal one.

There are two large distal hooks. The larger one (Fig. 14A & 14F: h1, 14E) is 84–89 µm long ($\bar{x}$= 87 µm; n = 3) and 63–77 µm wide at its base ($\bar{x}$= 68 µm; n = 3), curved, and carries a funnel-like and 65–80 µm long ($\bar{x}$= 70 µm; n = 3) projection at its base (Fig. 14E–F: fh). This structure is straight, makes a ±90º angle with the main hook, and ends in a blunt tip. The hook proper is strongly curved and ends in a sharp tip. At its base, there is a small, more or less square and folded projection (Fig. 14E: fp). The smaller hook (Fig. 14A & 14F: h2, 14D) is 57–89 µm long ($\bar{x}$= 59 µm; n = 3) and 54–62 µm wide ($\bar{x}$= 59 µm; n = 3) at its base. The base of this hook is asymmetrical. The hook is slightly curved and ends in a sharp tip.

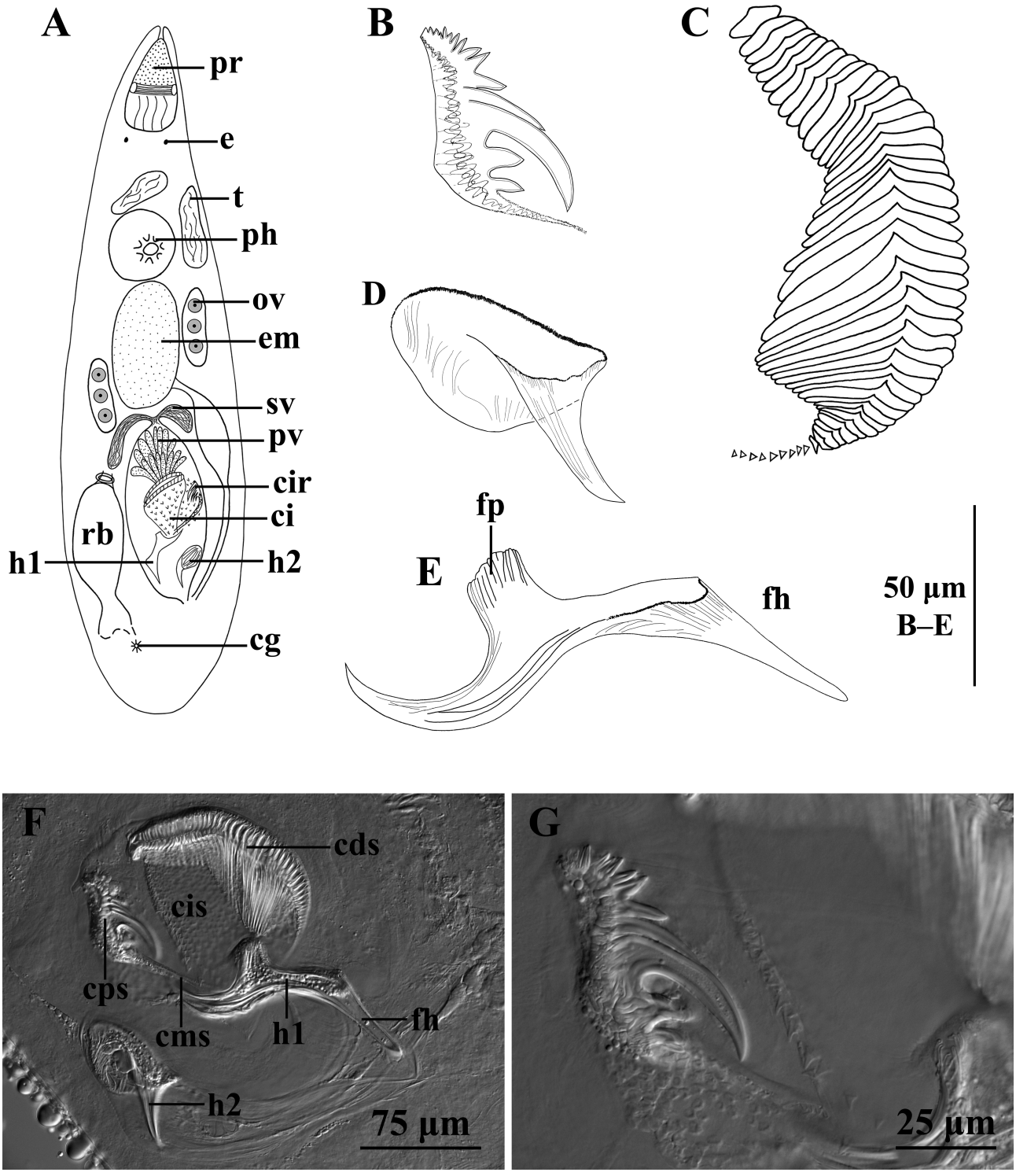

FIGURE 14. *Reinhardorhynchus soror* **sp. n.**. A, general organisation (from a live animal). B & G, proximal spines of the spiny row of the cirrus. C, distal spines of the spiny row of the cirrus. D, smaller hook. E, larger hook. F, sclerotised structures of the copulatory bulb. B–G, from the holotype. All with proximal end toward top of figure.

Vitellaria were not observed. The ovaries are oval shaped (Fig. 14A: ov), located rostral to the copulatory bulb, with the oocytes organised in a row. The oviducts open into the female duct. The female duct opens into the receptacle bursa (terminology of Karling 1980) (Fig. 14A: rb) through a strong sphincter. In a live specimen one embryo (Fig. 14A: em), apparently not surrounded by a shell, was observed, suggesting the species is (ovo-)viviparous. The common gonopore (Fig. 14A: cg) is located ventrally, at 90%.

***Reinhardorhynchus tahitiensis* Jouk, Diez, Yurduseven, Reygel & Artois sp. n.**
(Fig. 15)
urn:lsid:zoobank.org:act:EBAAD8FF-E519-48FE-8846-20693BD0C5A3

Material and distribution. Observations on live specimens. Three whole mounts, one of which designated holotype (FMNH https://id.luomus.fi/KV.652), from Puna'auia (17°38'15"S; 149°36'47"W) (Type Locality), Pape'ete, Tahiti, Society Islands, French Polynesia (March 20, 2016), in front of the Méridien Hotel, sandy beach in front of coral heads with strong periodic currents, fine sand with detritus, about 0.5 m deep. Another whole mount from the same locality (March 1, 2016), in mixed sand with shell gravel, 1 m deep. Two serially-sectioned specimens from the type locality (October 3, 2017), 100 m from the seafront, sand patch in between coral heads, medium grained sand with some coral debris, 1.5 m deep. Three whole mounts from Avatoru, Rangiroa (14°58'48"S; 147°37'25"W), Tuamotu Archipelago, French Polynesia (March 7, 2016), second harbour, fine sand with detritus, 1.5 m deep. All the reference material deposited in HU (XIII.4.20–XIII.4.27).

Etymology. Species named after Tahiti, where most of the specimens were found.

Diagnosis. Species of *Reinhardorhynchus* **gen. n.** with the copulatory bulb encompassing the prostate vesicle, an armed cirrus and two distal hooks. Cirrus armed with four rows of triangular, ±3-µm-long spines. Rows ±93 µm, ±96 µm, ±41 µm, and ±49 µm long respectively. Longest two rows end in curved spines, which increase in length from the most proximal one (±6 µm long) to the most distal one (±27 µm long). Hooks ±24 µm long and ±18 µm wide at their base, ending bluntly with a very small, sharp tip directed sideways.

Description. The specimens are 1.1–1.3 mm long ($\bar{x}$ = 1.2 mm; n = 4), yellowish, with two eyes. Habitus and general organisation as in *R. riae* **sp. n**. The epidermis is 6 µm thick. Rhabdites, 7–9 µm long, more numerous in the posterior 2/3 of the specimen, deeply embedded within the epidermis. Some rhabdites stain pinkish, others yellowish. At the distal end, caudal glands are present (Fig. 15A: cgl).

The proboscis (Fig. 15A: pr) is of the typical koinocystidid construction (see Brunet 1972; Karling 1980). It represents 10% of the body length and has the same detailed morphology as that of *R. riae* **sp. n.**; see above. Only two kinds of glands open through the caudal wall of the proboscis: coarse-grained basophilic glands and fine-grained eosinophilic ones.

The pharynx (Fig. 15A: ph) has a diameter of 15% of the body length, and is located at 40%. Its morphology does not differ from that in *R. riae* **sp. n**. There are two types of pharyngeal glands: coarse-grained basophilic and coarse-grained eosinophilic ones. In one specimen several diatoms were observe. Proximally, the pharynx opens into the oesophagus (Fig. 15A: oe).

A pair of testes (Fig. 15A: t) is located rostrally from the pharynx. In the caudal body fourth, the vasa deferentia are swollen and form the seminal vesicles (Fig. 15A & 15D: sv), which are lined by longitudinal muscles and fuse with each other just before entering the copulatory bulb. The copulatory bulb (Fig. 15A & 15C: cb) is 208–245 µm long ($\bar{x}$ = 228 µm; n = 7). It is lined by a coat of strong circular muscles, which are weakest distally. Proximally, prostate glands (Fig. 15A: pg) open into the copulatory bulb. The prostate vesicle (Fig. 15D: pv) contains two types of coarse-grained secretions: a basophilic and an eosinophilic one. Additionally, some fine-grained eosinophilic glands (Fig. 15D: gl) lie inside the muscular wall of the copulatory bulb. The prostate ducts open into the cirrus. Nuclei of both the basophilic and the eosinophilic glands are extracapsular and could only be observed in live specimens. The cirrus is armed with four rows of spines (Fig. 15A & 15D: spr). One row (Fig. 15B–C: spr1) is 88–104 µm long ($\bar{x}$ = 93 µm; n = 3), the second one (Fig. 15B–C: spr2) 93–99 µm ($\bar{x}$ = 96 µm; n = 3), the third one (Fig. 15C: spr3) 40–42 µm ($\bar{x}$ = 41 µm; n = 3), and the last one (Fig. 15C: spr4) 49 µm (n = 3). The triangular spines that make up these rows are 2–4 µm long ($\bar{x}$ = 3 µm; n = 30). The two largest rows distally end in large, curved, somewhat shark-tooth-shaped spines, increasing in length from the most proximal one (6 µm long) to the most distal one (27 µm long) ($\bar{x}$ = 16 µm; n = 21). The two distal hooks (Fig. 15B–D: h) are similar to each other: broad-funnel shaped, 23–26 µm long ($\bar{x}$ = 24 µm; n = 12) and 13–23 µm wide at their base ($\bar{x}$ = 18 µm; n = 12), and end bluntly. Depending on the degree of the squeezing and the orientation of the hooks, some specimens reveal that these distal ends bear a small sharp tip directed sideways. The copulatory bulb opens into the male atrium (Fig. 15D: ma), which itself enters the common genital atrium (Fig. 15D: ca) through the latter's rostro-dorsal wall.

The ovaries (Fig. 15A: ov) are oval-shaped and located rostrally from the copulatory bulb. The vitellaria occur as a large mass throughout almost the complete body of the animal. In some specimens, however, they seemingly extend as one or two rows of large follicles from just caudally of the testes to alongside the copulatory organs (Fig. 15A: vi). The female duct is bipartite, with the proximal part (Fig. 15A & 15D: fd1) more or less globular and filled

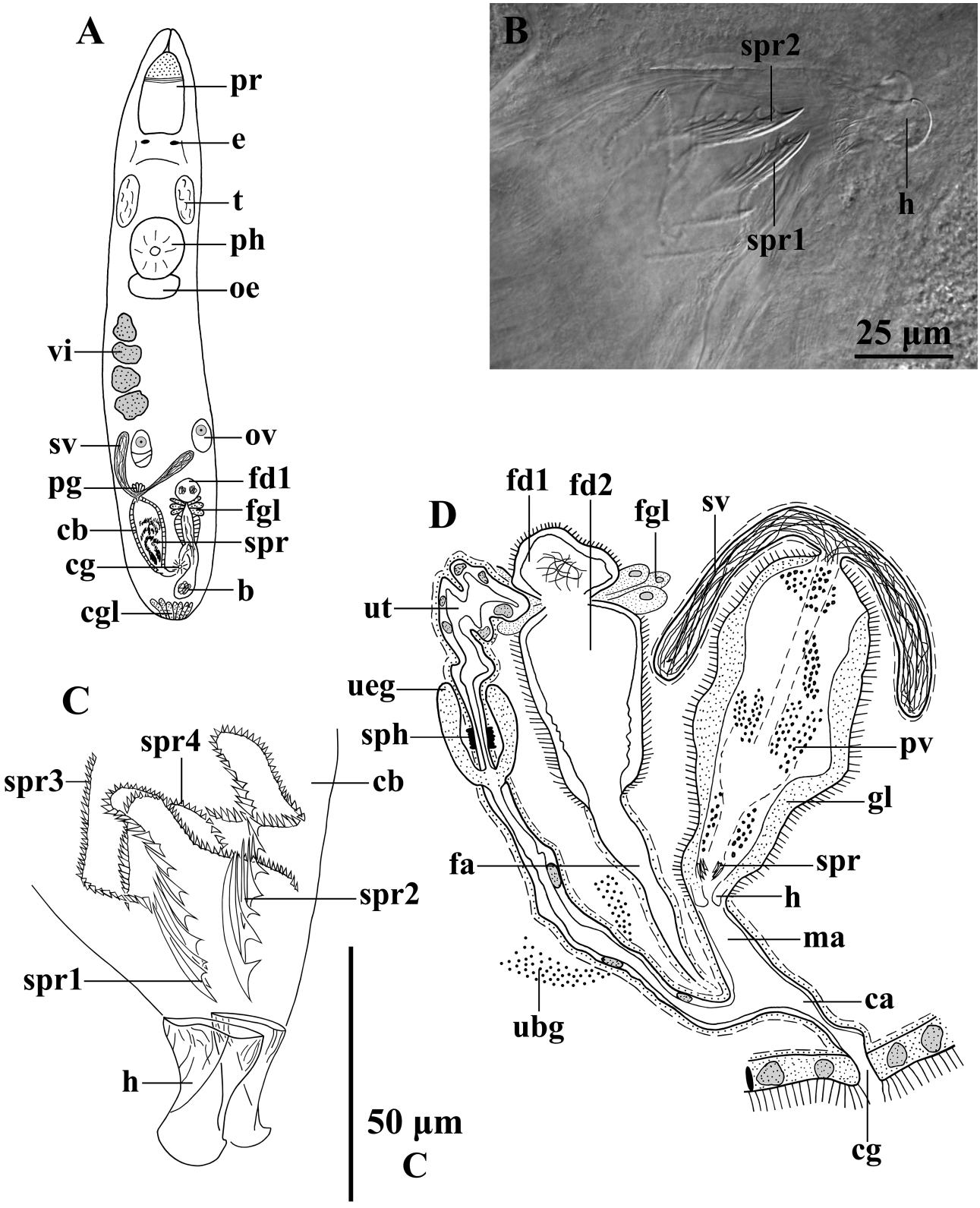

FIGURE 15. *Reinhardorhynchus tahitiensis* **sp. n.**. A, general organisation (from a live animal). B–C, sclerotised structures of the copulatory bulb (from the holotype). D, sagittal reconstruction of the genital system from the left hand side. C with proximal end toward top of figure, B with proximal end toward left of figure.

with living sperm, the distal part (Fig. 15D: fd2) more elongated. In one of the live specimens two separate sperm-packages were observed within the proximal part of the female duct. A bundle of glands enters at the transition between the two compartments (Fig. 15A & 15D: fgl). The female duct is lined by an anucleated epithelium and a layer of strong circular muscles. Distally, the female duct opens into the female atrium (Fig. 15D: fa). The female atrium is surrounded by an inner weak circular and an outer longitudinal muscle layer. The epithelium of the female atrium could not be observed, probably because it is very low. The female duct enters the common atrium caudo-dorsally, but the exact point of entry could not be observed in the available material. The exact course of the oviducts could not be determined.

The common genital atrium is lined by a low, anucleated epithelium. The uterus (Fig. 15D: ut) enters the common atrium caudally. It is lined by a nucleated epithelium and is surrounded by an inner layer of circular and an outer layer of longitudinal muscles. A sphincter separates the proximal third of the uterus from the distal part (Fig. 15D: sph). Distally from the sphincter, a bundle of fine-grained eosinophilic glands (Fig. 15D: ueg) enters the uterus. At its distal third, the uterus is surrounded by coarse-grained basophilic glands (Fig. 15D: ubg). The common gonopore (Fig. 15A & 15D: cg) is located at 90%. Caudally of the gonopore, a bursa (Fig15A: b) is present.

Reinhardorhynchus unicornis Diez, Aguirre, Reygel & Artois sp. n.

(Fig. 16)
urn:lsid:zoobank.org:act:B5662028-C218-43A0-9A93-7B2557629C76

Material and distribution. One specimen studied alive, whole mounted afterwards, designated holotype (FMNH https://id.luomus.fi/KV.653), collected in Guardalavaca (21°07’32”N; 75°49’39”W) (Type Locality), Banes, Holguín, Cuba (February 28, 2017), fine-grained sand in a bed of *Syringodium filiforme*, 0.2 m deep, salinity 35 ‰.

Etymology. The epithet refers to the copulatory organ, which is armed with a single accessory hook only.

Diagnosis. Species of *Reinhardorhynchus* **gen. n.** with a copulatory bulb encompassing an ejaculatory cirrus, a papillary cirrus, and an accessory hook. Ejaculatory cirrus 73 µm long, armed with 5-µm-long, triangular spines. Papillary cirrus 119 µm long, armed with triangular, ±1-µm-long spines which become longer distally, up to ±11 µm. Curved hook 100 µm long and 40 µm wide at its asymmetrical base.

Description. The specimen is 1.6 mm long, unpigmented, with a pair of eyes. The proboscis is about 20% of the body length in the live specimen. As far as could be seen on the live specimen, it shows the distinctive features of the typical koinocystidid proboscis (see Brunet 1972; Karling 1980), with a strong juncture sphincter. The pharynx (Fig. 16B: ph) has a diameter of 15% of the body length in live specimens, and is located at 40%.

A pair of testes is located rostrally from the pharynx. The seminal vesicles (Fig. 16A–B & 16E: sv) fuse just before entering the copulatory bulb and form a short ejaculatory duct (Fig. 16A: ed). The extracapsular prostate glands (Fig. 16A: pg) open proximally into the copulatory bulb. The copulatory bulb (Fig. 16A) encompasses the prostate vesicle (Fig. 16A–B: pv), an ejaculatory cirrus, a papillary cirrus, and one distal hook. Proximally, a bundle of prostate glands opens into the copulatory bulb. The ejaculatory cirrus (Fig. 16A–B & 16E–F: ci) is 73 µm long and armed with 4–7-µm-long triangular spines ($\bar{x}$ = 5 µm; n = 12). The papillary cirrus (Fig. 16A–B & 16E–F: pc, 16D) is proximally enclosed in a globular papilla (Fig. 16A: pa). It is 119 µm long and 24 µm wide, and armed with triangular and ±1-µm-long spines; some spines are larger distally (±11 µm long). The caudally-located hook (Fig. 16A–B & 16E: h, 16C) is 100 µm long and 40 µm wide at its asymmetrical base.

The pair of ovoid ovaries is situated rostrally from the copulatory bulb, with the oocytes organised in a row. The vitellaria (Fig. 16B: vi) extend from beside the pharynx to the body end.

Galapagetula Reygel, Willems & Artois, 2011

Emended diagnosis of *Galapagetula* (after Reygel *et al.* 2011). Koinocystididae with proboscis of the typical koinocystidid construction without proboscis juncture sphincter. Testes lie at mid-body or more caudally. Copulatory organ pear shaped, distal part cylindrical, containing an unarmed or armed cirrus. Female duct widened proximally, functioning as a seminal receptacle, only surrounded with muscles in its tube-shaped distal part. Two bursae open separately into the female atrium, a muscular one (accessory bursa) and a resorptive one.

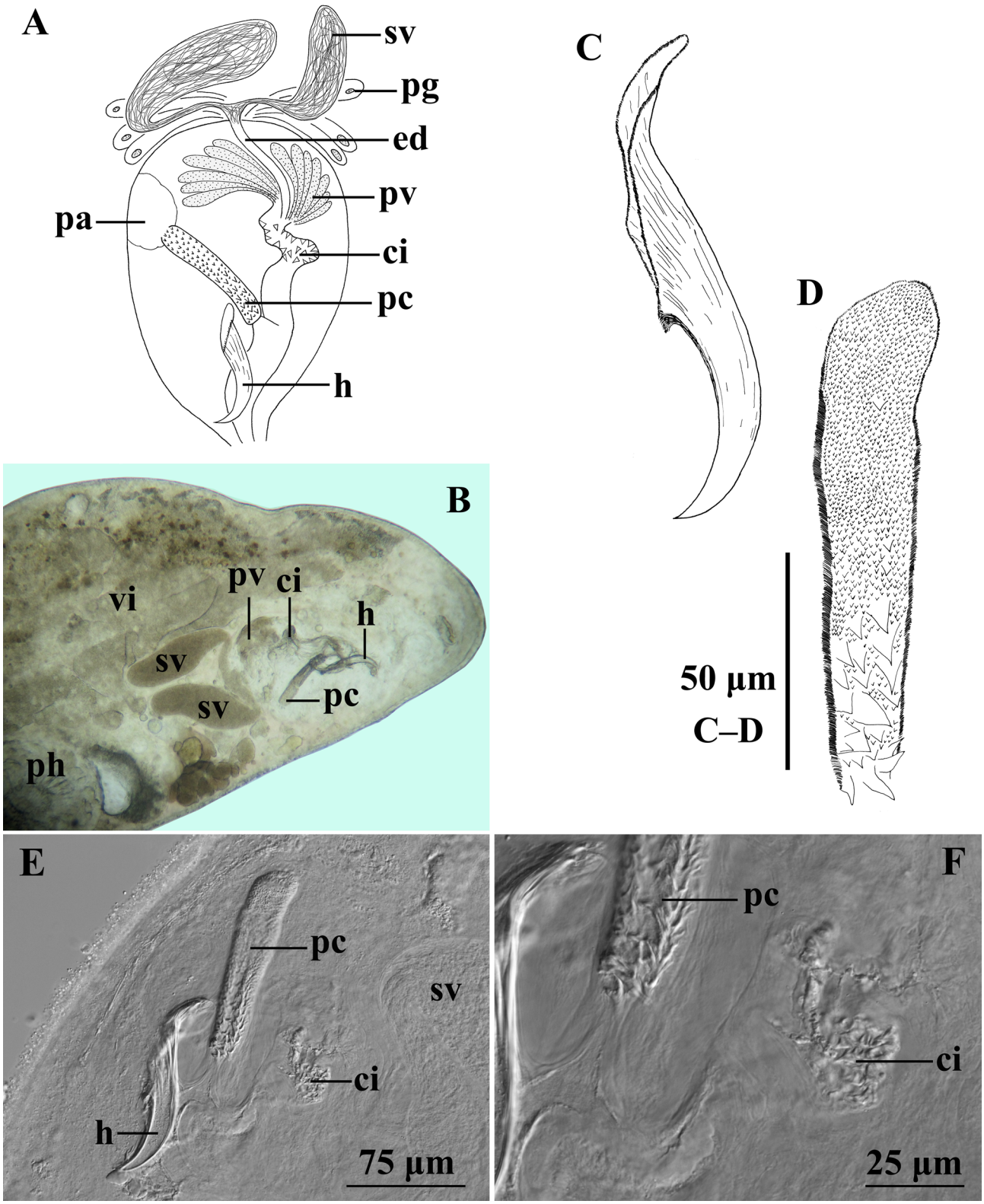

FIGURE 16. *Reinhardorhynchus unicornis* **sp. n.**. A, copulatory bulb. B, caudal body end. C, hook. D, papillary cirrus. E–F, sclerotised structures of the copulatory bulb. A–B, from the live animal. C–F, from the holotype. A–D & E–F with proximal end toward top of figure, B with proximal end toward left of figure.

Emended diagnosis of *Galapagetula annikae* (after Reygel *et al.* 2011). Species of *Galapagetula* without a mouth sphincter. Copulatory organ of the conjucta duplex-type, with a folded cirrus, armed with small spines. Female duct distally highly muscular with strong sphincter. Bursae without sphincters. Common gonopore at 85%.

***Galapagetula cubensis* Diez, Reygel & Artois sp. n.**
(Fig. 17–19)
urn:lsid:zoobank.org:act: 54453AD2-50DE-4451-AB22-86999485DCB8

Material and distribution. Observation on live specimens. One serially-sectioned specimen from Bueycabón (19°57'38"N; 76°57'28"W) (Type Locality), Santiago de Cuba, Cuba (November 18, 2017), designated holotype (FMNH https://id.luomus.fi/KV.654), intertidal, scraping the upper 10 cm of the fine sand. One whole mount from Las Sardinas (19°56'24"N; 76°46'41"W), Santiago de Cuba, Cuba (June 22, 2016), fine, silty sand, 0.1 m deep, salinity 33 ‰, and two from El Masío (19°59'21"N; 76°16'35"W), Santiago de Cuba, Cuba (June 30, 2016), intertidal, upper 10 cm of the medium-coarse sand, salinity 33 ‰ (HU XIII.4.28– XIII.4.30).

Etymology. The epithet refers to the occurrence of the new species in Cuba.

Diagnosis of *Galapagetula cubensis* sp. n. Species of *Galapagetula* with mouth sphincter. The copulatory bulb encompasses a prostate vesicle, a seminal duct, and the ejaculatory duct, which distally ends in a small and unarmed penis papilla. Prostate glands enter the male duct separately from the seminal duct, forming a divisa-type copulatory organ. Stalk of the resorptive bursa with a strong sphincter. Female duct lacking a sphincter. Common gonopore caudal.

Description. Live specimens about 1.5 mm long, translucent, with a pair of small eyes (Fig. 17A: e). Epidermis syncytial, 5–8 µm thick, fully ciliated. Cilia 5 µm long. The epidermis shows many vacuoles, some of which are empty, others are filled with a dark, granular secretion. The dark-stained rhabdites are 2–3 µm long.

The proboscis (Fig. 17A & 19A: pr, 17B) is of the typical koinocystidid construction (see Brunet 1972; Karling 1980), without a juncture sphincter. In live specimens it represents about 20% of the body length in live specimens. The exact number of fixators (Fig. 17B & 19A: pfix) and retractors (Fig. 17B: pret) muscles could not be determined. The cone retractors (Fig. 17B: cret) are well developed. A pair of ventral and a pair of dorsal integument retractors (Fig. 17B: iret) are present. Proboscis sheath surrounded by an external layer of longitudinal muscles. Several dilatators (Fig. 17B & 19A: dil) connect the proboscis sheath with the body wall. Most of these dilatators are very thin, except for some in the proximal half of the proboscis sheath. The proboscis pore (Fig. 17B & 19A: prp) is not surrounded by a sphincter. The proboscis sheath is lined by a nucleated and thick epithelium (Fig. 17B: pep). This epithelium is continuous with the epithelium covering the proboscis cone. Both epithelia contain oval to circular-shaped glands (reddish stained) (Fig. 17B & 19A: epg), albeit the sheath epithelium only in its most proximal part. Several proboscis glands lie just caudal to the proboscis: ventrally and dorsally there are coarse-grained basophilic glands (Fig. 17B: prg1), and in between them fine-grained eosinophilic (light-pink) (Fig. 17B: prg2) and medium-coarse-grained eosinophilic (dark-pink) (Fig. 17B: prg3) ones.

The pharynx (Fig. 17A & 19A–D: ph, 17B) is located at 30%. It has a diameter of about 15% of the body length. The prepharyngeal cavity is lined by a nucleated epithelium and is surrounded by a layer of longitudinal muscles. Additional circular muscles occur externally from the longitudinal ones in the distal half of the cavity. The mouth (Fig. 17B: m) can be closed by a sphincter (Fig. 17B: sph). Two types of glands open into the pharynx lumen: coarse-grained eosinophilic ones distally (Fig. 17B: phg1), and more to the middle part of the pharynx, additional coarse-grained basophilic glands occur (Fig. 17B: phg2). An epithelium lining the pharynx lumen was not observed. The musculature of the pharynx consists of a layer of longitudinal muscles outside of the septum (Fig. 17B: lm1), which is continuous with the longitudinal muscles surrounding the prepharyngeal cavity, and a thick circular layer just inside (Fig. 17B: cm1). The longitudinal muscles at the inside of the septum, observed in several species of *Itaipusa*, are not observed in this species. The pharynx lumen is surrounded by an inner circular muscle layer (Fig. 17B: cm2) and an outer longitudinal one (Fig. 17B: lm2). Internal strong longitudinal muscles are present (Fig. 17B: ilm). Radial muscles (Fig. 17B: rm) run between the septum and the wall of the pharynx lumen. The oesophagus (Fig. 17B & 19A: oe) is surrounded by the digestive parenchyma (Fig. 17B: dip). This parenchyma shows several nuclei and dark-stained vacuoles.

The gonads and atrial organs are located in the caudal fourth of the body. The pair of testes (Fig. 17A: t) is ventral. The vasa deferentia each form a seminal vesicle (Fig. 17A & 18: sv), and these fuse at the point where they enter the copulatory bulb (Fig. 17A & 19B–C: cb). At the same point, also the prostate glands (Fig. 17A, 18 & 19D: pg) open into the copulatory bulb. The copulatory bulb encompasses the free prostate vesicle (Fig. 18 & 19B–D: pv), the seminal duct (Fig. 18 & 19D: sd) and the male duct, which ends in an unarmed penis papilla (Fig. 17A, 18 & 19B: pp). The rest of the space of the copulatory bulb is filled with parenchymatic tissue, which appears syncytial (Fig. 18 & 19B: np). The seminal vesicles and the seminal duct are lined by a nucleated epithelium. The copulatory

bulb is surrounded by a thick coat of circular muscles, which gradually becomes thinner distally and eventually disappears toward the penis papilla. The prostate vesicle opens proximally into the ejaculatory duct (Fig. 18: ed), next to the opening of the seminal duct (Fig. 18: sd), hence the copulatory organ is of the divisa type (see Karling 1956 for details). The prostate vesicle consists of a number of a coarse-grained eosinophilic glands. A connection with these prostate glands and the ones entering the copulatory bulb could not be observed, but as nuclei are only found in the extracapsular parts it is most likely that both are part of the same glandular system. The male duct is lined by a nucleated epithelium and surrounded by a layer of longitudinal muscles. Distally, the epithelium is thicker, and the male duct forms the penis papilla, which protrudes into the male atrium (Fig. 18: ma). Only the distal part of the male atrium seems to be surrounded by muscles, which are longitudinal; no muscles were seen around the proximal part.

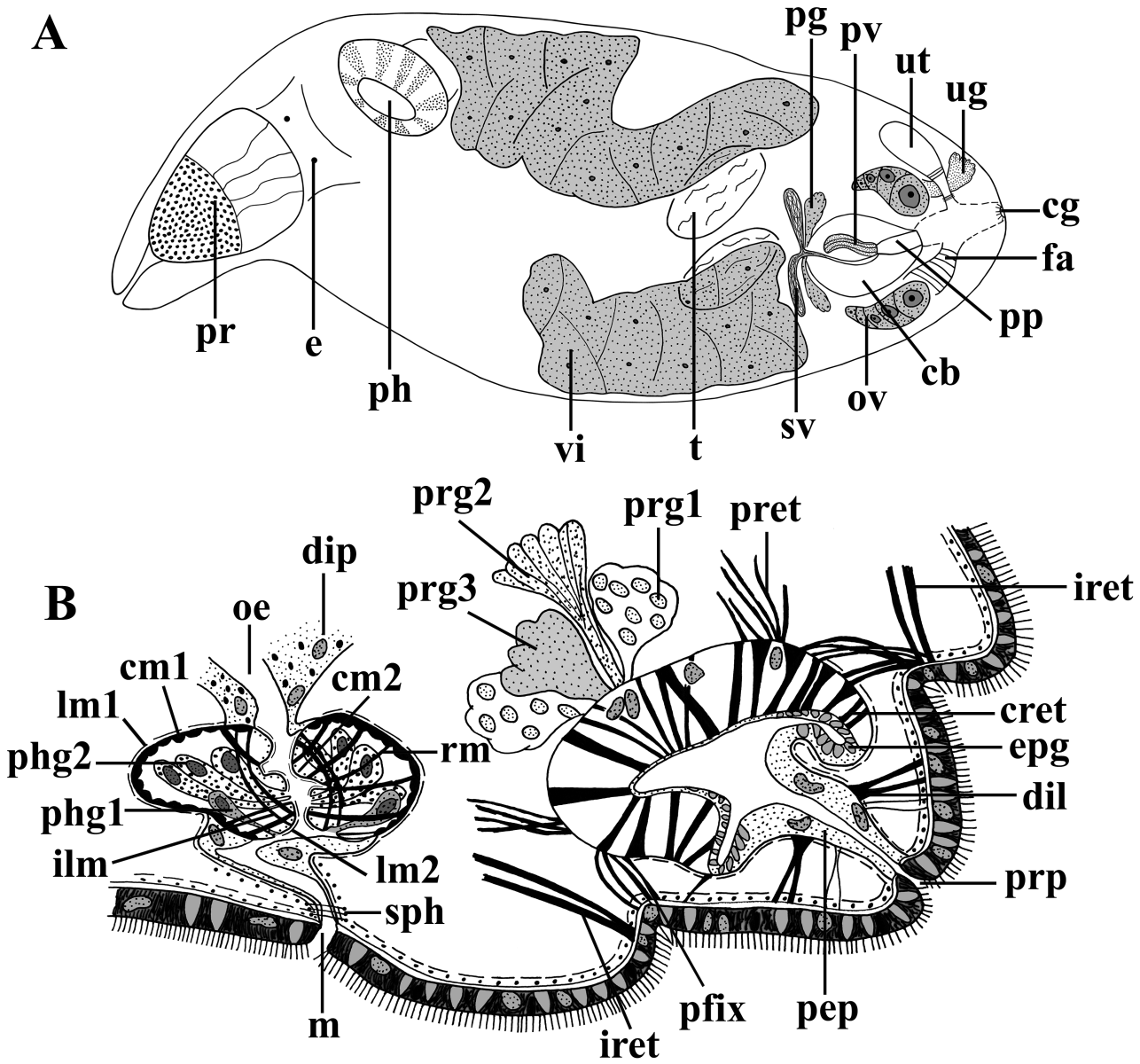

FIGURE 17. *Galapagetula cubensis* **sp. n.**. A, general organisation (from a live animal). B, sagittal reconstruction of the anterior body end from the right hand side.

The vitellaria (Fig. 17A & 19A–D: vi) extend along both sides of the body from behind the pharynx up to the level of the copulatory bulb. The elongated ovaries (Fig. 17A: ov) are located on either side of the copulatory bulb. The oocytes are organised in a row, increasing in diameter from the most proximal to the most distal one. The oviducts (Fig. 18: od) open into the female duct, which distally is a bit swollen (Fig. 18 & 19C–D: fd). Both the oviducts and the female duct are lined by a nucleated epithelium. Distally, the female duct is surrounded by a thin lon-

gitudinal muscle layer. It enters the female atrium through the latter's rostro-ventral wall (Fig. 17A, 18 & 19B: fa). Two bursae open into the female atrium. A resorptive bursa (Fig. 18 & 19B–C: b1) opens rostrally into the female atrium and contains degraded material. It is lined by a nucleated epithelium. Its distal, tubiform part (bursal stalk) is surrounded by thin longitudinal muscles. A well-developed sphincter occurs at the place where this bursa opens into the female atrium (Fig. 18: sph1, 19B–D: sph). A second, muscular bursa [Fig. 18 & 19D: b2; accessory bursa in the terminology of Reygel *et al.* (2011)] opens dorsal-rostrally into the female atrium. It is lined by a nucleated epithelium and surrounded by a layer of longitudinal muscles. The female atrium is lined by a nucleated epithelium and surrounded by an internal layer of longitudinal muscles and an external layer of very strong circular muscles (Fig. 19C: cm). The uterus (Fig. 17A, 18 & 19B–C: ut) is lined by a nucleated epithelium and by a longitudinal muscle layer. Coarse-grained basophilic (Fig. 18 & 19B: ubg) and fine-grained eosinophilic (Fig. 18 & 19B: ueg) glands open into the distal part of the uterus. Proximally and distally from these glands sphincters are present (Fig. 18: sph2 & sph3). The common genital atrium (Fig. 18: ca) is lined by a nucleated epithelium and by a longitudinal muscle layer. It opens to the outside through the common gonopore, which is situated exactly terminally (Fig. 17A, 18 & 19D: cg). The gonopore is surrounded by a sphincter (Fig. 18: sph4).

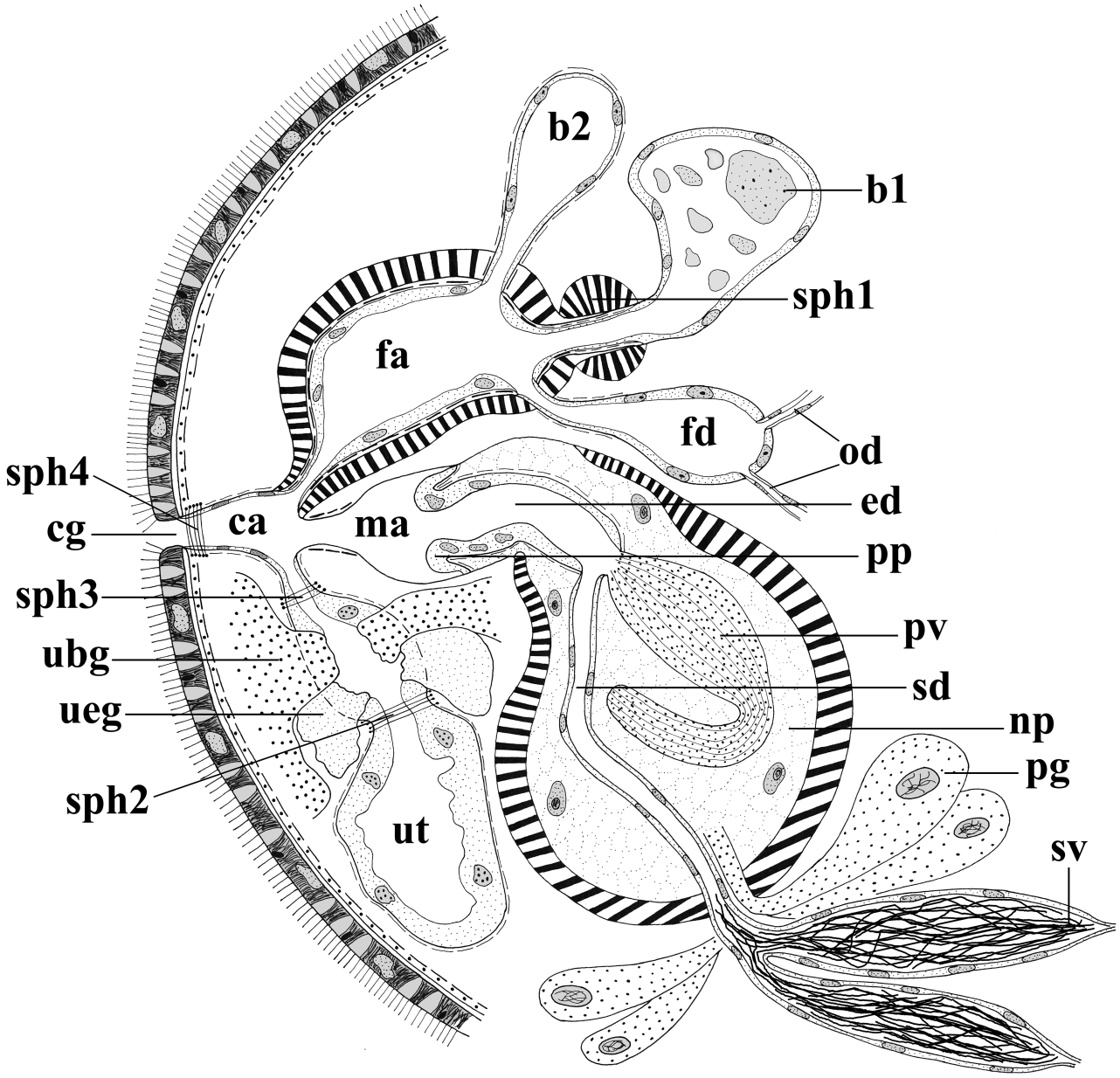

FIGURE 18. *Galapagetula cubensis* **sp. n.**. Sagittal reconstruction of the genital system from the right hand side.

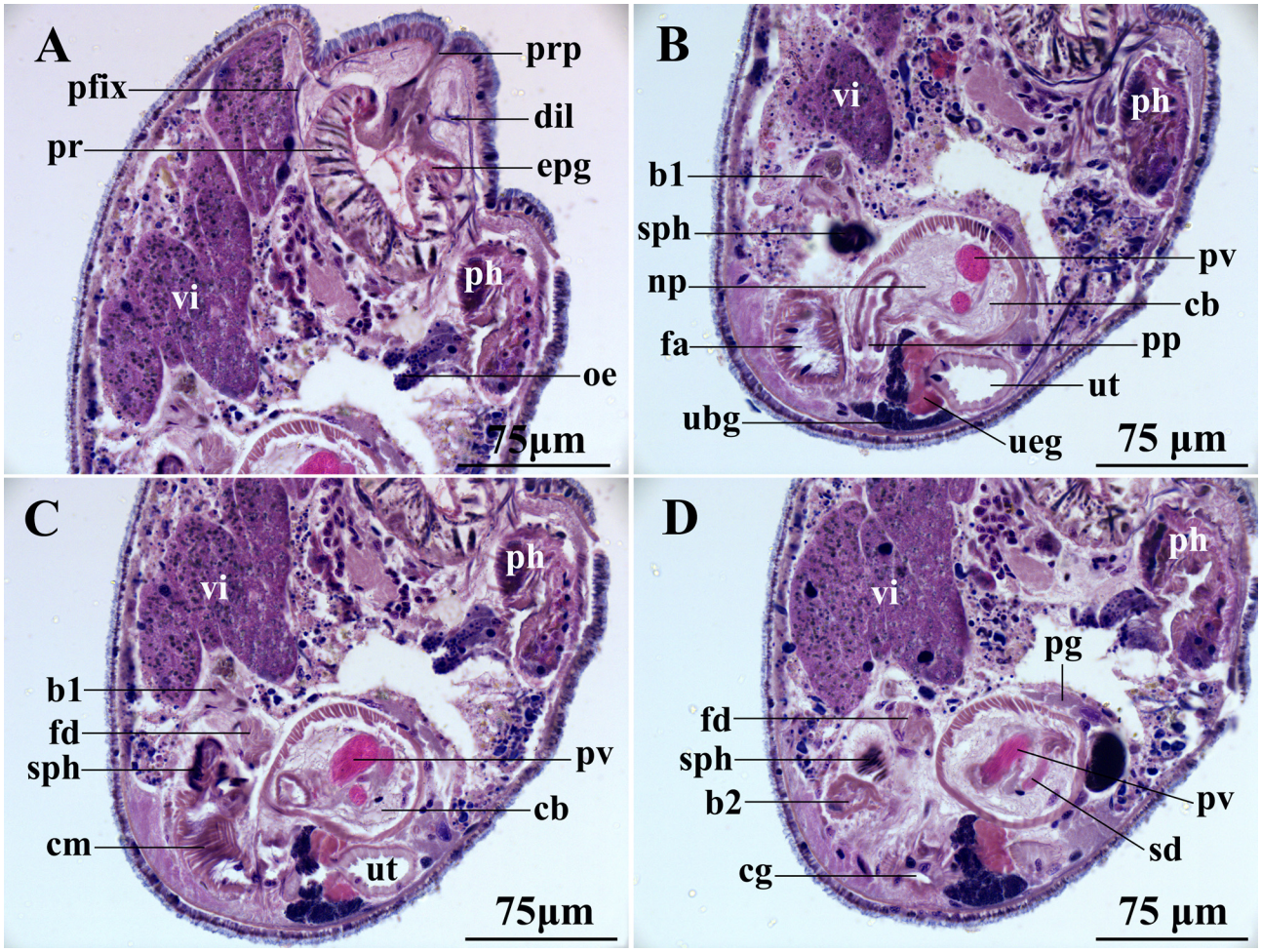

FIGURE 19. *Galapagetula cubensis* **sp. n.**. A, sagittal section through the anterior body end. B–D, sagittal sections through the genital system.

Utelga Marcus, 1949

Utelga heinckei (Attems, 1897) Karling, 1954

(Fig. 20A–C)

Known distribution. Western coast of USA, North Sea, Skagerrak, Irish Sea, Irish Atlantic coast (Karling 1980 and references therein). Skagerrak (Willems *et al.* 2007). Galapagos Islands (Reygel *et al.* 2011). British Columbia, Canada (Van Steenkiste & Leander 2018).

New records and material. Observations on live specimens. One whole mount (HU XIII.4.31) from Las Sardinas (19°56'24"N; 76°46'41"W), Santiago de Cuba, Cuba (June 21, 2017), on *Cladophoropsis macromeres* covered by silt, 0.7 m deep, salinity 32 ‰. One whole mount (HU XIII.4.32) and one serially-sectioned specimen (HU XIII.4.33) from Mala (29°05'0.53"N; 13°26'59"W), Lanzarote, Canary Islands (October 8, 2011), medium coarse calcareous sand, from a very steep slope, 48 m deep, salinity 35 ‰.

Remarks. The morphology of our specimens corresponds with the description of Karling (1980). Live specimens about 1 mm long, unpigmented, with a pair of eyes. The proboscis is about 10% of the body length. It shows the typical koinocystidid construction (see Brunet 1972; Karling 1980), without a juncture sphincter. The pharynx is located in the first body half. The testes lie caudal to the pharynx and ventral to the vitellaria. Two elongated ovaries are situated at the level of the copulatory bulb.

Copulatory bulb surrounded by a sheath of strong circular muscles. At the distal end of the copulatory bulb three sclerotised hooks (Fig. 20A–C) occur, which differ from each other in size. The largest hook is 13–14 µm long

(n = 2) and 5–6 μm wide proximally (n = 2). The smaller hooks are 4–6 μm long ($\bar{x}$ = 5 μm; n = 4) and 2–4 μm wide proximally ($\bar{x}$ = 3 μm; n = 4).

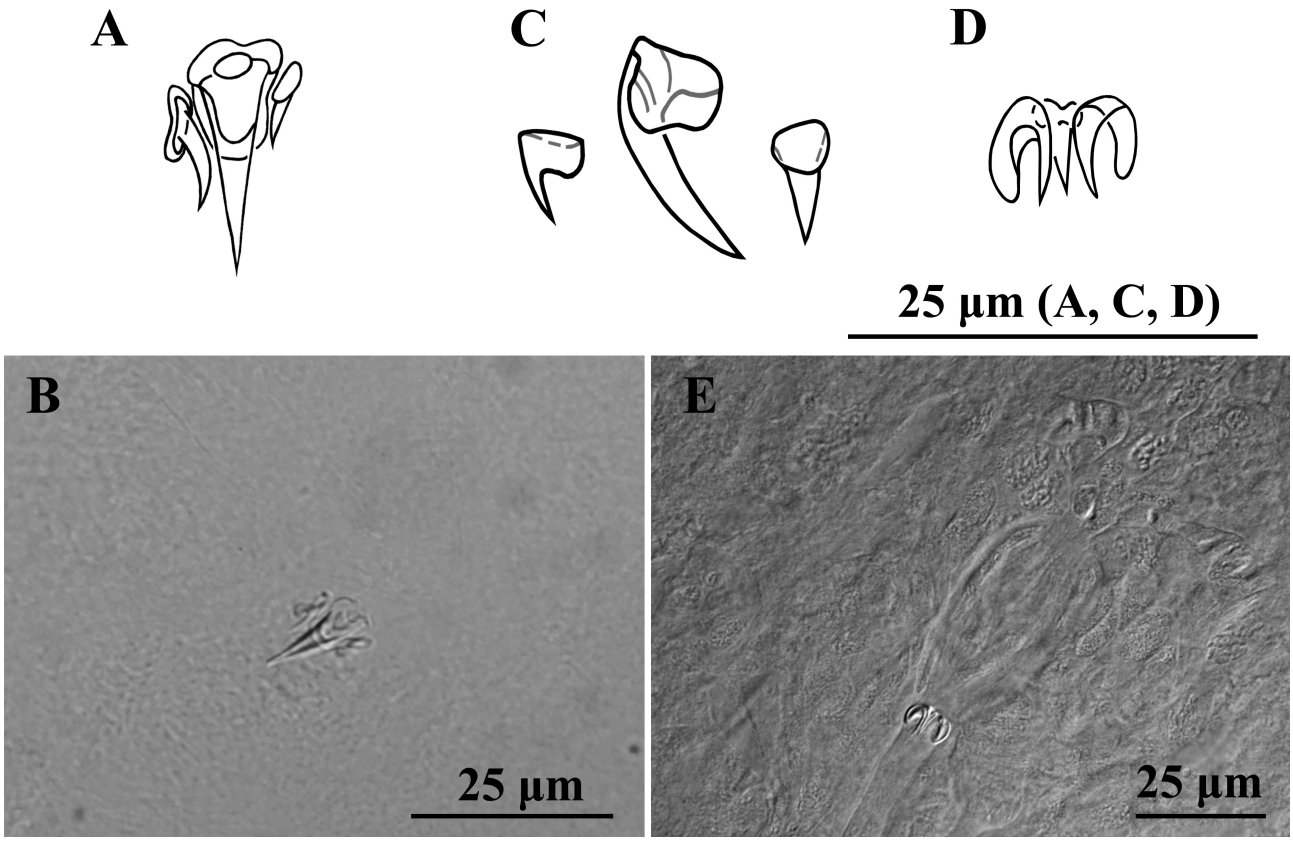

FIGURE 20. Hooks in species of *Utelga*. A–C, *Utelga heinckei*. D–E, *Utelga pseudoheinckei* (specimen from Sardinia). A–B, specimen from Cuba. C, specimen from Lanzarote. All with proximal end toward top of figure.

***Utelga pseudoheinckei* Karling, 1980**
(Fig. 20D–E)
urn:lsid:zoobank.org:act:27A436A5-2FD7-4059-A2D3-F75FF5104526

Syn. *Utelga heinckei* in Brunet (1965) and Mack-Fira (1974).

Known distribution. Korsfjord (Tekslo Island, Hordaland Fylke), Kleppholmen Island, and Fugloy Island, Norway; California, USA (Karling 1980). Marseille area, France (Brunet 1965); Black Sea, Romania (Mack-Fira 1974).

New records and material. Observations on live specimens. Four whole mounts (HU XIII.4.34–XIII.4.37) from Punta Negra (40°57'12"N, 8°13'43"E), Stintino, Sardinia, Italy (September 2018), on silty algae, 0.5 m deep, salinity 40 ‰.

Remarks. The morphology of the specimens corresponds with the description of Karling (1980). The general habitus and internal organisation are very similar to those in *U. heinckei*. The elongated copulatory bulb is 92–108 μm long ($\bar{x}$ = 100 μm; n = 2) and 35 μm wide (n = 2). In a third specimen, not fully developed, the copulatory bulb is 49 μm long and 21 μm wide. The three hooks (Fig. 20D–E) at the distal end of the copulatory bulb are all of the same length, 5–8 μm long ($\bar{x}$ = 7 μm; n = 6), with a broad base, curved and with a sharp tip.

***Simplexcystis* Diez, Reygel & Artois gen. n.**
urn:lsid:zoobank.org:act:27A436A5-2FD7-4059-A2D3-F75FF5104526

***Simplexcystis asymmetrica* Diez, Reygel & Artois gen. n. sp. n.**
(Fig. 21–23)
urn:lsid:zoobank.org:act:BB2226F6-C526-47E4-8B49-F5CF45AB242E

Material and distribution. Observations on one live specimen, serially sectioned afterwards, designated holotype (FMNH https://id.luomus.fi/KV.655), collected in Playa Chica (28°55'05"N, 13°40'07"W) (Type Locality), Puerto del Carmen, Lanzarote, Canary Islands (October 10, 2011), fine sand accumulated at the end of the rocky reef, 18 m deep, salinity 35 ‰.

Etymology. The genus name refers to the fact that the construction of the atrial organs in the new genus is relatively simple compared to that of other koinocystidids. The species name refers to the fact that the copulatory bulb is asymmetric due to the seminal duct entering laterally.

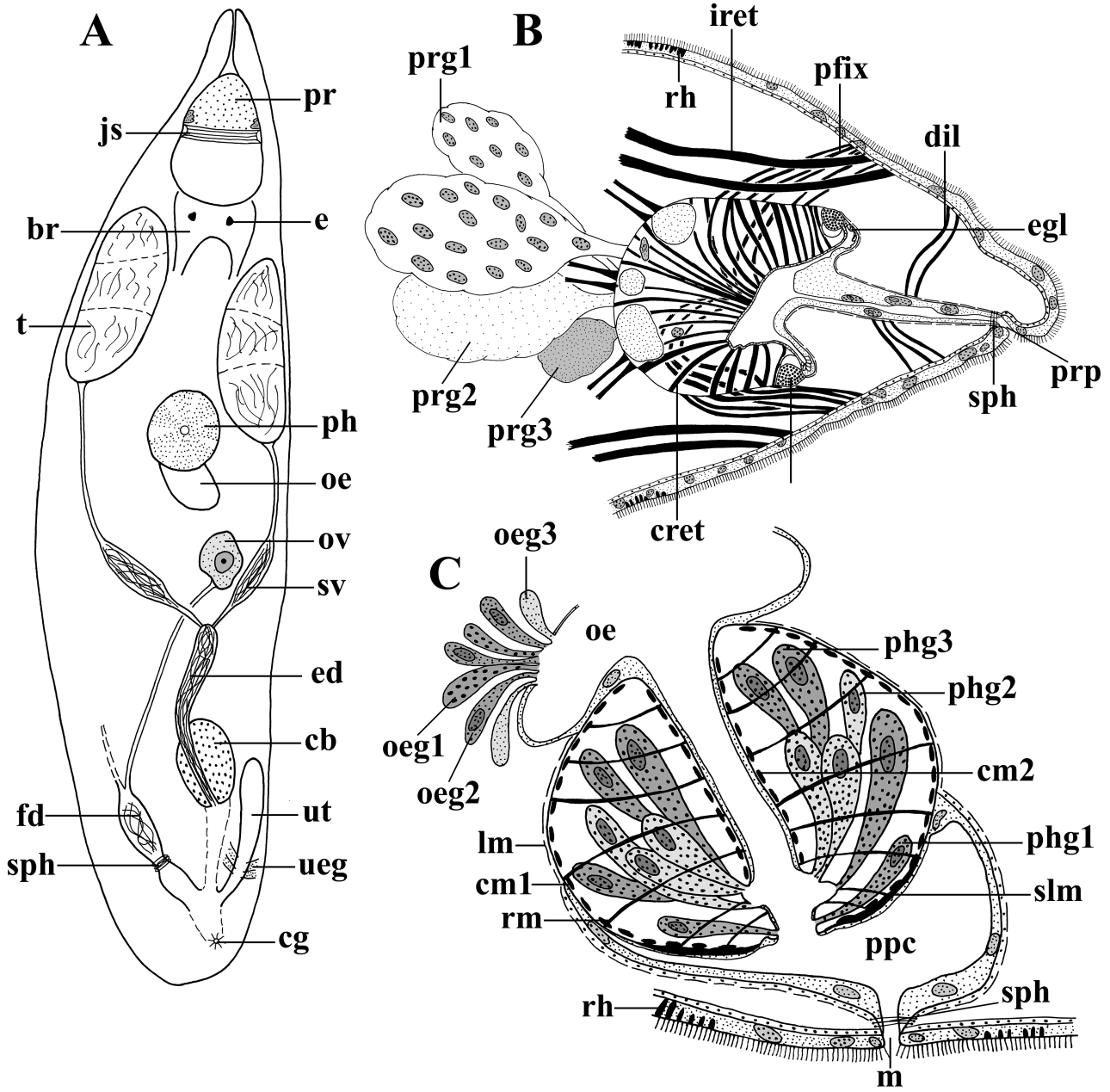

FIGURE 21. *Simplexcystis asymmetrica* **gen. n. sp. n.** A, general organisation (from a live animal). B, sagittal reconstruction of the proboscis from the right hand side. C, sagittal reconstruction of the pharynx from the right hand side.

Diagnosis of *Simplexcystis* gen. n. Representative of Koinocystididae with strong juncture sphincter in between proboscis bulb and cone. Male duct running eccentrically through the copulatory bulb, the latter also enclos-

ing the prostate vesicle. Copulatory organ devoid of any hard structure. Without bursa. Epithelium of the female, the male, and part of the common atrium lined by a brush border. All these structures surrounded by a sheath of muscles in different orientations.

Type species: *S. asymmetrica* **sp. n.** (by monotypy). Provisionally with the same diagnosis as the genus.

Description. Live specimen about 1.5 mm long, translucent, with pinkish parenchymal glands and a pair of eyes (Fig. 21A: e). The brain (Fig. 21A: br) is located caudally from the proboscis. The syncytial and fully ciliated epidermis is 5–7 µm thick, with cilia 3–4 µm long. The epidermis shows many vacuoles some of which are empty, others filled with a dark, granular secretion. The epidermis shows many rhabdites (Fig. 21B–C, 22 & 23C–E: rh) all over the body, except for the part anterior to the proboscis. Rhabdites are also lacking around the mouth and gonopore. The rhabdites situated near the apical surface of the epithelium are globular, 1–2 µm in diameter, while those more to the basal part of the epithelium are more elongated (3–4 µm long).

The proboscis (Fig. 21A: pr, 21B, 23A) is of the typical koinocystidid construction (see Brunet 1972; Karling 1980), with well-developed cone retractors (Fig. 21B & 23A: cret) and nuclei in the parenchyma of the proboscis bulb. In between the bulb and the cone there is a strong juncture sphincter (Fig. 21A–B & 23A: js). In the live specimen, the proboscis is about 15% of the body length. Several types of glands enter the proboscis through its caudal wall: dorsally coarse-grained basophilic ones (Fig. 21B: prg1), more centrally larger, fine-grained eosinophilic glands (stained pinkish) (Fig. 21B: prg2), and ventrally small fine-grained eosinophilic glands (stained yellowish) (Fig. 21B: prg3). There are three pairs of proboscis retractors (Fig. 21B: pret). The exact number of fixators (Fig. 21B & 23A: pfix) and dilatators (Fig. 21B: dil) could not be determined. There is one pair of ventral and one pair of dorsal integument retractors (Fig. 21B: iret). The proboscis sheath is lined by a high, nucleated epithelium and is surrounded by an external longitudinal muscle layer. The sheath epithelium is continuous with the epithelium of the proboscis cone, which is very low and devoid of nuclei. The most proximal part of the sheath epithelium contains some oval to circular-shaped eosinophilic gland cells (Fig. 21B & 23A: egl). The epithelium surrounding the cone is lined by a brush border (Fig. 23A: bb). The proboscis pore (Fig. 21B: prp) is surrounded by a sphincter (Fig. 21B: sph).

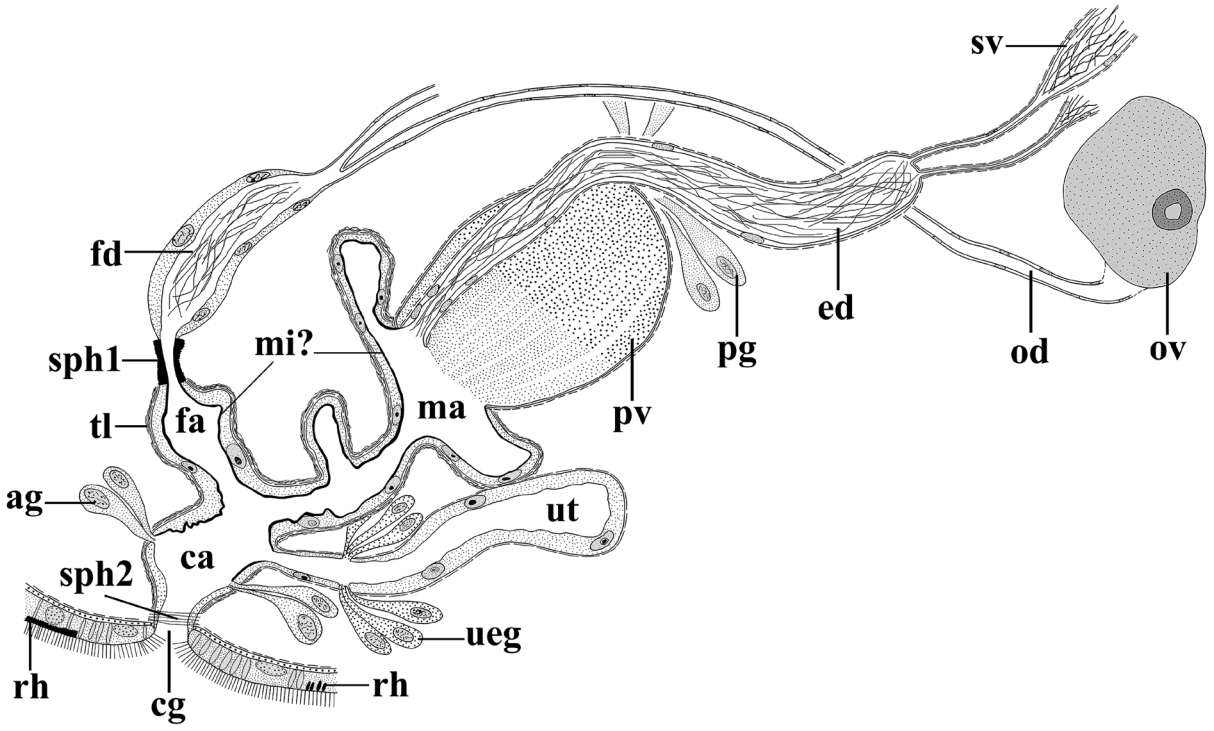

FIGURE 22. *Simplexcystis asymmetrica* **gen. n. sp. n.** Sagittal reconstruction of the genital system from the right hand side.

The pharynx (Fig. 21A: ph, 21C, 23B) is located at 40%. In the live specimen, it has a diameter of 10% of the body length. The prepharyngeal cavity (Fig. 21C: ppc) is lined by a nucleated epithelium, and is surrounded by an internal circular and an outer longitudinal muscle layer. The mouth (Fig. 21C: m) can be closed by a sphincter (Fig. 21C: sph). Three types of glands open into the pharynx lumen: coarse-grained eosinophilic ones (stained reddish) opening most distally (Fig. 21C & 23B: phg1), and, opening more proximally coarse-grained eosinophilic ones

(stained dark pinkish) (Fig. 21C & 23B: phg2) and coarse-grained basophilic ones (stained greenish) (Fig. 21C & 23B: phg3). The oesophagus (Fig. 21A, 21C & 23B: oe) is lined by a nucleated epithelium. A bundle of glands (Fig. 23B: oeg) opens into the oesophagus. It consists of coarse-grained basophilic glands (Fig. 21C: oeg1), fine-grained basophilic ones (Fig. 21C: oeg2), and fine-grained eosinophilic ones (Fig. 21C: oeg3). The pharynx lumen is surrounded by a low, nucleated epithelium. The musculature of the pharynx consists of a layer of longitudinal muscles outside of the septum (Fig. 21C: lm), which is continuous with the longitudinal muscles surrounding the prepharyngeal cavity, and a circular one just inside of the septum (Fig. 21C: cm1). The distal opening of the pharynx is lined by a thick layer of longitudinal muscles, which in sagittal section, gives the impression of forming a lip-like structure (Fig. 21C & 23B: slm). The pharynx lumen is surrounded by a circular muscle layer (Fig. 21C: cm2). Radial muscles run (Fig. 21C & 23B: rm) between the wall of the pharynx lumen and the outer septum.

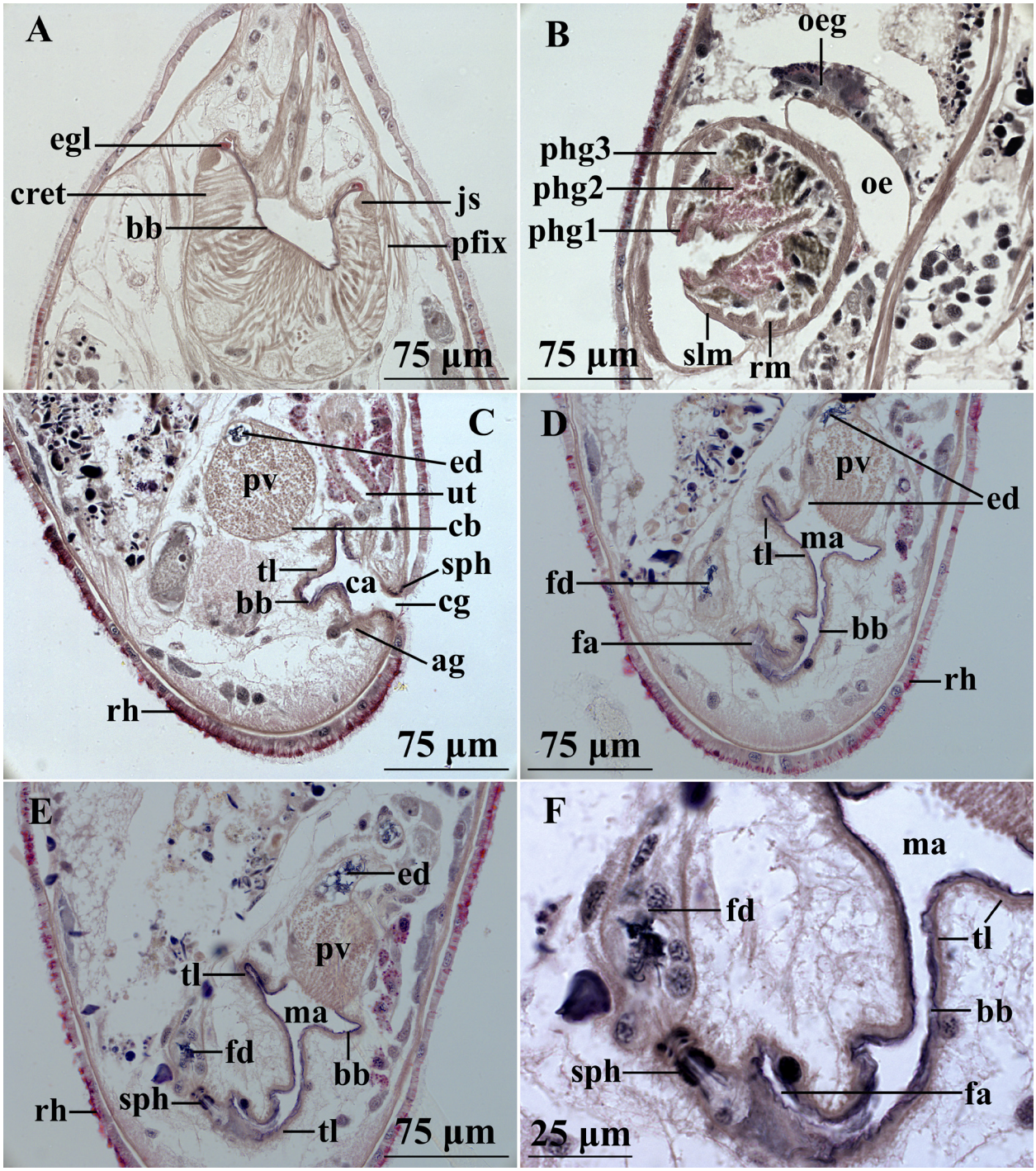

FIGURE 23. *Simplexcystis asymmetrica* **gen. n. sp. n.** A, sagittal section through the proboscis. B, sagittal section through the pharynx. C–F, sagittal sections through the atrial organs.

The two elongated testes (Fig. 21A: t) are located rostrally from the pharynx. They seem to be divided into three follicles that are closely packed together. However, this could also be an optic effect caused by the testes being heavily folded. The vasa deferentia run towards the caudal body end, and distally form the elongated seminal vesicles (Fig. 21A & 22: sv). The seminal vesicles are lined by a low, nucleated epithelium, and are surrounded by longitudinal muscles. The copulatory bulb is oviform, and lies in the caudal body third (Fig. 21A & 23C: cb). It is surrounded by a longitudinal muscle layer. Distally from the seminal vesicles, the vasa deferentia enter the ejaculatory duct separately (Fig. 21A, 22 & 23C–E: ed). The ejaculatory duct is elongated, with its distal half situated eccentrically within the copulatory bulb (Fig. 21A & 23C: cb). Distally the seminal duct opens into the male atrium, surrounded by the prostate vesicle (Fig. 22 & 23C–E: pv), which also opens in the male atrium. The seminal duct is lined by a low nucleated epithelium, and is surrounded by longitudinal muscles. The prostate glands (Fig. 22: pg) are extracapsular, without clearly separated gland necks in the prostate vesicle. The latter contains a coarse-grained eosinophilic secretion in its proximal half and a fine-grained one in its distal half. The male atrium (Fig. 22 & 23D–F: ma) is divided into a short, broad proximal part, and a tubiform distal part, which ends in the common genital atrium (Fig. 22 & 23C: ca). The male atrium, the female atrium, and the common genital atrium are lined by a nucleated epithelium and are surrounded by longitudinal muscles. Outside of this longitudinal muscle layer, a thick layer of muscles with different orientations (probably circular and oblique ones) and connective tissue occurs (Fig. 22 & 23C–F: tl). At its apical side the epithelium is lined by a brush border (Fig. 22 & 23D–F: bb), which is lacking in the most distal part of the common genital atrium.

In the live specimen, we only observed a single, poorly differentiated ovary (Fig. 21A & 22: ov), located at the level of the seminal vesicles. In the serially-sectioned specimen, we observed two weakly developed oviducts, suggesting that the female system in full maturity has two ovaries. The very long oviducts (Fig. 22: od) are lined by a nucleated epithelium; muscles were not observed. They open proximally into the female duct (Fig. 21A, 22 & 23D–F: fd). The female duct is lined by a nucleated epithelium and contains sperm. It opens into the female atrium (Fig. 22, 23D & 23F: fa) through a strong sphincter (Fig. 21A & 23E–F: sph, 22: sph1). The female atrium enters the common genital atrium dorsally. There is no bursa. The uterus (Fig. 21A, 22, 23C: ut) is lined by a nucleated epithelium and surrounded by longitudinal muscles. Coarse-grained eosinophilic uterine glands (Fig. 22: ueg) open into the uterus somewhat proximally from the entry point into the common genital atrium. Just distally from the entry point of the uterus, some fine-grained eosinophilic atrial glands (Fig. 22: ag) enter the common genital atrium. The common gonopore lies ventrally, at about 95% (Fig. 21A, 22 & 23C: cg), and can be closed by a sphincter (Fig. 22: sph2, 23C: sph).

Molecular phylogenetic account

The 18S and 28S rRNA sequence data sets include sequences from 20 specimens and 17 taxa, and 1,765 bp and 1,659 bp, respectively (concatenated data set 18S + 28S of 3,424 bp). Bayesian and ML topologies were congruent. The results of the phylogenetic analyses are shown in Figure 24. The monophyly of Koinocystididae is confirmed (pp = 0.99; SH-aLRT = 94.4; UFboot = 91). Our results show a basal trichotomy within Koinocystididae: (1) *Mesorhynchus terminostylis*, (2) a clade with the two species of *Utelga*, and (3) a clade comprising all other included koinocystidids. Within the latter clade, another polytomy is retrieved, consisting of three clades each of which containing species that were considered to belong to *Itaipusa*: (1) clade 'sinensis' including *Rhinolasius dillonicus* and *Koinogladius sinensis* (Wang & Lin, 2017) **comb. n.** (pp = 1; SH-aLRT = 99.5; UFboot = 98); (2) clade 'divae' including *Itaipusa biglandula*, *I. karlingi*, *I. divae* and *I. novacaledonica* **sp. n.** (pp = 1; SH-aLRT = 100; UFboot = 100), in which *I. biglandula* and *I. karlingi* are sister taxa (pp = 1; SH-aLRt = 99.1; UFboot = 100), as are *I. divae* and *I. novacaledonica* **sp. n.** (pp = 1; SH-aLRt = 100; UFboot = 100); (3) a clade including *Sekerana stolzi*, *Reinhardorhynchus riegeri* **comb. n.**, *R. anamariae* **sp. n.**, *R. hexacornutus* **sp. n.**, *R. tahitiensis* **sp. n.** and two undescribed species (*Itaipusa* n. sp. 1 and Koinocystididae sp1) (pp = 0.99; SH-aLRT = 95.7; UFboot = 97). The above-mentioned species of *Reinhardorhynchus* **gen. n.** and Koinocystididae sp1 together form a well-supported monophylum: clade 'riegeri' (pp = 0.99; SH-aLRT = 100; UFboot = 86). Deep relationships within the latter clade are not resolved; however, *R. riegeri* **comb. n.**, *R. anamariae* **sp. n.** and *Itaipusa* n. sp. 1 together form a monophyletic group (pp = 1; SH-aLRT = 100; UFboot = 100).

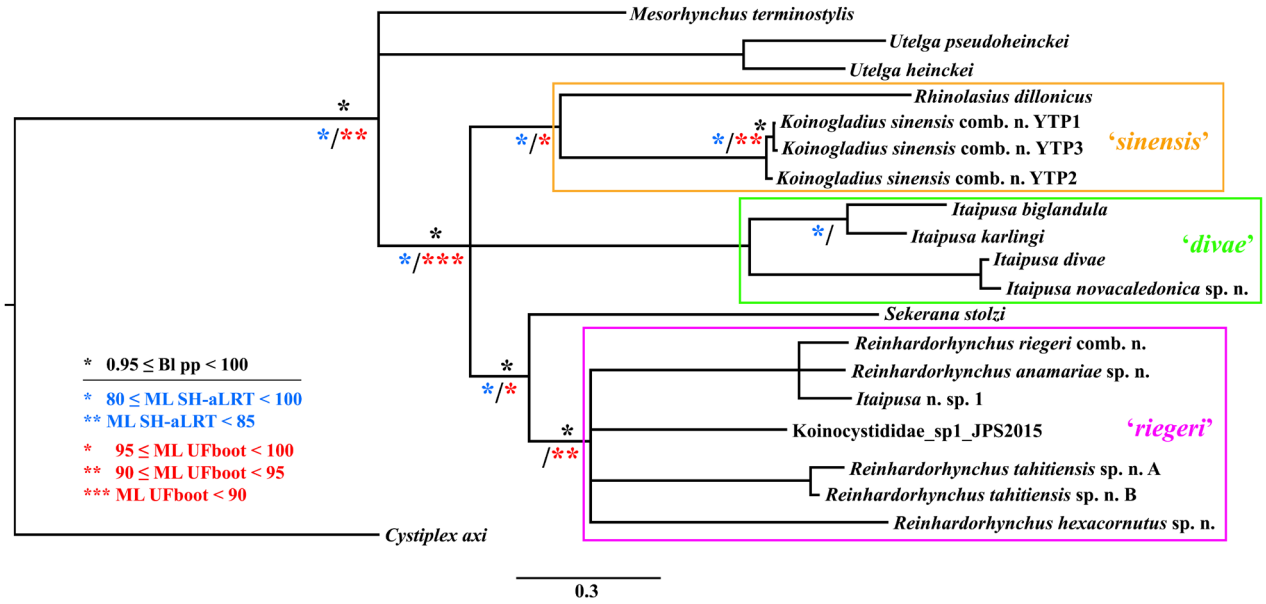

FIGURE 24. Majority-rule consensus tree from the Bayesian analysis of the concatenated 18S+28S rDNA dataset. Branches with support values below the thresholds in the legend of the three analyses were collapsed. Symbols above branches represent posterior probabilities (*: 0.95 ≤ pp < 100). Symbols below branches indicate bootstrap values (*: 80 ≤ SH-aLRT < 100, **: SH-aLRT < 85) and ultrafast bootstrap values (*: 95 ≤ bootstrap ≤ 100, **: 90 ≤ UFboot < 95, ***: UFboot < 90) from the maximum likelihood analysis. Branches without symbols have pp = 1, bootstrap = 100 and UFboot = 100).

Discussion

Interrelationships of Koinocystididae. To this date, the family Koinocystididae has largely been neglected in molecular phylogenetic studies. Indeed, only a small fraction (< 5%) of the known species was included in the analyses by Tessens *et al.* (2014), Smith *et al.* (2015), and Lin *et al.* (2017). Due to this poor taxon coverage, the interspecific relationships within Koinocystididae remain elusive to this day. However, the above-mentioned studies already indicated that the family is monophyletic, which is here confirmed based on a more comprehensive dataset (pp = 0.99; SH-aLRT = 94.4; UFboot = 91). *Mesorhynchus terminostylis* is part of Koinocystididae, but its intrafamilial position remains unresolved. In the following section, an in-depth taxonomic discussion of all the species of koinocystidids included in this work is presented. The value of the respective morphological traits used to delineate species and genera are discussed in the framework of the newly-presented phylogeny.

Utelga. *Utelga* appears as a monophyletic clade in all analyses. *Utelga pseudoheinckei* is distinguished from *U. heinckei* by the presence of three identical hooks in the copulatory bulb, whereas the hooks differ in length from each other in *U. heinckei*. The hook lengths in the specimens from Sardinia (5–8 µm) fall within the size range of 4–12 µm reported by Karling (1980). In the newly-collected specimens of *U. pseudoheinckei*, the length/wide ratio of the fully developed copulatory bulb is 2.8, while Karling (1980) recorded a ratio of 4–5.

Our specimens of *U. heinckei* have smaller hooks than those reported for the populations occurring in the northern and western Atlantic (22–36 µm long) (Karling 1980) and from the Skagerrak area (10–23 µm) (Willems *et al.* 2007). Specimens of *U. heinckei* recorded by Reygel *et al.* (2011) from Galapagos and by Van Steenkiste & Leander (2018) from Vancouver Island possess much larger hooks (34–40 µm). Moreover, the large hook and two small hooks differ 8–9 µm in size in our specimens, a larger length difference compared to the 5 µm reported by Reygel *et al.* (2011) and the 3 µm reported by Van Steenkiste & Leander (2018).

Overall, the new findings indicate a high degree of morphological variation within these two species. Combined with their widespread distribution (see Willems *et al.* 2007 and references therein), it is reasonable to conjecture that these species might constitute species complexes, reflected in their hook morphologies. To resolve this, a more thoroughly-sampled dataset is imperative, including specimens of *Utelga* sampled at different localities and with differing (hook) morphologies.

Three clades (previously) known as *Itaipusa.* The genus *Itaipusa* as it was conceived up to now is not recovered in the topology. After collapsing the weakly supported nodes, three separate groups containing species of *Itaipusa* emerge within Koinocystididae. These clades are labelled '*sinensis*', '*divae*' and '*riegeri*' in Figure 24. The taxonomy and phylogeny of and within these three clades will be discussed in the following sections. Both ML and BI analyses recovered *S. stolzi* as the sister taxon to clade '*riegeri*' (pp = 0.99; SH-LRT = 100; UFboot = 86). *Sekerana stolzi* is an atypical, poorly-known species, with strongly-reduced internal structures (proboscis, pharynx, copulatory bulb) (see Karling 1980). It is known exclusively from freshwater, in contrast to all species of *Itaipusa* which are either marine or brackish.

Clade '*sinensis*': *Koinogladius* gen. n. and *Rhinolasius.* Clade '*sinensis*' contains three previously-published sequences of *Itaipusa sinensis* and is strongly supported (pp = 0.98; SH-LRT = 84.6; UFboot = 94). *Itaipusa sinensis* is an aberrant koinocystidid, being the only described species with a copulatory bulb enclosing a cirrus, two hooks and a stylet. *Rhinolasius dillonicus* appears as the sister taxon to *I. sinensis* (pp = 1, SH-LRT = 99.5; UFboot = 98). As the type species of *Itaipusa* (*I. divae*) falls outside this clade, the phylogeny warrants erection of a new genus: *Koinogladius* Diez, Monnens & Artois **gen. n.** (Etymology: composed by the prefix *Koino*, referring to the family Koinocystididae, and the suffix *gladius* (Lat.) = sword, which refers the presence of the stylet within the copulatory bulb) (urn:lsid:zoobank.org:act:1D672D44-5695-416E-A24D-B2F25BCCD80B). Both *Koinogladius sinensis* (Wang & Lin in Lin *et al.*, 2017) **comb. n.** and *R. dillonicus* have the testes at midbody, caudally from the pharynx. In *K. sinensis* **comb. n.**, the ejaculatory duct runs through the stylet, a feature which differentiates the new genus from *Brunetia* Karling, 1980, the only other koinocystidid genus with a stylet. In *Brunetia camarguensis* (Brunet, 1965) Karling, 1980, the ejaculatory duct indeed runs beside the stylet. Another distinguishing feature between these two genera is the lack of an armed cirrus in *Brunetia* (see Brunet 1965; Karling 1980).

It is also worth noting that the topology shows that the presence or absence of a proboscis juncture sphincter cannot be used to differentiate between groups within Koinocystididae, as was already apparent from the morphological phylogeny of Karling (1980). Indeed, this structure is lacking in *Utelga* and *R. dillonicus*, each of which are positioned at different locations in the tree, implying that this structure has been lost and/or acquired multiple times.

Clades '*divae*' and '*riegeri*'. Apart from *I. sinensis* (now *K. sinensis* **comb. n.**), the genus *Itaipusa* contained 16 species up to now (Karling 1980; Reygel *et al.* 2011; Willems *et al.* 2017). Traditionally, representatives of *Itaipusa* were identified by the presence of a strong proboscis juncture sphincter and a pharynx without a closing mouth sphincter (Marcus 1949; Karling 1980, but see further). The copulatory bulb is globular-oviform and muscular, with an irregular spiny cirrus or spiny papilla, except in *I. biglandula,* which lacks any hard parts (see Reygel *et al.* 2011; Van Steenkiste & Leander 2018). In several species, robust accessory hooks are also present.

The present phylogeny shows that the remaining species of *Itaipusa* form two separate, well-supported clades that together do not form a monophyletic group, as clade 'riegeri' forms a sister group relationship with *Sekerana stolzi*. Therefore, these two clades are better considered separate genera. Clade '*divae*' contains the type species of *Itaipusa* (*I. divae*), and, therefore, remains *Itaipusa*. For clade '*riegeri*' a new genus was erected: *Reinhardorhynchus* Diez, Monnens & Artois **gen. n**.

Clade '*divae*': *Itaipusa* sensu novo. The four species of this group included in the molecular phylogenetic analyses cluster together in a clade (Clade '*divae*' in Figure 24; pp = 1; SH-LRT = 100; UFboot = 100). All these species lack accessory hooks in the male system, a feature distinguishing them from species of *Reinhardorhynchus* **gen. n.** Based on this diagnostic feature, eight previously-described and two new species can be placed in *Itaipusa*: *I. aberrans* **sp. n.,** *I. acerosa*, *I. biglandula*, *I. divae*, *I. karlingi*, *I. novacaledonica* **sp. n**., *I. sbui*, *I. similis*, *I. sophiae*, and *I. spinibursa*.

The presence or absence of a mouth sphincter was not included as a diagnostic character in the genus diagnosis by Marcus (1949), but its presence was later added by Karling (1980). A mouth sphincter was observed in *I. divae* (from New Caledonia), making it clear that the absence of this structure cannot be considered as diagnostic for the genus as it is conceived now. A novel feature never before described for *Itaipusa* or any other koinocystidid is the fact that the longitudinal muscles inside the septum of the pharynx form a lip-like structure distally. This feature was observed in all the species of which serial sections were available: *I. divae*, *I. karlingi*, and *I. sbui*.

Of all species in this group, only *I. biglandula* lacks hard structures in the male system, its copulatory organ proper consisting of an unarmed penis papilla (see Reygel *et al.* 2011). According to Graff (1905), also *I sophiae* has a copulatory organ proper that is a penis papilla, but in this species it is covered with spines of different sizes

and morphology. In our phylogenetic reconstruction, *I. biglandula* **n. sp.** forms a sister group relationship with *I. karlingi*, a species with a spiny cirrus (see further), which suggests the unarmed cirrus is a derived condition.

Itaipusa acerosa, *I. similis*, *I. sophiae*, and *I. spinibursa* can easily be distinguished from all other species in this genus by the presence of spines in the bursa (*I. spinibursa* and *I. sophiae*) or the fact that there is only a single row of spines in the cirrus (*I. acerosa* and *I. similis*).

Itaipusa aberrans **n. sp.** is the only species of *Itaipusa* that has a cirrus consisting of two folded plates bearing triangular spines, both of which are connected by a duct armed with small, folded, sclerotised structures. This unique construction of the armament of the cirrus diagnostic.

In *I. divae*, the armed cirrus consists of a compact structure built up by at least three transverse spiny rows consisting of scale-shaped spines, a situation unique within the group. The remaining three species (*I. karlingi*, *I. novacaledonica* **n. sp.**, and *I. sbui*) all have an armed cirrus that consists of at most two rows of triangular spines, but these rows are never organised in transverse bands as is the case in *I. divae*. In our phylogeny, *I. novacaledonica* **n. sp.** is recovered as the sister species of *I. divae*. Both species can easily be distinguished from each other by the construction of the armed cirrus, which *in I. novacaledonica* **n. sp.** contains two bands of spines that run longitudinally within the copulatory bulb, a situation clearly distinguishing it not only from *I. divae* (see above), but also from *I. karlingi* and *I. sbui*. In these two species, the two spiny cirrus belts are more or less perpendicular to the longitudinal axis of the cirrus. In *I. novacaledonica* **sp. n.**, the two spiny belts are M shaped and inverted U shaped, respectively, while in *I. sbui*, one belt has the appearance of a twisted figure eight and the other one is U shaped (see Willems *et al.* 2017).

In both *I. novacaledonica* **sp. n.** and *I. karlingi* the copulatory bulb ends in a penis papilla, which is not the case in the other species of *Itaipusa.* This papilla is sclerotised in *I. novacaledonica* **n. sp.**, but not so in *I. karlingi*. Moreover, the bursa of *I. karlingi* is ornamented with sclerotised belts, which is not the case in *I. novacaledonica* or *I. sbui*.

Clade '*riegeri*': *Reinhardorhynchus* gen. n. Four species characterised by the presence of accessory hooks in the male system were included in the phylogenetic analyses, and they form a well-supported clade with an unidentified species of koinocystidid from North Carolina and with *Itaipusa* n. sp. 1 (Clade '*riegeri*' in Figure 24; pp = 0,99; SH-LRT = 100; UFboot = 86). The former has accessory hooks (Julian Smith, pers. comm.), while *Itaipusa* n. sp. 1 also has a copulatory bulb armed with spiny rows and at least one accessory hook (own unpublished data).

The hard structures of the copulatory bulb of *R. riegeri* **comb. n.** are considerably smaller in the specimens from Cuba compared with those of the specimens from Bermuda. In the specimens from Bermuda the papillary cirrus is 135 µm long (vs. 117 µm in the Cuban specimens), armed with spines of maximum 15 µm long (vs. 2–8 µm); the ejaculatory cirrus is 45 µm long (vs. 64 µm), armed with spines of maximum 40 µm long (vs. 7–17 µm), and the accessory hooks are 115 µm and 145 µm long, respectively (vs. 56 µm and 107 µm) (see Karling 1978). However, as these are the only differences that can be found, we include the Cuban population within *R. riegeri* **comb. n**.

The specimens of *R. ruffinjonesi* **comb. n.** from the different localities show small morphological differences in the hard structures of the copulatory bulb. The length of the spiny belt varies from 165 µm in the specimen from Brazil to ±260 µm in specimens collected in Panama. In the specimens from Cuba a length of ±176 µm is recorded. Accessory hooks are largest in the specimen from Bermuda (72 µm and 45 µm long, respectively). In the new material, these structures vary in size from 54 to 62 µm (large hook) and from 27 to 33 µm (small hook), respectively. The distal spines of the spiny belt are slightly variable in shape, but all are more or less triangular and distally curved (see Fig. 5C, 5F, 5I, 6B–D, 6F). However, this variation might be attributed to the orientation of the spines and squeezing of the specimens.

Four species in this group, *R. riegeri* **comb. n.**, *R. variodentata* **comb. n.**, *R. pacificus* **sp. n.** and *R. unicornis* **sp. n.** have a copulatory bulb with two armed cirri: the ejaculatory cirrus and the papillary cirrus (terminology of Karling 1978). A third additional cirrus is present in *R. pacificus* **sp. n**. *Reinhardorhynchus unicornis* **sp. n.** is easily distinguished from the other three species mentioned, and from all other species with accessory hooks, by the presence of only one accessory hook in the copulatory bulb. All other species have two accessory hooks.

The presence of three cirri in the copulatory bulb of *R. pacificus* **sp. n.** is unique within *Reinhardorhynchus* **gen. n.**, and hence clearly diagnostic. The morphology of the hooks of *R. pacificus* **sp. n.** is similar to that in *R. variodentata* **comb. n**. In both species the hooks are funnel-shaped and have a broad base. However, they clearly differ in size from each other in *R. variodentata* **comb. n.** (90 µm and 50 µm long respectively, measured in the holotype), whereas they are similar in size in *R. pacificus* **sp. n.** (83 µm and 81 µm). The proximal sphincter in the papillary cirrus was only observed in *R. pacificus* **sp. n.**, and not in any of the other species.

Another species bearing a papillary cirrus inside the copulatory bulb is *R. hexacornutus* **sp. n.** However, this species lacks an armed ejaculatory cirrus. In addition, *R. hexacornutus* **sp. n.** is the only known species of *Reinhardorhynchus* in which the ejaculatory duct opens into the male atrium distally, independently of the prostate vesicle, hence forming a divisa-type copulatory organ (terminology of Karling, 1956). This is an uncommon organisation in Koinocystididae, previously only reported in the unrelated taxon *Mesorhynchus terminostylis* and in this contribution also in *Galapagetula cubensis* **sp. n**. (see further). The entire copulatory system in both *R. hexacornutus* **n. sp.** and *G. cubensis* **sp. n.** is surrounded by a muscular septum. As such, it could be considered as a divisa-duplex type copulatory organ, a situation unique within eukalyptorhynchs. The nail-shaped cirrus spines are unique for *R. hexacornutus* **sp. n.**, as these spines are consistently triangular or scale-shaped in all other species of *Reinhardorhynchus* **gen. n.** The copulatory bulb of *R. hexacornutus* **sp. n.** carries six hooks, the largest number within the genus. Only two other species of *Reinhardorhynchus* **gen. n.** have more than two hooks: three in *R. evelinae* **comb. n.** and five in *R. scotica* **comb. n.**

Reinhardorhynchus beatrizae **sp. n.** and *R. soror* **sp. n.** both have a cirrus armed with triangular spines and a belt of large spines. This combination of armature is only known from *R. ruffinjonesi* **comb. n.** and *R. anamariae* **sp. n**. Both new species differ from *R. ruffinjonesi* **comb. n.** because of their broad hook bases, a funnel-like structure on the larger hook, and well-developed spines in the spiny belts. These characters are all absent in *R. ruffinjonesi* **comb. n.**

Reinhardorhynchus beatrizae **sp. n.** differs from *R. soror* **sp. n.** in the morphology of the proximal spines of the spiny row. These spines are curved, hook-like, and fused at their bases in *R. soror* **sp. n.**, while they are scale-like and not fused in *R. beatrizae* **sp. n**. Moreover, the spines are larger in *R. soror* **sp. n.** (largest proximal spines ±57 μm long and distal ones ±39 μm long) than in *R. beatrizae* **sp. n.** (largest proximal spines ±23 μm long and distal ones ±32 μm long). The spiny belt is ±347 μm long in *R. beatrizae* **sp. n.** and ±437 μm in *R. soror* **sp. n**. Furthermore, the accessory hooks are larger in *R. beatrizae* **sp. n.** (±101 μm long and ±89 μm long, respectively) than in *R. soror* **sp. n.** (±87 μm long and ±59 μm long, respectively). The funnel-like structure of the larger hook is ±70 μm long in *R. soror* **sp. n.** and ±45 μm long in *R. beatrizae* **sp. n**. The general outline of the larger hook of *R. soror* **sp. n.** is more slender than that of *R. beatrizae* **sp. n**.

Reinhardorhynchus anamariae **sp. n.** is easily recognisable because it is the only known species of *Reinhardorhynchus* **gen. n.** without eyes. This is an uncommon feature within Koinocystididae, until now exclusively known from *Leguta chelifera* (Karling, 1954) Karling, 1980 and *Paratenerrhynchus triplex* Brunet, 1972 (see Karling 1954, 1980; Brunet 1972). The cirrus morphology in *R. anamariae* **sp. n.** also distinguishes it from its congeners: it is ornamented with rows of fine, ±1-μm-long spines and an L-shaped row of larger spines (±116 μm long). *R. curvicirra* **comb. n.** and *R. ruffinjonesi* **comb. n**. have a cirrus with comparable features. However, in *R. curvicirra* **comb. n.** the spiny row is longer (120–160 μm), U-shaped, and carries larger lamellar spines (20–40 μm, compared to 9–34 μm in *R. anamariae* **sp. n.**). Furthermore, in *R. curvicirra* **comb. n.** the rows of small spines which are present in *R. anamariae* **sp. n.** are absent. The spiny row of the cirrus of *R. ruffinjonesi* **comb. n.** is considerably larger (165–260 μm) than in *R. anamariae* **sp. n**. The spiny row of the former species is also differentiated in a proximal and a distal part, but the spines in this area distinctly differ in morphology and length from those of *R. anamariae* **sp. n**. In *R. anamariae* **sp. n.**, the proximal hook-like spines are ±22 μm long, hollow and distally curved, whereas in *R. ruffinjonesi* **comb. n.** the proximal spines are ±5 μm (specimen from Brazil) to ±8 μm long (specimens from Bermuda and Punta Culebra), triangular, and not hollow or distally curved. Furthermore, the proximal and the distal parts of the spiny belt in *R. ruffinjonesi* **comb. n.** are connected by an area of 2–3-μm-long spines, which are absent in *R. anamariae* **sp. n**. The spiny armature of the cirrus also differentiates *R. anamariae* **sp. n.** (fine spines ±1 μm long, organised in rows) from *R. ruffinjonesi* **comb. n.** (triangular spines 1–3 μm long, not organised in rows). Finally, the shape and size of the distal hooks in *R. anamariae* **sp. n.** (31 μm and 51 μm long, respectively, ending in a rounded tip) differ from those in *R. ruffinjonesi* **comb. n.** (36 μm and 59 μm long, respectively, ending in a sharp tip).

Both *R. tahitiensis* **sp. n.** and *R. riae* **sp. n.** possess a cirrus armed with spiny rows and two symmetric, distal hooks in the copulatory bulb. In *R. riae* **sp. n.**, the cirrus spines are all similar in size and organised in two spiny rows, while the cirrus of *R. tahitiensis* **sp. n.** carries four rows of spines of variable size, the most distal ones being the largest. In addition, the accessory hooks are ±24 μm long and conical, with a small distal hook in *R. tahitiensis* **sp. n.**, whereas in *R. riae* **sp. n.** they measure ±14 μm, are more flattened and never carry a distal hook. The only other species of *Reinhardorhynchus* **gen. n.** with distal symmetric hooks is *R. bispina* **comb. n.**, which also bears

two spiny rows in the copulatory bulb. However, in *R. bispina* **comb. n.**, these rows are longitudinally oriented and 100–150 μm long, while they are transversally oriented and 55–72 μm long in *R. riae* **sp. n**. In *R. tahitiensis* **sp. n.**, three rows are more or less longitudinally oriented and one is transversally oriented. In addition, the symmetric hooks of *R. bispina* **comb. n.** are needle-shaped and larger (40–50 μm) compared to those of the new species (Karling 1980).

Reinhardorhynchus riae **sp. n.** is the only species of *Reinhardorhynchus* **gen. n.** that has a prostate vesicle surrounded by a muscular bulb, with the spiny rows of the cirrus extending over the distal end of this muscular bulb. The female system is also peculiar, with the female duct divided into two compartments similar to the female duct in *R. tahitiensis* **sp. n**. However, in *R. riae* **sp. n.**, the proximal compartment of the female duct is not muscular and contains vitelline material, while the distal compartment is surrounded by well-developed circular muscles and contains sperm. In *R. tahitiensis* **sp. n.**, both compartments are muscular and it is the proximal one that contains sperm.

Galapagetula. *Galapagetula cubensis* **sp. n.** displays the main diagnostic features of the genus (see Reygel *et al.* 2011): proboscis without juncture sphincter, testes located at midbody, copulatory organ pear-shaped, female duct proximally widened and functioning as seminal receptacle. The most typical feature of species of *Galapagetula*, however, is the presence of an accessory bursa (see Reygel *et al.* 2011). *Galapagetula cubensis* **sp. n.** and *G. annikae*, the only known species up to now, differ in many features. One of the most important differences is the fact that in *G. annikae* the cirrus is provided with many small teeth, while in *G. cubensis* **sp. n.** it is completely unarmed. An unarmed copulatory organ is uncommon within Koinocystididae, and reported only in the unrelated taxa *I. biglandula*, *Tenerrhynchus magnus* Brunet, 1972, *Parautelga bilioi* Karling, 1964, *Neoutelga inermis* Karling, 1980, *S. stolzi*, and *Simplexcystis asymmetrica* **gen. n. sp. n** (see further).

Moreover, in *G. cubensis* **sp. n.** the ejaculatory duct and prostate vesicle open separately in the male atrium (a so-called divisa type copulatory organ; terminology of Karling 1956; see also the discussion on *R. hexacornutus* **n. sp**. above), whereas in *G. annikae* the copulatory organ is of the conjuncta-duplex type, typical of Koinocystididae. Also, the fact that the gonopore is located completely caudally in *G. cubensis* **sp. n.** clearly distinguishes it from *G. annikae*. In fact, within Koinocystididae, only *M. terminostylis* has a gonopore that is completely terminal. This species, however, is entirely different from a morphological point of view (for details: see Karling 1956). Other differences between the species of *Galapagetula* is the absence of a pseudocuticular lining in the female duct and accessory bursa in *G. cubensis* **sp. n.** (present in *G. annikae*), and the lack of a mouth sphincter in *G. annikae*.

***Simplexcystis* gen. n.**

Simplexcystis asymmetrica **gen. n. sp. n.** possesses all diagnostic features of Koinocystididae (see Karling 1980). However, the new species, *S. asymmetrica* **sp. n.**, shows a unique combination of features which does not allow allocation to any existing koinocystidid genus, including a copulatory bulb with unarmed cirrus, seminal duct entering the copulatory bulb eccentrically, oviducts very long, bursa lacking, and male, female, and common atrium lined by a brush border.

As previously discussed, a copulatory organ without hard structures is uncommon in Koinocystididae (see above). *Simplexcystis asymmetrica* **sp. n.** also lacks a bursa, a feature only found in *T. magnus* and *Bhambathorhynchus abursalis* Willems & Artois in Willems *et al.*, 2017 (see Brunet 1972; Karling 1980; Willems *et al.* 2017). However, the latter two species lack the unique combination of features typical of *Simplexcystis* **gen. n**. Moreover, *S. asymmetrica* **sp. n.** shows a strong sphincter caudally from the female duct typical of koinocystidids, a feature lacking in *B. abursalis*. The latter species also has a complex and bipartite receptacle bursa (see Willems *et al.* 2017), which is not present in *S. asymmetrica* **sp. n**. Furthermore, in *B. abursalis* there are two hooks in the copulatory bulb, while the copulatory system is completely unarmed in *S. asymmetrica* **sp. n**. Many features allow to differentiate *S. asymmetrica* **sp. n.** from *T. magnus*; for instance, the fact that the testes are located rostral to the pharynx in *S. asymmetrica* **sp. n.**, caudal to it in *T. magnus*. The ejaculatory duct is very long and broad before entering the copulatory bulb in *S. asymmetrica* **sp. n.** while it is short and tubiform in *T. magnus*. Moreover, the copulatory bulb lacks a penis papilla in *S. asymmetrica* **sp. n.**, while such a papilla is present in *T. magnus*.

Conclusions

Both species richness and morphological diversity of koinocystidids has been greatly underestimated in the past. Here, we exemplify that even a relatively small sampling effort can lead to the discovery of many new species, often with such an aberrant morphology that they cannot be placed in any existing genus. In this contribution 12 new species are described, raising the number of known species of koinocystidids from 51 to 63. The family is also morphologically very diverse, especially as to the construction of the genital system. In a few species the copulatory bulb is devoid of any hard structures (*I. biglandula*, *T. magnus*, *P. bilioi*, *N. inermis*, *S. stolzi*, *G. cubensis* **sp. n.**, and *S. asymmetrica* **gen. n. sp. n.**). In the other species, the copulatory bulb encompasses a diversity of cirri, spines, stylets and hooks. The female genital system can be very simple, as in *S. asymmetrica* **gen. n. sp. n.**, but in most other koinocystidids it is very complex and includes a diversity of bursae, glands, and even armature in the form of spines or sclerotised membranes. The number of species included in phylogenetic analyses is still very limited, even with the new sequences provided in this contribution. It is imperative to sample many more taxa for future analyses, especially taxa with 'aberrant' morphologies, which are now mostly represented by monospecific genera. In that way, the diversity of koinocystidids could be better appreciated and their phylogenetic relationships unravelled.

Acknowledgements

Mrs. Natascha Steffanie is thanked for making the histological sections. We would like to thank Ria Vanderspikken for her valuable assistance in the laboratory. Sampling campaigns were organised by Alejandro Martínez García and Katrine Worsaae (Lanzarote, 2010), Jon Norenburg (Panama, 2011), Maikon Di Domenico (Brazil, 2012), Francesca Leasi (Panama, 2016), and Marco Curini-Galletti (Sardinia, 2018). Jean-Lou Justine hosted ES in New Caledonia (2003). Mare Geraerts helped during the collects in Sardinia. This work is partially supported by VLIR-UOS under the project "Risk mitigation plan for biodiversity and food production to face climatic change in the eastern region of Cuba" with Universidad de Oriente. YLD is supported by BOF-Hasselt University under grant BOF15BL09. MM is supported by a PhD fellowship of the Research Foundation Flanders (FWO-Vlaanderen). The research leading to results presented in this publication was carried out with infrastructure funded by EMBRC Belgium - FWO project GOH3817N. PJ wants to thank Dr. N. Gaertner-Mazouni and Dr. M. Taquet from the Université de la Polynésie Française, Unité Mixte de Recherche 241, Écosystèmes lnsulaires Océaniens (UMR 241-EIO), for their support and the access to the laboratory facilities during the field research. NWLVS and BSL were supported by grants from the Hakai Institute and the National Science and Engineering Research Council of Canada (NSERC 2019-03986). We thank two anonymous reviewers for their valuable comments in an earlier version of the manuscript.

References

Altschul, S.F., Gish, W., Miller, W., Myers, E.W. & Lipman, D.J. (1990) Basic local alignment search tool. *Journal of Molecular Biology*, 215, 403–410.
https://doi.org/10.1016/S0022-2836(05)80360-2

Attems, C.G. (1897) Beitrag zur Kenntnis der rhabdocoelen Turbellarien Helgolands. *Wissenschaftliche Meeresuntersuchungen der Kommission Abteilung Kiel*, 2 (1), 219–232.

Benson, D.A., Karsch-Mizrachi, I., Clark, K., Lipman, D.J., Ostell, J. & Sayers, E.W. (2012) GenBank. *Nucleic Acids Research*, 40, D48–D53.
https://doi.org/10.1093/nar/gkr1202

Brunet, M. (1965) Turbellariés calyptorhynques de substrats meubles de la région de Marseille. *Recueil des Travaux de la Station Marine d'Endoume*, 39 (55), 128–218.

Brunet, M. (1972) Koinocystididae de la région de Marseille. *Zoologica Scripta*, 1, 157–174.
https://doi.org/10.1111/j.1463-6409.1972.tb00673.x

Castresana, J. (2000) Selection of conserved blocks from multiple alignments for their use in phylogenetic analysis. *Molecular Biology and Evolution*, 17, 540–552.
https://doi.org/10.1093/oxfordjournals.molbev.a026334

Claus, C. (1887) *Lehrbuch der Zoologie. 4. Auflage*. N. G. Elwertsche Verlagsbuchhandlung, Marburg, Leipzig, 1279 pp.

Ehlers, U. (1985) Cytoskelette bei freilebenden Plathelminthen. *Verhandlungen der Deutschen Zoologischen Gesellschaft*, 78, 161.

Ehrenberg, C.G. (1831) Animalia evertebrata exclusis insectis recensuit C.G. Ehrenberg. Series prima cum Tabularum decade prima. *In*: Hemprich, F.G. & Ehrenberg, C.G. (Eds.), *Symbolae Physicae 2. Phytozoa Turbellaria*. Officina Academica, Berolina, pp. 1–15.

Fuhrmann, O. (1904) Ein neuer Vertreter eines marinen Turbellariengenus in Süsswasser. *Zoologischer Anzeiger*, 27, 381–384.

Graff, L. von (1905) Marine turbellarien Orottavas und der Küsten Europas. *Zeitschrift für wissenschaftliche Zoologie*, 83, 68–148.

Guindon, S., Dufayard, J.-F., Lefort, V., Anisimova, M., Hordijk, W. & Gascuel, O. (2010) New Algorithms and Methods to Estimate Maximum-Likelihood Phylogenies: Assessing the Performance of PhyML 3.0. *Systematic Biology*, 59 (3), 307–321.
https://doi.org/10.1093/sysbio/syq010

Hoang, D.T., Chernomor, O., Haeseler, Arndt von, Minh, B.Q. & Vinh, L.S. (2013) UFBoot2: Improving the Ultrafast Bootstrap Approximation. *Molecular Biology and Evolution*, 35 (2), 518–522.
https://doi.org/10.1093/molbev/msx281

Kalyaanamoorthy, S., Minh, B.Q., Wong, T.K.F., Haeseler, A. von & Jermiin, L.S. (2017) ModelFinder: Fast Model Selection for Accurate Phylogenetic Estimates. *Nature Methods*, 14 (6), 587–589.
https://doi.org/10.1038/nmeth.4285

Karling, T.G. (1952a) Kalyptorhynchia (Turbellaria). *Further Zoological Results of the Swedish Antarctic Expedition*, 4 (9), 1–50.

Karling, T.G. (1952b) Studien über Kalyptorhynchien (Turbellaria) IV. Einige Eukalyptorhynchia. *Acta Zoologica Fennica*, 69, 1–49.

Karling, T.G. (1954) Einige marine Vertreter der Kalyptorhynchien-Familie Koinocystididae. *Arkiv för Zoologi*, 7, 165−183.

Karling, T.G. (1956) Morphologisch-histologische Untersuchungen an den männlichen Atrialorganen der Kalyptorhynchia (Turbellaria). *Arkiv för Zoologi*, Serie 2, 9 (7), 187–279.

Karling, T.G. (1964) Über einige neue und ungenügend bekannte Turbellaria Eukalyptorhynchia. *Zoologischer Anzeiger*, 172, 159−183.

Karling, T.G. (1978) Anatomy and Systematics of Marine Turbellaria from Bermuda. *Zoologica Scripta*, 7, 25–248.

Karling, T.G. (1980) Revision of Koinocystididae (Turbellaria). *Zoologica Scripta*, 9, 241–269.
https://doi.org/10.1111/j.1463-6409.1980.tb00666.x

Karling, T.G., Mack-Fira, V. & Dörjes, J. (1972) First report on marine microturbellarians from Hawaii. *Zoologica Scripta*, 1, 251–269.
https://doi.org/10.1111/j.1463-6409.1972.tb00575.x

Katoh, K. & Standley, D.M. (2013) MAFFT multiple sequence alignment software version 7: improvements in performance and usability. *Molecular Biology and Evolution*, 30 (4), 772–780.
https://doi.org/10.1093/molbev/mst010

Katoh, K., Rozewicki, J., Yamada, K.D. (2017) MAFFT online service: multiple sequence alignment, interactive sequence choice and visualization. *Briefings in Bioinformatics*, 20 (4), 1160–1166.
https://doi.org/10.1093/bib/bbx108

Kearse, M., Moir, R., Wilson, A., Stones-Havas, S., Cheung, M., Sturrock, S., Buxton, S., Cooper, A., Markowitz, S., Duran, C., Thierer, T., Ashton, B., Meintjes, P. & Drummond, A.A. (2012) Geneious Basic: An integrated and extendable desktop software platform for the organization and analysis of sequence data. *Bioinformatics*, 28 (12), 1647–164.
https://doi.org/10.1093/bioinformatics/bts199

Lanfear, R., Calcott, B., Ho, S.Y.W. & Guindon, S. (2012) Partition Finder: Combined selection of partitioning schemes and substitution models for phylogenetic analyses. *Molecular Biology and Evolution*, 29, 1695–1701.
https://doi.org/10.1093/molbev/mss020

Lin, Y.-T., Feng, W.-T., Zhuang, J.-Y., Zhang, Y. & Wang, A.-T. (2017) Two new species of Kalyptorhynchia (Koinocystididae and Gnathorhynchidae) from China. *Zootaxa*, 4337 (4), 573-583.
https://doi.org/10.11646/zootaxa.4337.4.8

Mack-Fira, V. (1968) Turbellariés de la Mer Noire. *Rapport de la Commission pour la Mer Méditerranée*, 9 (2), 179–182.

Mack-Fira, V. (1974) The turbellarian fauna of the Romanian littoral waters of the Black Sea and its annexes. *In*: Riser, N.W. & Morse, M.P. (Eds.), *Biology of Turbellaria*. McGraw-Hill, New York. pp. 248–290.

Marcus, E. (1949) Turbellaria Brasileiros (7). *Boletins da Faculdade de Filosofia Ciencias e Letras, Universidade de São Paulo Zoologia*, 7 (14), 7−155.
https://doi.org/10.11606/issn.2526-4877.bsffclzoologia.1949.129106

Marcus, E. (1951) Turbellaria Brasileiros (9). *Boletins da Faculdade de Filosofia, Ciencias e Letras, Universidade de São Paulo Zoologia*, 16, 1−215.
https://doi.org/10.11606/issn.2526-4877.bsffclzoologia.1951.125221

Marcus, E. (1954) Turbellaria Brasileiros (11). *Papéis Avulsos*, 11, 419−489.
https://doi.org/10.11606/issn.2526-4877.bsffclzoologia.1946.125301

Meixner, J. (1924) Studien zu einer Monographie der Kalyptorhynchia und zum System der Turbellaria Rhabdocoela. *Zoologischer Anzeiger*, 60, 89−105.

Meixner, J. (1925) Beitrag zur Morphologie und zum System der Turbellaria-Rhabdocoela. I. Die Kalyptorhynchia. *Zeitschrift*

für Morphologie und Ökologie der Tiere, 3, 255–343.
https://doi.org/10.1007/BF00408146
Meixner, J. (1928) Der Genitalapparat der Tricladen und seine Beziehungen zu ihrer allgemeinen Morphologie, Phylogenie, Ökologie und Verbreitung. *Zeitschrift für Morphologie und Ökologie der Tiere*, 11 (5), 570–612.
https://doi.org/10.1007/BF02424587
Miller, M.A., Pfeiffer, W. & Schwartz, T. (2010) Creating the CIPRES Science Gateway for inference of large phylogenetic trees. *Proceedings of the Gateway Computing Environments Workshop*, 2010, 1–8.
https://doi.org/10.1109/GCE.2010.5676129
Nguyen, L.-T., Schmidt, H.A., Haeseler, A. von & Minh, B.Q. (2015) IQ-TREE: A fast and effective stochastic algorithm for estimating maximum-likelihood phylogenies. *Molecular Biology and Evolution*, 32 (1), 268–274.
https://doi.org/10.1093/molbev/msu300
Rambaut, A. (2006–2019) FigTree: Tree Figure Drawing Tool. Computer program distributed by the author. Available from: http://tree.bio.ed.ac.uk/software/figtree/ (accessed 14 August 2020)
Reygel, P.C., Willems, W.R. & Artois, T.J. (2011) Koinocystididae and Gnathorhynchidae (Platyhelminthes: Rhabdocoela: Kalyptorhynchia) from the Galapagos, with the description of three new species. *Zootaxa*, 3096 (1), 27–40.
https://doi.org/10.11646/zootaxa.3096.1.3
Ronquist, F., Teslenko, M., Mark, P. van der, Ayres, D.L., Darling, A., Höhna, S., Larget, B., Liu, L., Suchard, M.A. & Huelsenbeck, J.P. (2012) MrBayes 3.2 efficient Bayesian phylogenetic inference and model choice across a large model space. *Systematic Biology*, 61 (3), 539–542.
https://doi.org/10.1093/sysbio/sys029
Schockaert, E.R. (1996) Turbellarians. *In*: Hall, G.S. (Ed.), *Methods for the Examination of Organismal Diversity in Soils and Sediments*. CAB International Wallingford, pp. 211–225.
Sekera, E. (1912) Monographie der Gruppe Olisthanellini. *Sitzungsberichte der Königlichen Böhmischen Gesellschaft der Wissenschaften. Classe für Mathematik und Naturwissenschaften*, 24, 1–93.
Strand, E. (1914) Neue Namen verschiedener Tiere. *Archiv für Naturgeschichte*, 80, 163–164.
Tessens, B., Janssen, T. & Artois, T. (2014) Molecular phylogeny of Kalyptorhynchia (Rhabdocoela, Platyhelminthes) inferred from ribosomal sequence data. *Zoologica Scripta*, 43 (5), 519–530.
https://doi.org/10.1111/zsc.12066
Trifinopoulos, J., Nguyen, L.-T., Haeseler, Arndt von & Minh, B.Q. (2017) W-IQ-TREE: a fast online phylogenetic tool for maximum likelihood analysis. *Nucleic Acids Research*, 44, W232–W235.
https://doi.org/10.1093/nar/gkw256
Tyler, S., Artois, T., Schilling, S., Hooge, M. & Bush, L.F. (Eds.) (2006–2019) World List of turbellarian worms: Acoelomorpha, Catenulida, Rhabditophora. Koinocystididae Meixner, 1924. World Register of Marine Species. Available from: http://www.marinespecies.org/aphia.php?p=taxdetails&id=142395 (accessed 28 November 2018)
Van Steenkiste, N., Tessens, B., Willems, W., Backeljau, T., Jondelius, U. & Artois, T. (2013) Comprehensive Molecular Phylogeny of Dalytyphloplanida (Platyhelminthes: Rhabdocoela) Reveals Multiple Escapes from the Marine Environment and Origins of Symbiotic Relationships. *PLoS ONE*, 8 (3), e59917.
https://doi.org/10.1371/journal.pone.0059917
Van Steenkiste, N.W.L. & Leander, B.S. (2018) Species diversity of eukalyptorhynch flatworms (Platyhelminthes, Rhabdocoela) from the coastal margin of British Columbia: Polycystididae, Koinocystididae and Gnathorhynchidae. *Marine Biology Research*, 14 (9–10), 899–923.
https://doi.org/10.1080/17451000.2019.1575514
Van Steenkiste, N.W.L., Herbert, E.R. & Leander, B.S. (2018) Species diversity in the marine microturbellarian *Astrotorhynchus bifidus* sensu lato (Platyhelminthes: Rhabdocoela) from the Northeast Pacific Ocean. *Molecular Phylogenetics and Evolution*, 120, 259–273.
https://doi.org/10.1016/j.ympev.2017.12.012
Willems, W., Reygel, P., Van Steenkiste, N., Tessens, B. & Artois, T. (2017) Kalyptorhynchia (Platyhelminthes: Rhabdocoela) from KwaZulu-Natal (South Africa), with the description of six new species. *Zootaxa*, 4242 (3), 441–466.
https://doi.org/10.11646/zootaxa.4242.3.2
Willems, W.R., Sandberg, M.I. & Jondelius, U. (2007) First report on Rhabdocoela (Rhabditophora) from deep parts of Skagerrak, with the description of four new species. *Zootaxa*, 1616 (1), 1–21.
https://doi.org/10.11646/zootaxa.1616.1.1